DISSERTATION

DEVELOPMENT OF MINIATURIZED CAPILLARY ELECTROPHORESIS SYSTEM WITH ELECTROCHEMICAL DETECTION

Submitted by

Yan Liu

Department of Chemistry

In partial fulfillment of the requirements

For the Degree of Doctor of Philosophy

Colorado State University

Fort Collins, Colorado

Fall 2005

COLORADO STATE UNIVERSITY

August 11, 2005

WE HEREBY RECOMMEND THAT THE DISSERTATION PREPARED UNDER OUR SUPERVISION BY YAN LIU ENTITLED "DEVELOPMENT OF MINIATURIZED CAPILLARY ELECTROPHORESIS SYSTEM WITH ELECTROCHEMICAL DETECTION" BE ACCEPTED AS FULFILLING IN PART REQUIREMENTS FOR THE DEGREE OF DOCTOR OF PHILOSOPHY.

Committee on Graduate Work

Advisor

Co-Advisor

Department Head

ABSTRACT OF DISSERTATION

DEVELOPMENT OF MINIATURIZED CAPILLARY ELECTROPHORESIS SYSTEM WITH ELECTROCHEMICAL DETECTION

Over the past decade, development of microanalytical devices has become an important trend in analytical research. An ideal miniaturized analytical device can shrink a laboratory full of instrumentation into one single lab-on-a-chip which incorporates sample acquisition, pretreatment, injection, separation, derivatization, and detection. The goal of this dissertation work was to develop a miniaturized capillary electrophoresis (CE) system with electrochemical detection (EC) to analyze biological and environmental samples.

The miniaturized CE-EC system was first demonstrated on PDMS/glass hybrid chip in a urinary 4-aminophenol determination. The fabrication of hybrid chip involved the microfabrication of a Au thin-film electrode and fabrication of PDMS piece with patterned channels. This system was found to be unstable and give poor performance. To improve the overall performance, several steps were taken. First, a portable and cheap power supply was developed which could provide up to 4 kV output and perform three different types of sample injections. Second, to overcome the drawbacks of the Au thin-film electrode, a new

microwire working electrode design was developed by placing a metallic microwire into the electrode alignment channel in the PDMS piece. The new working electrode proved to be more sensitive and flexible and have a higher collection efficiency than microfabricated electrode. The developed portable and sensitive microchip CE-EC system was then applied to aerosol analyses and antioxidant profiling.

Yan Liu

Chemistry Department

Colorado State University

Fort Collins, CO 80523

Fall 2005

ACKNOWLEDGMENTS

Grateful acknowledgment is expressed to Colorado State University and Mississippi State University for giving me the opportunity to work and study as a part of their graduate program.

I am so thankful for many individuals that help me reach this point in my life. Sincere appreciation is extended to all my committee members, which include Dr. Charles Henry, Dr. George Barisas, Dr. Tom Rovis, Dr. Kevin Lear, Dr. Michael Elliott, and Dr. Ellen Fisher. My sincerest gratitude is expressed to Dr. Henry for serving as my advisor. He showed me how to formulate scientific ideas, write proposals, carry out productive research, and publish scientific work. Very importantly, he served as a great mentor and friend both inside and outside of the lab.

I would like to thank Dr. David Wipf (MSU) and Dr. Jeffery Collett (CSU) for providing the conductivity detectors which were very important in my research. I would like to express my appreciation to Mr. Geoffrey Carter and Dr. Kevin Lear for the access to microfabrication equipment. Deep appreciation is also due to Paul Anderson for his help in building compact power supplies. Grateful acknowledgment is also due to my lab partners, including Jon Vickers, Dave MacDonald and Dr. Carlos Garcia. Their dedication helped me get through the projects smoothly. Thanks are also due to all members of Henry group for their help and friendship. Gratitude is also expressed to Fanguy's family for their love,

assistance, and friendship. I am so grateful to know such a warm American family. Although I only acknowledge a few people here, I express my greatest appreciation to all who have helped me along the way to get to this point.

Finally my deepest affection and gratitude are due to my family members including my wife, parents, and brothers. Their love is the best support for me to finish study here.

DEDICATION

I would like to dedicate this research to my father, LIU Guozhou.

TABLE OF CONTENTS

LIST OF TABLES

LIST OF FIGURES

CHAPTER I

INTRODUCTION

1.1 Background of capillary electrophoresis

Electrophoresis is a liquid phase analytical technique in which ions in solution are separated, based on their differences in size and charge, when a high voltage is applied to the solution.[1] Capillary electrophoresis (CE) has emerged as an alternative form of electrophoresis, with a capillary wall providing the mechanical stability for the carrier electrolyte.[2] Capillaries, with their relatively high surface-to-volume ratio, dissipate heat efficiently. This means greater separation potentials can be used.[3] With the application of higher potentials, separations can be achieved in much shorter analysis times than those obtained with traditional slab gel methods.[4] Moreover, the small dimensions of the capillary decrease the required sample sizes by a few orders of magnitude, compared to high performance liquid chromatography (HPLC).[5] CE did not become popular until 1981 when Jorgenson and Lukacs demonstrated the high resolving power of capillary zone electrophoresis (CZE).[2] Since then, CE has shown good improvement over other analytical separation techniques in terms of resolution power, separation speed, sample and reagent consumption, and cost.[6, 7] Although the initial start was slow, CE methods are now undergoing an exponential expansion. Today thousands of CE instruments are installed

worldwide and routine CE methods have been established in many academic and industrial laboratories. Due to their high separation power, sufficient selectivity, and versatility, CE and related capillary techniques have been applied in every major industry.[8-15]

1.2 Electroosmotic flow

In CE, separation is driven by two factors. The first is the movement of the analyte in the capillary due to the electric field, also called electrophoretic velocity. The second is the bulk flow of solution due to the surface charge on the capillary wall, also called electroosmotic flow (EOF).[1] The migration velocity of a particular species is the product of its mobility and the electric field and may be written as[1]

$$v = \mu E = (\mu_e + \mu_{eo})V / L \qquad (1\text{-}1)$$

where:

E = electric field strength

μ = the apparent mobility,

μ_e = electrophoretic mobility,

μ_{eo} = mobility of EOF,

V = the applied voltage,

L = the length of the capillary.

This electrophoretic mobility is dependent upon both the charge density and

mass of the analyte as well as buffer properties such as the dielectric constant and viscosity. In a fused silica capillary, the ionization of silanol groups gives rise to a negatively charged surface, which affects the distribution of nearby ions in solution. To balance the negative charges on the capillary inner walls, hydrated cations in the buffer are attracted to the negatively charged inner wall. A double layer thus forms, with a compact layer, tightly bound to the wall, and a loosely bound diffuse layer, shown in Figure 1.1. When an external electric field is applied, the diffuse layer moves toward the cathode. A bulk solution flow results from viscous drag and is termed EOF. EOF, however, will not behave as ideally as described because the ionic strength of the buffer, analyte adsorption on the walls, and external electric fields can influence it.[1]

Electroosmosis occurs in fused silica capillaries because the acidic silanol groups on the capillary wall dissociate when in contact with a basic electrolyte solution.

$$SiOH \longrightarrow SiO^- + H^+ \qquad (1\text{-}2)$$

The pK_a value for above dissociation is around 3.5. Below a pH of 3.0, there are few SiO^- ions; thus, the zeta potential (potential between the compact and diffuse layer) and the EOF are both zero. As the pH is increased, the zeta potential and EOF increase. The zeta potential is proportional to the thickness of the double layer. Increasing the buffer solution's ionic strength provides a higher

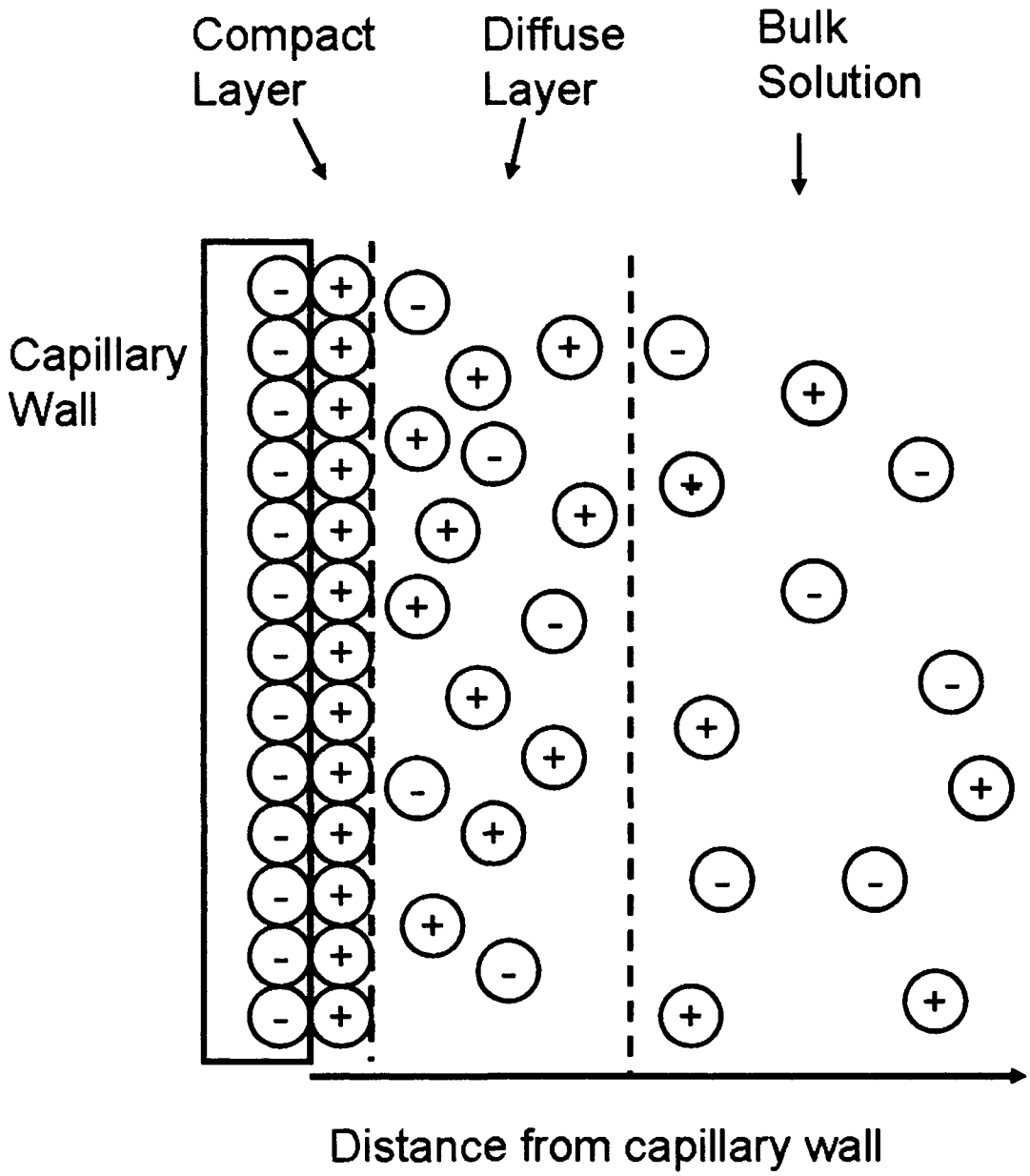

Figure 1.1 Schematic diagram of double layer close to the capillary wall

concentration of cations, decreasing the thickness of the double layer. The EOF value is directly related to the magnitude of the zeta potential, ζ, which is given by:[1]

$$\zeta = \frac{4\pi\eta\mu_{eo}}{\varepsilon} \qquad (1\text{-}3)$$

where:

η = the viscosity of the buffer,

ε = the dielectric constant of the buffer,

μ_{eo}= the zeta potential.

The dependence of mobility on ionic strength or concentration is given by:

$$\mu_{eo} = \frac{e}{3\times10^{-7}|Z|\eta c^{1/2}} \qquad (1\text{-}4)$$

where:

Z = the number of valence electrons of the electrolyte,

e = the total excess charge in solution per unit area,

c = the buffer concentration.

When the buffer concentration increases, the EOF will decrease as the square root of the buffer concentration. The addition of organic solvents to buffer alters the viscosity, partially decreases the ionic strength of buffer solution, and may also affect the intramolecular hydrogen bonding. The EOF is also affected by applied voltage. Increasing the applied voltage results in an increase of EOF.

1.3 Microchip CE

Over the past decade, miniaturization and integration of CE instruments has become an dominant trend in CE research.[16-27] The main driving force behind miniaturization is the need to reduce costs by reducing consumption of expensive reagent and by increasing throughput and automation. Ideal miniaturized analytical devices have the capacity of incorporating sample acquisition, pretreatment, injection, separation, derivatization, and detection into one single small chip. Microchip CE was developed initially in early of 1990s.[28-34] Typically, microchip CE systems consume only picoliters of sample.[32, 35] The second feature is short analysis times as a separation of a binary mixture in 0.8 ms on microchip CE has been achieved.[36] The third feature is that sample may potentially be prepared on-chip for a complete integration of sample preparation, chemical reactions, chromatographic or electrophoretic separations, and detection.[37-39] Moreover, the overall size of microfluidic chips is particularly suitable to CE for in situ and real-time analysis.[40] For polymeric microchips, the disposability is another attractive feature due to the low manufacturing costs.[41, 42] These features make microchip CE an attractive technology for the next generation of CE instrumentation. Work on microchip CE is now undergoing expanding growth.[43-48] It is anticipated that the current rate of progress and

interest in this area will lead to the next revolution in chemical, biological, and clinical analysis.

1.4 Substrate materials for microchip

As mentioned in section 1.2, CE relies electroosmotic pumping to propagate flow in microfluidic system. In electroosmotically driven systems, it is critical that the substrate material exhibits good electrical insulating properties so that the electric field will drop across the fluid-filled channel and not through the substrate. The second concern when using electrokinetic pump is Joule heating. The substrate should dissipate heat generated in microchannel effectively. The third consideration is surface charge properties of substrate material since EOF is generated by the surface charge on the microchannel walls in combination with an electric field along the microchannel.[49] Until the late 1990s, CE microchips were mainly fabricated using various silica-based substrates, from soda lime glass to high quality quartz.[16, 17, 50-53] Silica-based substrates are the most common mainly because the well-developed microfabrication methods from the microelectronics industry can be adapted in the fabrication of silica CE microchips. In addition, glass and quartz, being chemically similar to fused silica, maintain many of the properties already developed for conventional CE. The optical clarity of these substrates, especially that of quartz, is significant as early

work relied solely on laser-induced fluorescence (LIF) for detection. There are, however, several limitations to the use of glass, especially for the rapid development of microfluidic systems. The major drawback of glass and quartz CE chips is the time- and labor-intensive fabrication. For instance, in order to form a closed channel system, it is required to bond a cover plate at a high temperature (typically 600°C for 4 h) to the patterned substrate. In addition, reservoir holes providing access to the microchannels have to be drilled through the cover plate in a tedious procedure using a diamond tipped drill bit. Another concern with silica devices is the cost of manufacturing. Fabrication of the devices requires extensive use of clean-room facilities, which are expensive to both set up and maintain. Optical quality glass and quartz are expensive and fragile compared to polymers, raising the cost of each device. Moreover, the fabrication process produces a permanent seal between the two plates that make up the device. If a channel clogs, the device is useless.

The disadvantages of glass microchips have recently triggered the search for alternative substrate materials for the fabrication of microchip CE devices. Various polymer materials, such as polyester,[54, 55] polycarbonate,[56, 57] polymethylmethacrylate,[41, 58] polystyrene,[59, 60] and polydimethylsiloxane (PDMS),[61, 62] have been explored by a number of research groups to fabricate microchips for CE separations. Polymer substrates are advantageous as they are

much less expensive than glass, not as fragile as glass, and a wide range of material properties can be explored. The primary advantage of polymer substrates, however, lies in the ability to mass-produce devices. Unlike glass substrates, which use a second piece of glass to form the completed channel, polymer substrates have the advantage of good adhesion on clean, smooth surfaces of many different materials including other polymers and glass. Thus forming closed channel networks can be accomplished without special bonding procedures. Buffer and sample reservoirs can be simply punched through the bulk material. Finally, the overall process is faster than conventional micromachining, allowing numerous devices to be produced in a short time period.

1.5 PDMS substrate

One of the most successful polymer substrates used in microchip CE is cross-linked PDMS. PDMS was first used for microchip CE by Effenhauser and coworkers for the separation of DNA fragments in a gel filled capillary.[63] PDMS is a durable hydrophobic elastomer and is an attractive material for the fabrication of micropatterned objects. The water/PDMS contact angle measured immediately after curing at 75 °C for 3 h is 104.5 ± 2.0 °C.[64] The average contact angles measured over four months do not differ statistically from this value within the

95% confidence interval, demonstrating the remarkable stability of the cured elastomer. The patterned silicone substrate can be reversibly bonded to itself and other materials by van der Waals contact with the clear smooth surface at room temperature.[65] PDMS has a refractive index of 1.430 and is optically transparent down to ~230 nm facilitating LIF detection in the visible and high ultraviolet range of spectrum. Moreover, PDMS exibits high electrical volume resistivity (2×10^{15} Ωcm^{-1}), moderate heat conductivity (0.15 W/mK) and low surface energy (~ 22 mN/m), and can be molded with a variety of masters at very low cost.[64, 65] The primary advantage of PDMS over glass or quartz substrate is the ability to rapidly prototype very complex devices. Fabrication times from idea to chip completion can be less than 12 hours. There are several disadvantages to the use of PDMS due to its hydrophobic nature. The absorption and adsorption of non-polar species has been well documented for PDMS.[66-68] In addition, PDMS is known to absorb organic solvents, limiting buffer systems to water and some alcohols.[64]

1.6 Sample injection methods

Integrated sample injection is used to produce the small sample size (measured in picoliters) required for CE on microchips. Generally, the injection procedure for a cross-format microfluidic chip involves two discrete steps, loading and dispensing.[69] In the loading step, the sample fluid is transported through the

cross region from the sample reservoir. After the cross-region is filled with the sample, the dispensing step begins when a plug of sample is pushed into the separation channel by an electroosmotic pump. According to the forces employed in these two steps, different injection methods have been designed for microchip CE system. [69-71]

Electrokinetic injection includes gated[72, 73] and pinched injection.[74, 75] At the beginning of the gated injection, sample is electrokinetically transported from sample to sample waste reservoir while buffer is transported from buffer to buffer waste reservoir. This is done by application of a potential on buffer and sample reservoirs while maintaining both waste reservoirs at ground (Figure 1.2A). When the voltage on the buffer reservoir is temporarily turned off, sample will flow into the separation channel resulting in the formation of a sample plug (Figure 1.2B). When the voltage on the buffer reservoir is turned back on, the sample plug will move toward the detection area. The two main advantages of gated injection are the ability to vary the size of the dispensed sample and the continuous flow in separation channel.[76] However, there are problems such as sampling bias and difficulty in measuring the precise injection volume. Pinched injection is an improvement over gated injection. A high voltage is applied to the buffer reservoir, and the buffer waste reservoir is grounded, which allows buffer flow through the separation channel. Meanwhile, a pull-back voltage is applied to the sample and

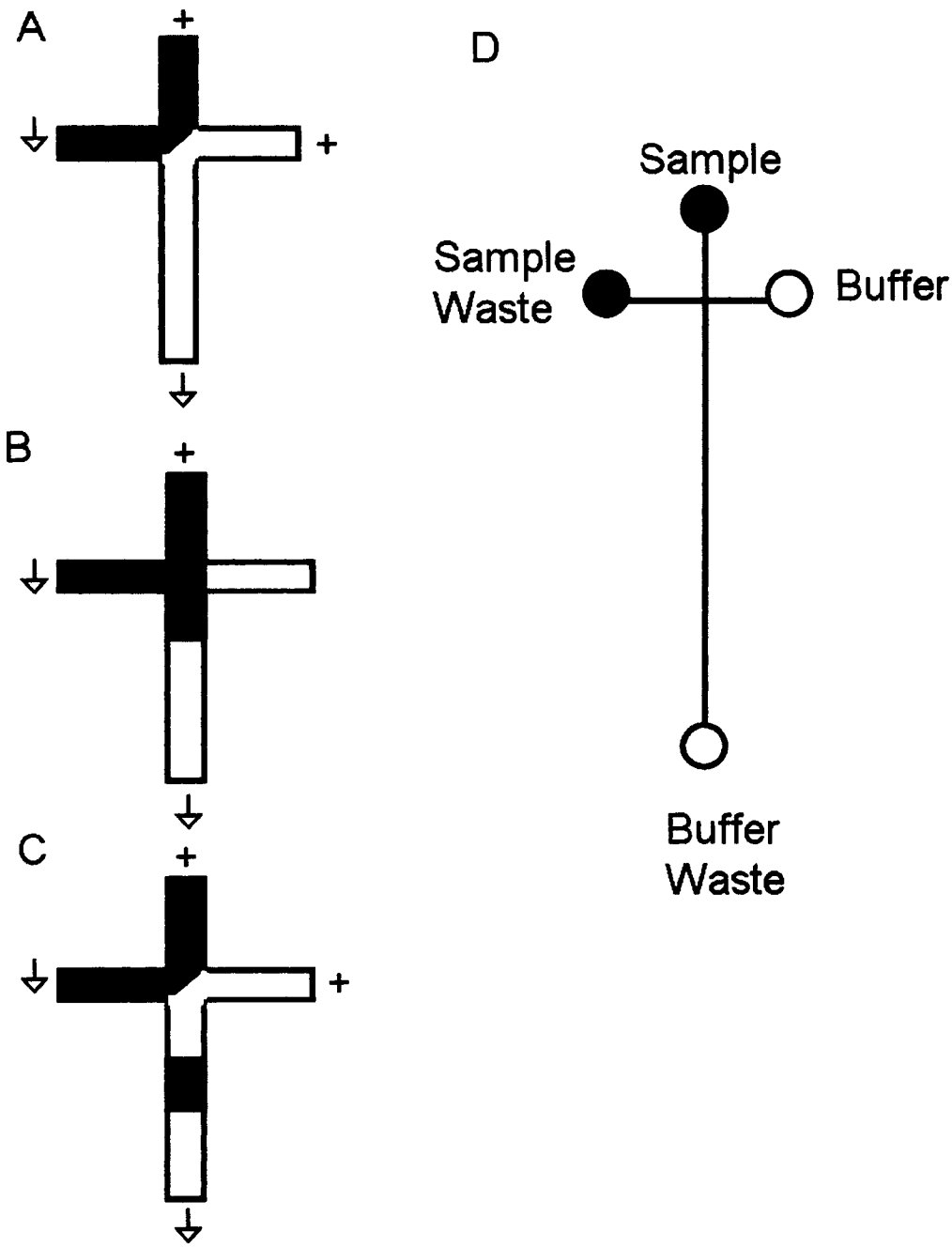

Figure 1.2 Gated injection: A. separation B. sample loading C. sample dispensing D. reservoir assignment

the sample waste reservoir to prevent leakage of sample into the separation channel (Figure 1.3.A). When a negative voltage is applied to the sample waste reservoir with positive potentials on the buffer and the sample reservoir, the flow of sample will pass through the cross section of two channels. When the potential is switched back, a sample plug is dispensed into the separation channel and moves toward the detection area (Figure 1.3.C). A precise control of injection volume can thus be obtained by pinched injection and no electrokinetic sample biasing occurs.

Besides electrokinetic injection, hydrodynamic injection is also employed in microchip CE systems.[77, 78] In separation mode, the voltage settings for hydrodynamic injection are the same as those for gated injection. Samples are loaded into the separation channel either using diffusion of molecules or applying a pressure to sample reservoir of channel after turning off all applied potentials (Figure 1.4).[77, 78] Hydrodynamic injection can effectively decrease sample electrokinetic biasing; however, the absolute amount injected is difficult to control. Hydrostatic injection employs pressure in conjunction with electrokinetic forces.[69, 78] This method avoids the species bias effect and could be used to load any samples. However, it increases the controlling complexity as compared to the complete electrokinetic or hydrodynamic injection.

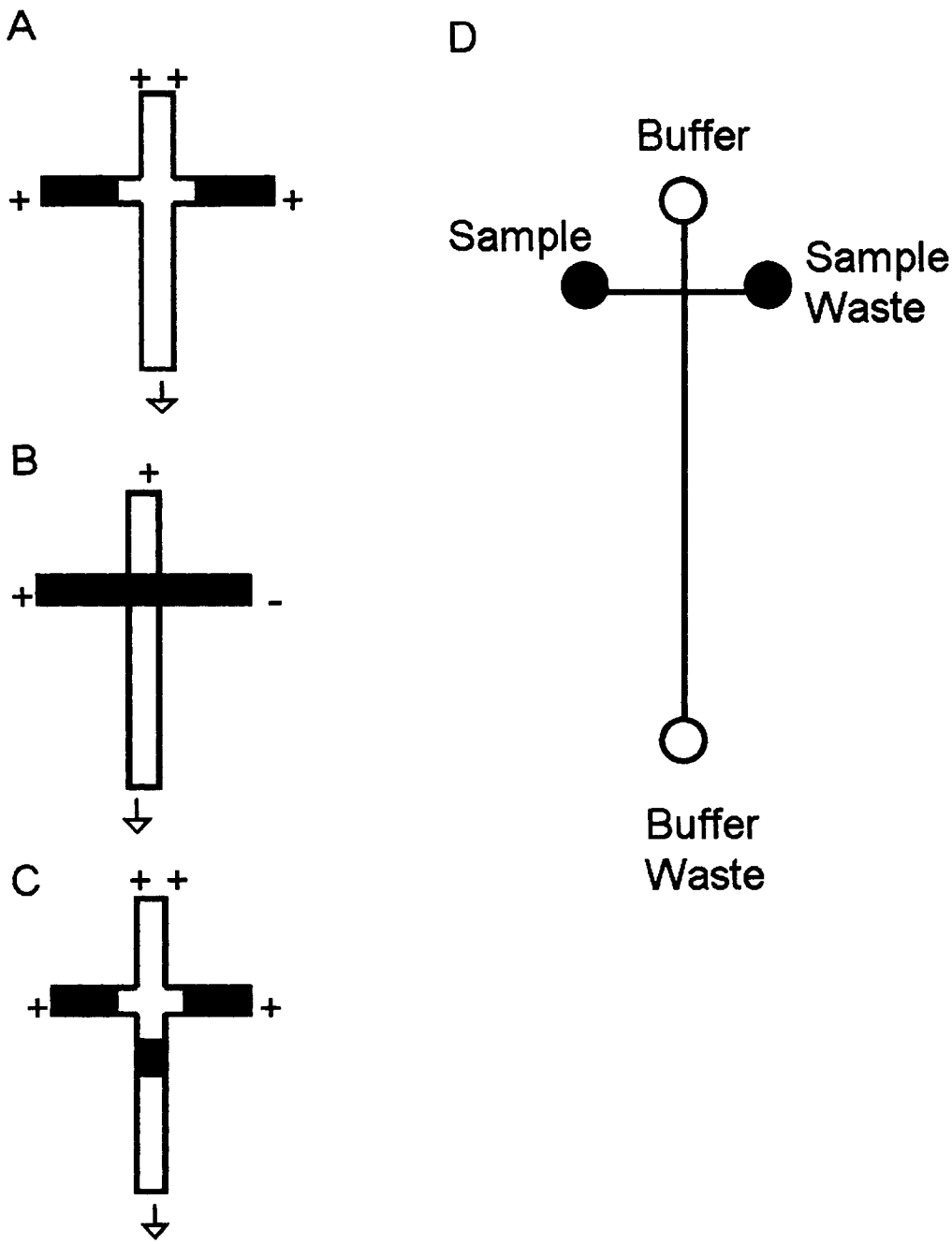

Figure 1.3 Pinched injection: A. separation B. sample loading C. sample dispensing D. reservoir assignment

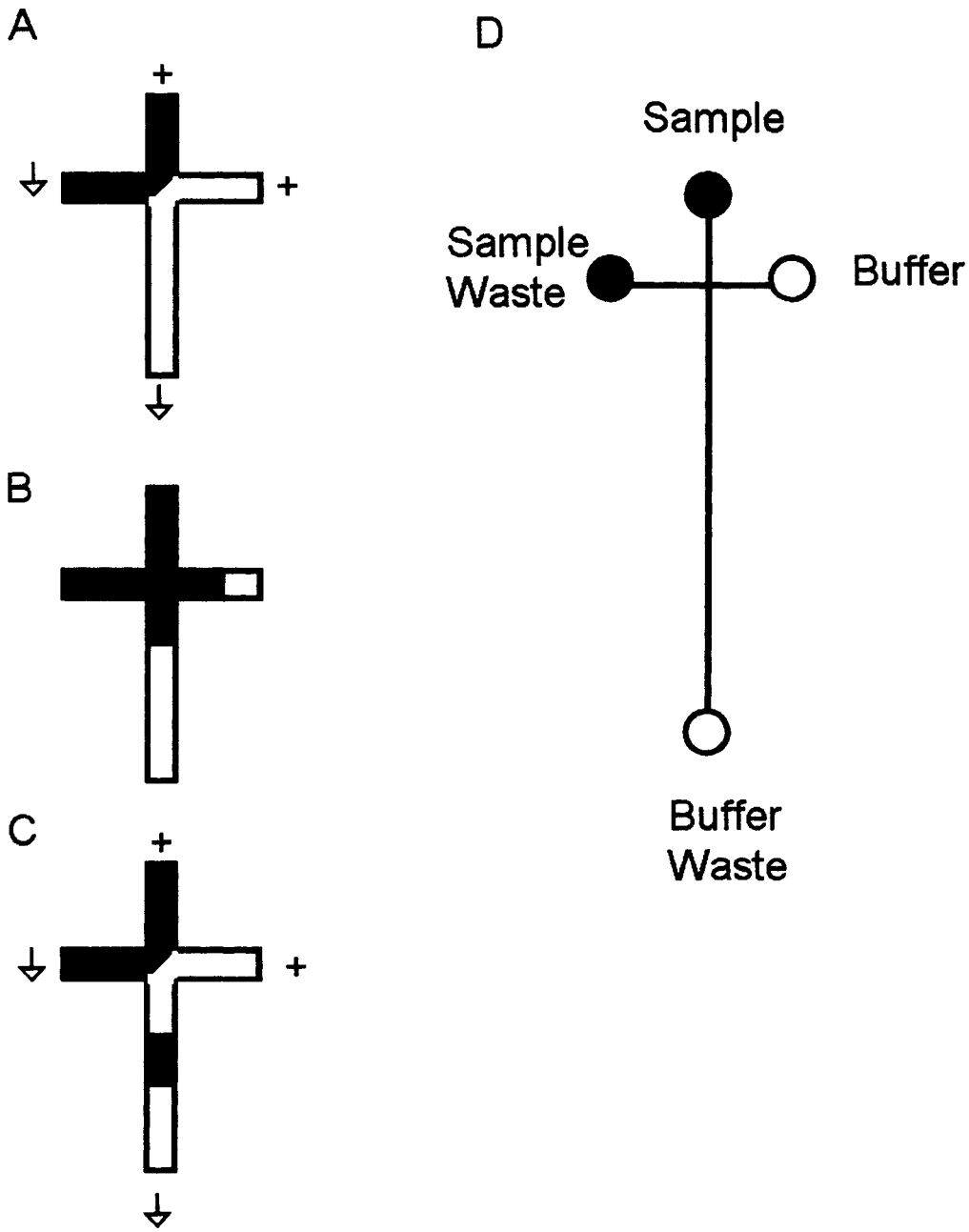

Figure 1.4 Diffusion injection: A. separation B. sample loading C. sample dispensing D. reservoir assignment

1.7 Detection methods

As the field of microfluidic devices continues to grow, there is an urgent need to develop detection modes. So far, many detection modes have been coupled to microchip devices, including UV,[79, 80] LIF,[47, 81] chemiluminescence,[82, 83] MS,[42, 84] electrochemistry,[85, 86] Raman,[87, 88] NMR,[89, 90] thermal lens microscopy,[43, 91] and refractive index methods.[51, 92] Absorbance detectors are commonly used for conventional CE systems. They are classified as selective or solute property detectors because the running buffer is chosen such that it exhibits little or no absorbance at the wavelength of interest.[93] Unfortunately, microchip CE devices generally have very shallow channel depths (10-50 μm). This means a short optical path length is used, which limits the performance of these devices according to Beer's Law. Several methods, including the use of Z-cells and U-shaped channels, or widening of the capillary at the detection point, can improve detection limits by increasing the optical path length.[94] The optical path length problem is still a constraint for the application of absorbance to microchip CE.

The primary mode of detection for microchip CE is laser-induced fluorescence (LIF).[46, 95] LIF is the most sensitive, small volume detection method developed to date,[96-98] with single molecule detection being demonstrated. Off-chip fluorescein detection is typically accomplished through the use of lasers

for excitation of florescent molecules and charge-coupled device (CCD) cameras or photmultiplier tubes (PMT) for the emitted fluorescent light.[99] Fluorescence is expected in molecules that contain multiple conjugated double bonds with a high degree of resonance stability. To detect many nonfluorophore bearing analytes, derivatization of the analytes with an appropriate fluorophore must be accomplished either before or after the separation has taken place.[100-102] This adds time, complexity, and cost to analysis. Moreover, expensive off-chip instrumentation and time-consuming alignment procedures are required.

Though optically based detectors continue to be actively explored for use in microchip CE, other detection methodologies remain to be explored for micro-separation systems. Mass spectrometry (MS) is a powerful tool in analytical chemistry. Not only can it determine the identity of analytes during the separation, but it also provides the structural information of analytes. Integrating MS with microfluidic devices has become a significant effort in recent years.[19, 42, 103, 104] The power of MS for analyte identification at low concentrations greatly complements the power of microfluidic for small volume sample handling and efficient separations. The principle of the MS detection on chip is the same as for conventional CE/MS, which loads samples into the MS using electroosmotic flow. The close match between flow rates required for ESI/MS and flow rates generated by CE chips makes MS a promising alternative for LIF detection. The

integration of the ionization process onto microfluidic devices, however, is challenging owing to the planar nature of microfabricated system. In addition, the coupling of CE/MS increases the cost of analysis due to the expensive MS instrumentation. Moreover, the size of the mass spectrometer constrains the portability of microfluidic devices. As a result, MS is not widely coupled to microchip CE system.

1.8 Electrochemical detection

Electrochemical method (EC) has been demonstrated as an attractive alternative detection approach for microchip CE. Many compounds can be detected without derivatization, and the sensitivity is comparable to that of fluorescence detection. Electrochemical signal from analyte is detected through the use of electrode which is by nature small and compact. Well-established microfabrication techniques provide the potential to fully integrate microelectrodes with microfluidic devices. EC detection on the microchip scale was first reported in 1996 by Mathies' group who constructed a microchip device containing a 10-μm-wide Pt working electrode patterned within 30 μm of the end of the CE channel.[105] Unlike optical detection methods, the analytical performance of EC is less compromised by miniaturization.[106] The associated EC instrumentation for microchip CE is less expensive than that for any other form of

detection – certainly compared to LIF or MS systems.[107] Finally, because of decades of earlier work with EC sensors, there already existed a wide variety of well-characterized electrode/analyte systems available for direct adaptation to microchip CE.[108]

Although four main categories, potentiometry, voltammetry conductivity, and amperometry, have been used for microchip CE-EC, only amperometry and conductivity detection are common.[107, 109, 110] Amperometric detection is based on electron transfer to or from the analyte of interest at an electrode surface.[106] With an applied DC voltage, a redox reaction occurs at the electrode resulting in a current that is directly related to the analyte concentration. Amperometry is the most popular electrochemical approach to quantify the redox reaction of analytes in microchip CE applications due to the high selectivity and sensitivity.[65, 85, 95, 111, 112] The major drawback of amperometric techniques is strong adsorption of the intermediate reaction products to the electrode surface, subsequently reducing the activity (electron transfer) of the electrode and interfering with detection. Conductivity detection (CD) is based on the change in bulk solution conductivity between two electrodes when an analyte band passes through the electrode gap.[113-115] Any molecule can be detected if it causes a change in the conductivity between electrodes.

1.9 Applications

Applications for microchip CE systems can be separated into different categories based on their target analytes and the method of analysis. These categories may include nucleic acids, proteins, cellular assays, small molecules, and environmental applications.

One of the leading applications of microchip CE is the analysis of nucleic acids.[116-118] Early demonstrations of applicability of CE-based DNA on-chip analysis included separations of oligonucleotides (10-25 bases) and sizing of longer DNA fragments (ΦX174 HAE-III digest sizing ladder, 70-1000 bp). Since the first applications of microchip CE to nucleic acid analysis in 1994,[119] integrated systems with DNA sample preparation, fragment separation, and on-chip detection have been reported by several research groups.[22, 120-122] More recently, microfluidic devices are being applied to genotyping experiments for screening of hereditary diseases or for forensic analyses.[123, 124] A significant advantage for applying microchips to DNA analyses is the decreased analysis time which is 10-times faster than conventional CE system. The main technology in DNA amplification is the polymerase chain reaction (PCR). PCR enzymatically amplifies a small amount of initial DNA, which expresses the information of the whole gene. The primary advantage of PCR on chip is the decreased thermal cycling times, which translate to shorter overall reaction times.

Proteins are essential constituents of all organisms. The additional chemical complexity has made their analysis on-chip more difficult than that of DNA. Protein analysis on-chip encompasses a wide range of application and technical developments, including immunoassay, enzyme assay, integration with MS, methods for sampling as well as considerable research on separations of amino acids, peptides and proteins. Since the first demonstration of chip-based CE separations of human serum proteins was presented,[125] there has been an expansion in the reported applications in this field.[126-130] Fully automated protein identification was realized on a microchip platform.[131] A primary advantage of chip-based protein analysis is the high throughput capability provided by microfluidic devices as supported by Bergman research group.[132]

Cells are the basic structural and functional units of living organisms.[133] Therefore, analysis of biochemical constituents and metabolism at cellular level is important for understanding the physiology and pathology of any organism. The similarity of microchannel dimensions to those of biological cells offers advantages over conventional CE systems for observing the cells. Currently, research in this area focuses on integration of cell lysing and target intracellular molecule detection.[126, 134-136] Gao et al. developed a microfluidic system for the analysis of single biological cells, with functional integration of cell sampling, single cell loading, docking, lysing, and CE separation with LIF detection.[75]

Besides detection of intracellular components, microchips can also be used for cell culturing in cellular analysis or cell sorting clinical applications.[134, 136, 137]

In addition to DNA, proteins, and the cellular components, microchip CE systems have also been applied to detection of small molecules relevant to clinical diagnostics. Large number of different compounds can fit in this category, including amines, carbohydrates, metabolites, and therapeutic drugs.[138-142] Fanguy et al. measured uric acid concentration in a true clinical urine sample via a PDMS/glass hybrid microchip system with electrochemical detection in less than 30 s.[143] The values obtained with the microchip were equivalent to a conventional urinase method which took 30 min to complete. Direct measurement of renal markers (creatinine, creatine, and uric acid) in urine was reported by Garcia et al. who used a microchip CE system with pulsed amperometric detection.[144]

Environmental analysis is another application for microchip CE systems.[145] Wakida et al proposed a high throughput analysis method to detect dissolved organic carbons at low level concentration. Samples from Lake Biwa, Japan were analyzed within 2 mins by using microchip-based capillary electrophoresis (CE) with LIF detection.[146] Besides dissolved organic carbons, analyses of atmospheric SO_2,[147] inorganic metal ions,[148-152] low-explosive ionic

components,[153, 154] chemical warfare agent,[155] and trinitroaromatic explosives[156, 157] have all been reported using microchip-based analytical systems.

In this dissertation, effort was to develop a microchip CE-EC system to study biological and environmental samples. The miniaturized CE system was first demonstrated on PDMS/glass hybrid chip. To produce a functional microchip, fabrication of mold and microchannels were required. Detailed information about microfabrication is described in chapter II. This PDMS/glass chip was successfully employed to determine the urinary p-aminophenol in spiked urine. A few problems that were common for PDMS/glass chip with microfabricated Au thin-film electrode were encountered in the electrochemical detection of p-aminophenol. The first problem was the size and weight of power supply for microchip CE system. To accomplish fully miniaturized system, the power supply needed to be portable too. The second concern was the flow in channel. The walls of the channel consisted of two different materials, PDMS and glass. The different surface chemistry of PDMS and glass leaded to different surface charge density. Non-uniform flow in channel was thus generated, which affected separation efficiency. The third problem was the costly fabrication of working electrode which required the clean room facility. Once the working electrode fouled, a new one needed to be fabricated which increased time and cost. In this

dissertation, improvements were made to overcome these drawbacks. The construction of a compact and portable power supply was accomplished employing DC-DC converters and other electronic elements. The constructed power supply was able to provide 0 - 4 kV output which could meet the requirement of microchip CE system. Following this, the improvement of working electrode design was accomplished. A new microwire working electrode design proved to be more sensitive and flexible than the microfabricated electrode. The developed portable and sensitive microchip CE-EC system was applied to analyze aerosols and profile antioxidants. Finally, the whole project is summarized in Chapter VIII.

1.10 References

(1) Weston, A.; Brown, P. R. *HPLC and CE Principles and Practices*; Academic Press: San Diego, 1997.
(2) Jorgenson, J. W.; Lukacs, K. D. *Clin Chem* **1981**, *27*, 1551-1553.
(3) Voegel, P. D.; Baldwin, R. P. *Electrophoresis* **1997**, *18*, 2267-2278.
(4) Jorgenson, J. W.; Lukacs, K. D. *Science* **1983**, *222*, 266-272.
(5) Figeys, D.; Pinto, D. *Anal Chem* **2000**, *72*, 330A-335A.
(6) Ewing, A. G.; Wallingford, R. A.; Olefirowicz, T. M. *Analytical Chemistry* **1989**, *61*, 292A-294A, 296A, 298A, 300A-303A.
(7) Wallingford, R. A.; Ewing, A. G. *Advances in Chromatography (New York, NY, United States)* **1989**, *29*, 1-76.
(8) Lunte, S. M.; O'Shea, T. J. *Electrophoresis* **1994**, *15*, 79-86.
(9) Holland, L. A.; Chetwyn, N. P.; Perkins, M. D.; Lunte, S. M. *Pharmaceutical Research* **1997**, *14*, 372-387.
(10) Lunte, S. M.; Martin, R. S.; Lunte, C. E. *Electroanalytical Methods for Biological Materials* **2002**, 461-490.
(11) Shihabi, Z. K. *Ann Clin Lab Sci* **1992**, *22*, 398-405.

(12) von Heeren, F.; Thormann, W. *Electrophoresis* **1997**, *18*, 2415-2426.
(13) Jenkins, M. A.; Guerin, M. D. *J Chromatogr B Biomed Appl* **1996**, *682*, 23-34.
(14) Mitchelson, K. R.; Cheng, J.; Kricka, L. J. *Trends Biotechnol* **1997**, *15*, 448-458.
(15) Schmalzing, D.; Buonocore, S.; Piggee, C. *Electrophoresis* **2000**, *21*, 3919-3930.
(16) Jacobson, S. C.; Hergenroder, R.; Koutny, L. B.; Ramsey, J. M. *Anal Chem* **1994**, *66*, 1114-1118.
(17) Moore, A. W., Jr.; Jacobson, S. C.; Ramsey, J. M. *Analytical Chemistry* **1995**, *67*, 4184-4189.
(18) Parinov, S.; Barsky, V.; Yershov, G.; Kirillov, E.; Timofeev, E.; Belgovskiy, A.; Mirzabekov, A. *Nucleic Acids Res* **1996**, *24*, 2998-3004.
(19) Ramsey, R. S.; Ramsey, J. M. *Anal Chem* **1997**, *69*, 1174-1178.
(20) Service, R. F. *Science* **1998**, *282*, 396-399.
(21) Soper, S. A.; Ford, S. M.; Xu, Y.; Qi, S.; McWhorter, S.; Lassiter, S.; Patterson, D.; Bruch, R. C. *J Chromatogr A* **1999**, *853*, 107-120.
(22) Stomakhin, A. A.; Vasiliskov, V. A.; Timofeev, E.; Schulga, D.; Cotter, R. J.; Mirzabekov, A. D. *Nucleic Acids Res* **2000**, *28*, 1193-1198.
(23) Sung, W. C.; Lee, G. B.; Tzeng, C. C.; Chen, S. H. *Electrophoresis* **2001**, *22*, 1188-1193.
(24) Wang, J.; Ibanez, A.; Chatrathi, M. P. *Electrophoresis* **2002**, *23*, 3744-3749.
(25) Yan, J.; Du, Y.; Liu, J.; Cao, W.; Sun, X.; Zhou, W.; Yang, X.; Wang, E. *Analytical Chemistry* **2003**, *75*, 5406-5412.
(26) Xu, J.-J.; Bao, N.; Xia, X.-H.; Peng, Y.; Chen, H.-Y. *Analytical Chemistry* **2004**, *76*, 6902-6907.
(27) Kelly, R. T.; Pan, T.; Woolley, A. T. *Analytical Chemistry* **2005**, *77*, 3536-3541.
(28) Harrison, D. J.; Manz, A.; Fan, Z.; Luedi, H.; Widmer, H. M. *Analytical Chemistry* **1992**, *64*, 1926-1932.
(29) Harrison, D. J.; Glavina, P. G.; Manz, A. *Sensors and Actuators, B: Chemical* **1993**, *B10*, 107-116.
(30) Manz, A.; Graber, N.; Widmer, H. M. *Sensors and Actuators, B: Chemical* **1990**, *B1*, 244-248.
(31) Manz, A.; Harrison, D. J.; Verpoorte, E. M. J.; Fettinger, J. C.; Luedi, H.; Widmer, H. M. *Chimia* **1991**, *45*, 103-105.
(32) Manz, A.; Harrison, D. J.; Verpoorte, E. M. J.; Fettinger, J. C.; Paulus, A.; Luedi, H.; Widmer, H. M. *J Chromatogr* **1992**, *593*, 253-258.
(33) Manz, A.; Miyahara, Y.; Miura, J.; Watanabe, Y.; Miyagi, H.; Sato, K.

Sensors and Actuators, B: Chemical **1990**, *B1*, 249-255.
(34) Manz, A.; Fettinger, J. C.; Verpoorte, E.; Luedi, H.; Widmer, H. M.; Harrison, D. J. *TrAC, Trends in Analytical Chemistry* **1991**, *10*, 144-149.
(35) Manz, A. *Biochemical Society Transactions* **1997**, *25*, 278-281.
(36) Jacobson, S. C.; Culbertson, C. T.; Daler, J. E.; Ramsey, J. M. *Analytical Chemistry* **1998**, *70*, 3476-3480.
(37) Chiem, N.; Harrison, D. J. *Anal Chem* **1997**, *69*, 373-378.
(38) Effenhauser, C. S.; Manz, A. *American Laboratory (Shelton, CT, United States)* **1994**, *26*, 15-16, 18.
(39) Effenhauser, C. S. *Topics in Current Chemistry* **1998**, *194*, 51-82.
(40) Lai, C. C.; Chen, C. H.; Ko, F. H. *J Chromatogr A* **2004**, *1023*, 143-150.
(41) Horng, R.-H.; Han, P.; Chen, H.-Y.; Lin, K.-W.; Tsai, T.-M.; Zen, J.-M. *Journal of Micromechanics and Microengineering* **2005**, *15*, 6-10.
(42) Dahlin, A. P.; Wetterhall, M.; Liljegren, G.; Bergstrom, S. K.; Andren, P.; Nyholm, L.; Markides, K. E.; Bergquist, J. *Analyst* **2005**, *130*, 193-199.
(43) Uchiyama, K.; Tokeshi, M.; Kikutani, Y.; Hattori, A.; Kitamori, T. *Analytical Sciences* **2005**, *21*, 49-52.
(44) Tabuchi, M.; Baba, Y. *Electrophoresis* **2005**, *26*, 376-382.
(45) Stettler, A. R.; Schwarz, M. A. *Journal of Chromatography, A* **2005**, *1063*, 217-225.
(46) Shintani, T.; Torimura, M.; Sato, H.; Tao, H.; Manabe, T. *Analytical Sciences* **2005**, *21*, 57-60.
(47) Qin, J.; Leung, F. C.; Fung, Y.; Zhu, D.; Lin, B. *Anal Bioanal Chem* **2005**, *381*, 812-819.
(48) Nagata, H.; Tabuchi, M.; Hirano, K.; Baba, Y. *Electrophoresis* **2005**.
(49) Becker, H.; Locascio, L. *Talanta* **2002**, *56*, 267-287.
(50) Wang, H. Y.; Foote, R. S.; Jacobson, S. C.; Schneibel, J. H.; Ramsey, J. M. *Sensors and Actuators, B: Chemical* **1997**, *B45*, 199-207.
(51) Burggraf, N.; Krattiger, B.; de Rooij, N. F.; Manz, A.; de Mello, A. J. *Analyst* **1998**, *123*, 1443-1447.
(52) Ocvirk, G.; Tang, T.; Jed Harrison, D. *Analyst* **1998**, *123*, 1429-1434.
(53) Kricka, L. J.; Faro, I.; Heyner, S.; Garside, W. T.; Fitzpatrick, G.; McKinnon, G.; Ho, J.; Wilding, P. *J Pharm Biomed Anal* **1997**, *15*, 1443-1447.
(54) Uchiyama, K.; Xu, W.; Qiu, J.; Hobo, T. *Fresenius J Anal Chem* **2001**, *371*, 209-211.
(55) Rossier, J. S.; Schwarz, A.; Reymond, F.; Ferrigno, R.; Bianchi, F.; Girault, H. H. *Electrophoresis* **1999**, *20*, 727-731.
(56) Chen, J.; Wabuyele, M.; Chen, H.; Patterson, D.; Hupert, M.; Shadpour, H.; Nikitopoulos, D.; Soper, S. A. *Anal Chem* **2005**, *77*, 658-666.
(57) Beddows, D. C.; Donovan, R. J.; Harrison, R. M.; Heal, M. R.; Kinnersley,

R. P.; King, M. D.; Nicholson, D. H.; Thompson, K. C. *J Environ Monit* **2004**, *6*, 124-133.
(58) Wang, J.; Pumera, M.; Chatrathi, M. P.; Escarpa, A.; Konrad, R.; Griebel, A.; Dorner, W.; Lowe, H. *Electrophoresis* **2002**, *23*, 596-601.
(59) Sato, K.; Tokeshi, M.; Odake, T.; Kimura, H.; Ooi, T.; Nakao, M.; Kitamori, T. *Anal Chem* **2000**, *72*, 1144-1147.
(60) Sato, K.; Tokeshi, M.; Kimura, H.; Kitamori, T. *Anal Chem* **2001**, *73*, 1213-1218.
(61) Wang, J.; Pumera, M.; Chatrathi, M. P.; Rodriguez, A.; Spillman, S.; Martin, R. S.; Lunte, S. M. *Electroanalysis* **2002**, *14*, 1251-1255.
(62) Ro, K. W.; Lim, K.; Kim, H.; Hahn, J. H. *Electrophoresis* **2002**, *23*, 1129-1137.
(63) Effenhauser, C. S.; Bruin, G. J.; Paulus, A. *Electrophoresis* **1997**, *18*, 2203-2213.
(64) Ocvirk, G.; Munroe, M.; Tang, T.; Oleschuk, R.; Westra, K.; Harrison, D. J. *Electrophoresis* **2000**, *21*, 107-115.
(65) Wu, C. C.; Wu, R. G.; Huang, J. G.; Lin, Y. C.; Hsien-Chang, C. *Anal Chem* **2003**, *75*, 947-952.
(66) Badal, M. Y.; Wong, M.; Chiem, N.; Salimi-Moosavi, H.; Harrison, D. J. *J Chromatogr A* **2002**, *947*, 277-286.
(67) Erickson, D.; Sinton, D.; Li, D. *Lab Chip* **2003**, *3*, 141-149.
(68) Jin, L. J.; Ferrance, J.; Sanders, J. C.; Landers, J. P. *Lab on a Chip* **2003**, *3*, 11-18.
(69) Gai, H.; Yu, L.; Dai, Z.; Ma, Y.; Lin, B. *Electrophoresis* **2004**, *25*, 1888-1894.
(70) Tsai, C.-H.; Yang, R.-J.; Tai, C.-H.; Fu, L.-M. *Electrophoresis* **2005**, *26*, 674-686.
(71) Lin, Y. H.; Lee, G. B.; Li, C. W.; Huang, G. R.; Chen, S. H. *J Chromatogr A* **2001**, *937*, 115-125.
(72) Jacobson, S. C.; Hergenroder, R.; Moore, A. W., Jr.; Ramsey, J. M. *Anal Chem* **1994**, *66*, 4127-4132.
(73) Slentz, B. E.; Penner, N. A.; Regnier, F. *Anal Chem* **2002**, *74*, 4835-4840.
(74) Alarie, J. P.; Jacobson, S. C.; Ramsey, J. M. *Electrophoresis* **2001**, *22*, 312-317.
(75) Gao, J.; Yin, X. F.; Fang, Z. L. *Lab Chip* **2004**, *4*, 47-52.
(76) Sinton, D.; Ren, L.; Li, D. *J Colloid Interface Sci* **2003**, *266*, 448-456.
(77) Bai, X.; Josserand, J.; Jensen, H.; Rossier, J. S.; Girault, H. H. *Anal Chem* **2002**, *74*, 6205-6215.
(78) Solignac, D.; Gijs, M. A. M. *Analytical Chemistry* **2003**, *75*, 1652-1657.
(79) Xu, F.; Jabasini, M.; Zhu, B.; Ying, L.; Cui, X.; Arai, A.; Baba, Y. *Journal of*

Chromatography, A **2004**, *1051*, 147-153.
(80) Nakanishi, H.; Nishimoto, T.; Arai, A.; Abe, H.; Kanai, M.; Fujiyama, Y.; Yoshida, T. *Electrophoresis* **2001**, *22*, 230-234.
(81) Wang, Z.; El-Ali, J.; Engelund, M.; Gotsaed, T.; Perch-Nielsen, I. R.; Mogensen, K. B.; Snakenborg, D.; Kutter, J. P.; Wolff, A. *Lab Chip* **2004**, *4*, 372-377.
(82) Tsukagoshi, K. *Science and Engineering Review of Doshisha University* **2005**, *45*, 168-186.
(83) Qiu, H.; Yin, X.-B.; Yan, J.; Zhao, X.; Yang, X.; Wang, E. *Electrophoresis* **2005**, *26*, 687-693.
(84) Tachibana, Y.; Otsuka, K.; Terabe, S.; Arai, A.; Suzuki, K.; Nakamura, S. *J Chromatogr A* **2004**, *1025*, 287-296.
(85) Kovarik, M. L.; Li, M. W.; Martin, R. S. *Electrophoresis* **2005**, *26*, 202-210.
(86) Hwang, S.; Kim, E.; Kwak, J. *Analytical Chemistry* **2005**, *77*, 579-584.
(87) Walker, P. A., 3rd; Morris, M. D.; Burns, M. A.; Johnson, B. N. *Anal Chem* **1998**, *70*, 3766-3769.
(88) Pan, D.; Mathies, R. A. *Biochemistry* **2001**, *40*, 7929-7936.
(89) O'Neill, A. P.; O'Brien, P.; Alderman, J.; Hoffman, D.; McEnery, M.; Murrihy, J.; Glennon, J. D. *J Chromatogr A* **2001**, *924*, 259-263.
(90) Hafner, S.; Kuhn, W. *Magn Reson Imaging* **1994**, *12*, 1075-1078.
(91) Sato, K.; Yamanaka, M.; Hagino, T.; Tokeshi, M.; Kimura, H.; Kitamori, T. *Lab Chip* **2004**, *4*, 570-575.
(92) Jakeway, S. C.; De Mello, A. J. *Micro Total Analysis Systems 2001, Proceedings mTAS 2001 Symposium, 5th, Monterey, CA, United States, Oct. 21-25, 2001* **2001**, 347-348.
(93) Hu, T.; Zuo, H.; Riley, C. M.; Stobaugh, J. F.; Lunte, S. M. *Journal of Chromatography, A* **1995**, *716*, 381-388.
(94) Liang, Z.; Chiem, N.; Ocvirk, G.; Tang, T.; Fluri, K.; Harrison, D. J. *Anal Chem* **1996**, *68*, 1040-1046.
(95) Martin, R. S.; Gawron, A. J.; Lunte, S. M. *Anal Chem* **2000**, *72*, 3196-3202.
(96) Bullard, K. M.; Hietpas, P. B.; Ewing, A. G. *Biomedical Microdevices* **1998**, *1*, 27-37.
(97) Guetens, G.; Van Cauwenberghe, K.; De Boeck, G.; Maes, R.; Tjaden, U. R.; van der Greef, J.; Highley, M.; van Oosterom, A. T.; de Bruijn, E. A. *J Chromatogr B Biomed Sci Appl* **2000**, *739*, 139-150.
(98) Jacobson, S. C.; Koutny, L. B.; Hergenroeder, R.; Moore, A. W., Jr.; Ramsey, J. M. *Anal Chem* **1994**, *66*, 3472-3476.
(99) Fiorini, G. S.; Chiu, D. T. *Biotechniques* **2005**, *38*, 429-446.
(100) Jiang, G.; Attiya, S.; Ocvirk, G.; Lee, W. E.; Harrison, D. J. *Biosens Bioelectron* **2000**, *14*, 861-869.

(101) Lee, T. M.-H.; Carles, M. C.; Hsing, I. M. *Lab on a Chip* **2003**, *3*, 100-105.
(102) Lou, X. J.; Panaro, N. J.; Wilding, P.; Fortina, P.; Kricka, L. J. *Biotechniques* **2004**, *36*, 248-252.
(103) Song, Q. J.; Greenway, G. M.; McCreedy, T. *Journal of Analytical Atomic Spectrometry* **2003**, *18*, 1-3.
(104) Xue, Q.; Foret, F.; Dunayevskiy, Y. M.; Zavracky, P. M.; McGruer, N. E.; Karger, B. L. *Anal Chem* **1997**, *69*, 426-430.
(105) Woolley, A. T.; Hadley, D.; Landre, P.; deMello, A. J.; Mathies, R. A.; Northrup, M. A. *Analytical Chemistry* **1996**, *68*, 4081-4086.
(106) Lambrechets, M.; Sansen, W. *Biosensors: Microelectrochemical Devices*; Institute of Physical Publishing: Bristol, 1992.
(107) Lacher, N. A.; Garrison, K. E.; Martin, R. S.; Lunte, S. M. *Electrophoresis* **2001**, *22*, 2526-2536.
(108) Lapos, J. A.; Manica, D. P.; Ewing, A. G. *Anal Chem* **2002**, *74*, 3348-3353.
(109) Vandaveer, W. R. I. V.; Pasas-Farmer, S. A.; Fischer, D. J.; Frankenfeld, C. N.; Lunte, S. M. *Electrophoresis* **2004**, *25*, 3528-3549.
(110) Vandaveer, W. R. I. V.; Pasas, S. A.; Martin, R. S.; Lunte, S. M. *Electrophoresis* **2002**, *23*, 3667-3677.
(111) Einaga, Y.; Sato, R.; Olivia, H.; Shin, D.; Ivandini, T. A.; Fujishima, A. *Electrochimica Acta* **2004**, *49*, 3989-3995.
(112) Rossier, J.; Reymond, F.; Michel, P. E. *Electrophoresis* **2002**, *23*, 858-867.
(113) Galloway, M.; Stryjewski, W.; Henry, A.; Ford, S. M.; Llopis, S.; McCarley, R. L.; Soper, S. A. *Anal Chem* **2002**, *74*, 2407-2415.
(114) Wang, J.; Pumera, M. *Analytical Chemistry* **2003**, *75*, 341-345.
(115) Liu, Y.; Wipf, D. O.; Henry, C. S. *Analyst* **2001**, *126*, 1248-1251.
(116) Chung, Y. C.; Lin, Y. C.; Shiu, M. Z.; Chang, W. N. *Lab Chip* **2004**, *3*, 228-233.
(117) Micke, P.; Bjornsen, T.; Scheidl, S.; Stromberg, S.; Demoulin, J. B.; Ponten, F.; Ostman, A.; Lindahl, P.; Busch, C. *J Pathol* **2004**, *202*, 130-138.
(118) Guschin, D.; Yershov, G.; Zaslavsky, A.; Gemmell, A.; Shick, V.; Proudnikov, D.; Arenkov, P.; Mirzabekov, A. *Anal Biochem* **1997**, *250*, 203-211.
(119) Eggers, M.; Hogan, M.; Reich, R. K.; Lamture, J.; Ehrlich, D.; Hollis, M.; Kosicki, B.; Powdrill, T.; Beattie, K.; Smith, S.; et al. *Biotechniques* **1994**, *17*, 516-525.
(120) Yuen, P. K.; Kricka, L. J.; Fortina, P.; Panaro, N. J.; Sakazume, T.; Wilding, P. *Genome Res* **2001**, *11*, 405-412.
(121) Tillib, S. V.; Mirzabekov, A. D. *Curr Opin Biotechnol* **2001**, *12*, 53-58.
(122) Cheng, J.; Fortina, P.; Surrey, S.; Kricka, L. J.; Wilding, P. *Mol Diagn* **1996**,

1, 183-200.
(123) Footz, T.; Somerville, M. J.; Tomaszewski, R.; Elyas, B.; Backhouse, C. J. *Analyst* **2004**, *129*, 25-31.
(124) Ertl, P.; Emrich, C. A.; Singhal, P.; Mathies, R. A. *Anal Chem* **2004**, *76*, 3749-3755.
(125) Colyer, C. L.; Tang, T.; Chiem, N.; Harrison, D. J. *Electrophoresis* **1997**, *18*, 1733-1741.
(126) Chang, H.-T.; Huang, Y.-F.; Chiou, S.-H.; Chiu, T.-C.; Hsieh, M.-M. *Current Proteomics* **2004**, *1*, 325-347.
(127) Wang, J.; Chen, G.; Pumera, M. *Electroanalysis* **2003**, *15*, 862-865.
(128) Youssouf Badal, M.; Wong, M.; Chiem, N.; Salimi-Moosavi, H.; Harrison, D. J. *Journal of Chromatography, A* **2002**, *947*, 277-286.
(129) Rubina, A.; Pan'kov, S. V.; Ivanov, S. M.; Dement'eva, E. I.; Mirzabekov, A. D. *Dokl Biochem Biophys* **2001**, *381*, 419-422.
(130) Arenkov, P.; Kukhtin, A.; Gemmell, A.; Voloshchuk, S.; Chupeeva, V.; Mirzabekov, A. *Anal Biochem* **2000**, *278*, 123-131.
(131) Laurell, T.; Nilsson, J.; Marko-Varga, G. *J Chromatogr B Biomed Sci Appl* **2001**, *752*, 217-232.
(132) Gustafsson, M.; Hirschberg, D.; Palmberg, C.; Jornvall, H.; Bergman, T. *Anal Chem* **2004**, *76*, 345-350.
(133) Irimia, D.; Tompkins, R. G.; Toner, M. *Anal Chem* **2004**, *76*, 6137-6143.
(134) Tamaki, E.; Sato, K.; Tokeshi, M.; Aihara, M.; Kitamori, T. *Anal Chem* **2002**, *74*, 1560-1564.
(135) Wheeler, A. R.; Throndset, W. R.; Whelan, R. J.; Leach, A. M.; Zare, R. N.; Liao, Y. H.; Farrell, K.; Manger, I. D.; Daridon, A. *Anal Chem* **2003**, *75*, 3581-3586.
(136) Huang, W. H.; Cheng, W.; Zhang, Z.; Pang, D. W.; Wang, Z. L.; Cheng, J. K.; Cui, D. F. *Anal Chem* **2004**, *76*, 483-488.
(137) Cho, B. S.; Schuster, T. G.; Zhu, X.; Chang, D.; Smith, G. D.; Takayama, S. *Analytical Chemistry* **2003**, *75*, 1671-1675.
(138) Sato, K.; Hibara, A.; Tokeshi, M.; Hisamoto, H.; Kitamori, T. *Adv Drug Deliv Rev* **2003**, *55*, 379-391.
(139) Tao, S. L.; Desai, T. A. *Adv Drug Deliv Rev* **2003**, *55*, 315-328.
(140) Wang, J.; Chatrathi, M. P. *Anal Chem* **2003**, *75*, 525-529.
(141) Du, Y.; Yan, J.; Zhou, W.; Yang, X.; Wang, E. *Electrophoresis* **2004**, *25*, 3853-3859.
(142) Lee, H.-L.; Chen, S.-C. *Talanta* **2004**, *64*, 210-216.
(143) Fanguy, J. C.; Henry, C. S. *Electrophoresis* **2002**, *23*, 767-773.
(144) Garcia, C. D.; Henry, C. S. *Analyst (Cambridge, United Kingdom)* **2004**, *129*, 579-584.

(145) Vilkner, T.; Janasek, D.; Manz, A. *Anal Chem* **2004**, *76*, 3373-3385.
(146) Wakida, S.; Shen, S.; Kurosawa, S.; Fukushi, K.; Takeda, S. *Chemical Sensors* **2004**, *20*, 102-103.
(147) Ohira, S.; Toda, K.; Ikebe, S.; Dasgupta, P. K. *Anal Chem* **2002**, *74*, 5890-5896.
(148) Prest, J. E.; Baldock, S. J.; Fielden, P. R.; Goddard, N. J.; Kalimeri, K.; Brown, B. J.; Zgraggen, M. *J Chromatogr A* **2004**, *1047*, 289-298.
(149) Prest, J. E.; Baldock, S. J.; Fielden, P. R.; Goddard, N. J.; Brown, B. J. *Analyst* **2003**, *128*, 1131-1136.
(150) Prest, J. E.; Baldock, S. J.; Fielden, P. R.; Goddard, N. J.; Treves Brown, B. J. *Anal Bioanal Chem* **2003**, *376*, 78-84.
(151) Prest, J. E.; Baldock, S. J.; Fielden, P. R.; Goddard, N. J.; Treves Brown, B. J. *J Chromatogr A* **2003**, *990*, 325-334.
(152) Rech, I.; Restelli, A.; Cova, S.; Ghioni, M.; Chiari, M.; Cretich, M. *Sensors and Actuators, B: Chemical* **2004**, *B100*, 158-162.
(153) Wallenborg, S. R.; Bailey, C. G. *Anal Chem* **2000**, *72*, 1872-1878.
(154) Bromberg, A.; Mathies, R. A. *Electrophoresis* **2004**, *25*, 1895-1900.
(155) Wang, J.; Polsky, R.; Tian, B.; Chatrathi, M. P. *Anal Chem* **2000**, *72*, 5285-5289.
(156) Chen, G.; Wang, J. *Analyst (Cambridge, United Kingdom)* **2004**, *129*, 507-511.
(157) Hilmi, A.; Luong, J. H. *Anal Chem* **2000**, *72*, 4677-4682.

CHAPTER II

FABRICATION OF PDMS MICROCHIPS

Fabrication procedures for electrophoresis microchips are quite different for different substrate materials.[1-7] In general, microchannels are fabricated first followed by bonding this piece to a second piece of substrate to create a closed network of microchannels and reservoirs. For glass or quartz microchips, channels are made by using standard photolithographic and etching technologies originating from the microelectronic industry.[7-9] Various bonding methods, such as anodic bonding, silicon fusion bonding, and thermal bonding, have been developed.[10] The thermal bonding method is used often in quartz and glass chips, although channel deformation is possible due to the high temperature required.[10] Anodic bonding uses electrostatic attraction to attach a glass substrate to a silicon substrate and forms covalent bonds between the two substrates.[10] Compared with thermal bonding, anodic bonding has the advantage of using a lower temperature with lower residual stress and less stringent requirements for the surface quality of the substrates. The use of anodic boding is limited, however, because it is applicable only to glass and silicon substrates.[11]

Methods for polymeric microchip fabrication include photoablation[12] and molding,[13, 14] depending on the chip material. Photoablation involves absorption of a short wavelength laser pulse by the substrate to break

covalent bonds and eject them from the surface. Microchannels are patterned by controlling the position of the laser or using a mask with subsequent generation of channels in various geometries. The resulting structures are generally characterized as having little thermal damage, straight vertical walls, and well-defined depth. However, the process requires a high energy laser source. The formation of microchannels using molding methods generally involves two primary steps: (i) fabrication of a master mold, and (ii) channel pattern transferring. Replication of the mold to produce patterned microchips can be accomplished by injection molding,[13, 14] embossing,[6, 15, 16] or casting.[17-19] Injection molding involves injecting melted polymer against the mold in the molding chamber, allowing very high throughput production at low cost. Embossing involves heating the embossing tool and polymer substrate separately under vacuum to a temperature just above the glass transition temperature of the polymer materials. Embossing methods are useful in rapid prototyping of devices. Both methods require a high temperature working environment, which increases the fabrication cost. Casting involves pouring polymer materials on the top of the mold and curing at atmospheric pressure and an elevated temperature. Casting is the simplest of these three molding processes, but typically requires more time.

In this chapter, the procedures for making a complete PDMS microchip are described since this type of chip was used throughout my dissertation. The

process involves the mold fabrication, channel pattern transferring, electrode alignment, and chip sealing.

2.1 Fabrication of master mold

A 3-in. silicon wafer was cleaned and oxidized with piranha solution (2:1 H_2SO_4:H_2O_2) for 15 mins. The wafer could also be cleaned with 24% HF solution (Aldrich, St. Louis, MO). After sequentially rinsing with deionized water and iso-propanol (Fisher, Fair Lawn, NJ), the wafer was dried under a stream of nitrogen. The wafer was then coated with SU-8 50 negative photoresist (Microchem, Newton, MA) using a spin coater (Laurell Technologies, North Wales, PA) operating at 2200 rpm for 30 seconds. A digitally produced mask containing the channel pattern was placed on the coated wafer and the sandwich was exposed to light via a near-UV flood source (Intell-Ray 400, Unitron, Dallas, TX) for 5 seconds. The wafer was then developed in XP SU-8 developer (Aldrich, St. Louis, MO) for 15 minutes during which the unexposed photoresist was removed, leaving a positive relief of the intended channel pattern as seen in Figure 2.1. The dimensions of the positive pattern, which are equal to channel dimensions created in the PDMS, were measured with a profilometer. The size of the microchannels normally varied from 80-120 μm wide and 40-50 μm deep. Detailed information of channel size is listed in the following individual chapter.

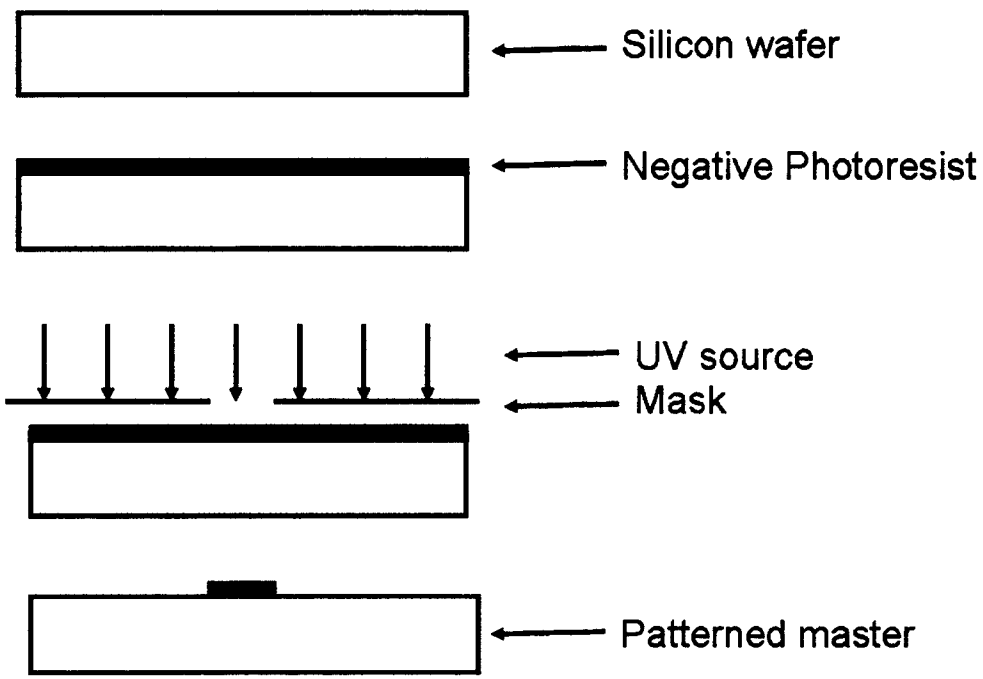

Figure 2.1 Fabrication of master mold

2.2 Fabrication of PDMS piece with microchannels

PDMS piece was patterned using casting method (Figure 2.2). A patterned silicon wafer or mold from above section was cleaned with methanol and dried in the oven. A degassed mixture of 10:1 ratio of PDMS (Sylgard 184 silicon elastomer, Dow Corning, Midland, MI) and its curing agent was poured on the master mold and set in the oven at 65 °C for 2 hrs. The PDMS replica was then peeled off the mold resulting in a pattern of negative relief channels, shown as a picture taken by SEM (Figure 2.3). The channel shown in Figure 2.3 is 120 μm wide and 40 μm deep. Holes were made by a circular punch for use as reservoirs and the PDMS piece was trimmed to size with a razor blade. Sometimes, the patterned wafer was coated with (tridecafluoro-1,1,2,2-tetrahydrooctyl)-1-trichlorosilane (United Chemical, Bristol, PA) to increase surface hydrophobicity of the mold to ease the separation of cured PDMS piece.

2.3 Microchip sealing

Modifications of previously published reversible and irreversible sealing methods[20] were used to assemble completed microchips. Reversible sealing uses van der Waals interaction between the PDMS replica and the second piece of substrate to create a bond. Both pieces were thoroughly rinsed by methanol and brought into contact with one another prior to drying. The assembled microchip was then dried in an oven at 65 °C for ten minutes. Air

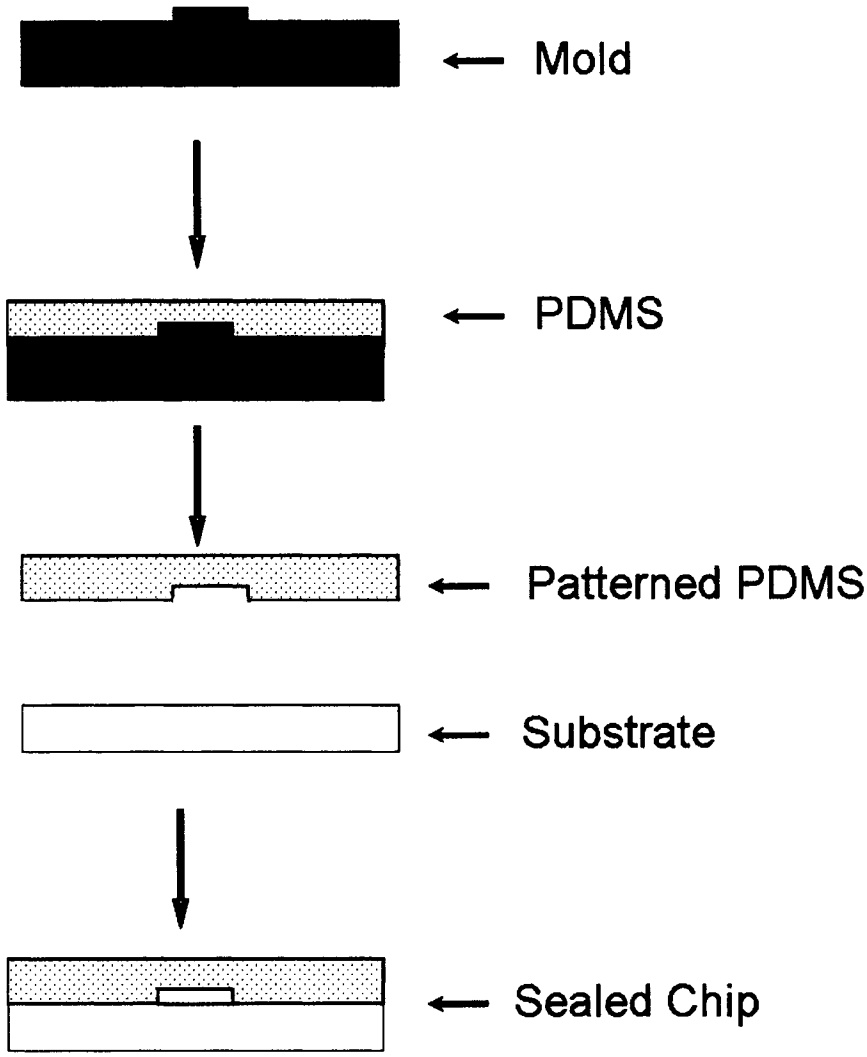

Figure 2.2 Fabrication of PDMS microchip

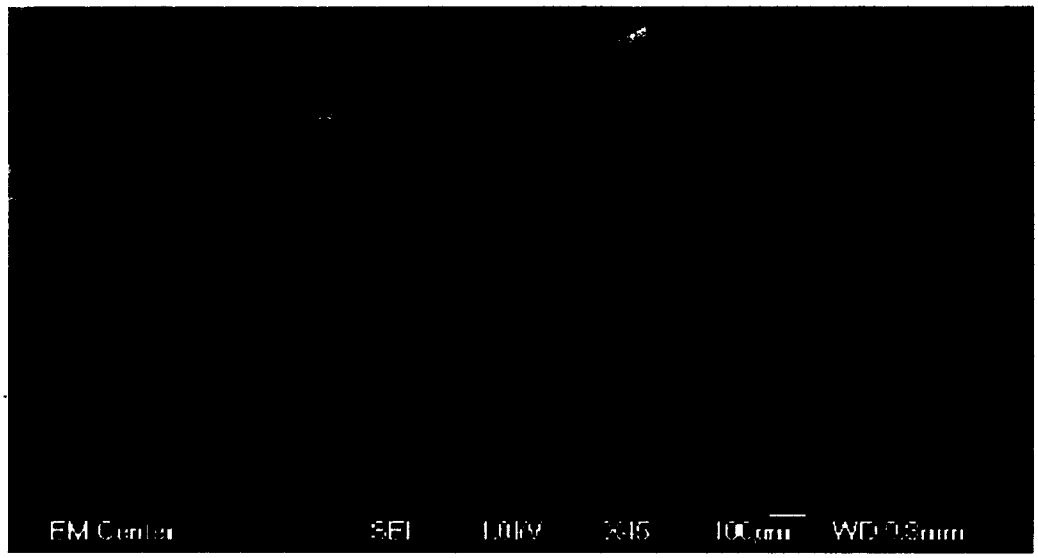

Figure 2.3 Picture of a patterned PDMS microchannel

bubbles formed between layers were driven out using finger pressure. The reversible bonding makes it possible to replace the separation channels without having to make a new detection layer. This form of sealing was very useful when microfabricated electrodes are being used. Irreversible sealing was also employed to assemble the microchips. First, two PDMS replicas were cleaned with methanol and then dried separately under a stream of nitrogen or in an oven at 65 °C for 10 minutes. The two pieces were placed in an air plasma cleaner (Harrick Plasma Cleaner/Sterilizer PDC-32G) and oxidized at high power for 35 seconds. The substrates were then brought into conformal contact immediately after removal from the plasma cleaner and an irreversible seal formed spontaneously. This seal was sufficiently strong that the two surfaces could not be separated without destroying the assembled microchip. This form of sealing was used when no reuse of both substrate pieces was needed.

2.4 Characterization of the system

One simple way to characterize the assembled system was to measure electroosmotic flow (EOF) in channel. A modification of a previously published current monitoring method was used to determine the EOF.[21] All reservoirs were filled with 18 mM buffer, and a 1 kΩ resistor was placed in line between the waste reservoir (reservoir 2 in Figure 2.4) and electrical ground to follow the separation current. A voltmeter was used to record the potential changes

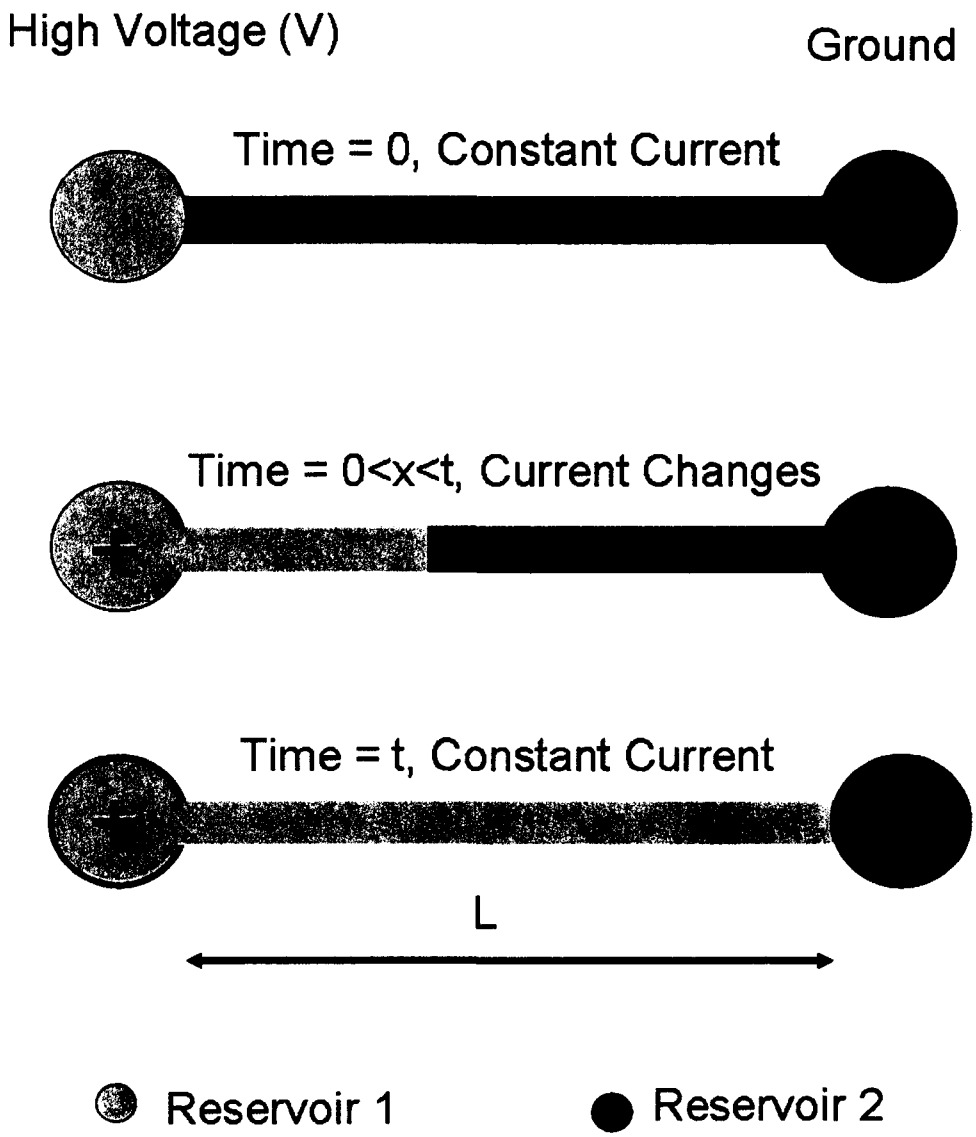

Figure 2.4 Layout of a microchip. Reservoir 1: sample reservoir; Reservoir 2: waste reservoir

across the resistor which correlates to the separation current through Ohm's Law. The channel was conditioned at a potential of 1200 V for 15 mins, and then the sample reservoir (reservoir 1 in Figure 2.4) was filled with 20 mM buffer, followed by applying the potential again. The time required for the current plateau was measured for each run and was the indicative of the concentrated buffer filling the separation channel. The sample reservoir was then filled with dilute buffer and the above procedure repeated. The time required for the current to reach this plateau was used as the migration rate of a neutral marker. The EOF was determined by

$$\mu_{EOF} = L^2/(V \bullet t) \qquad (2\text{-}1)$$

where:

L = the total length of microchannel,

V = the total applied voltage,

t = the time in second required to reach the new current plateau.

The typical voltage profile across the resistor is shown in Figure 2.5, and the time to reach a current plateau is 53 s for this microchip (4.2 cm length).

2.5 Conclusions

A simple and rapid prototyping method to fabricate PDMS microchips is described here. This methodology has two key components. First, the dimensions of microchannels can be varied by simply changing pattern size on mask. A similar procedure can be taken to modify the geometry of

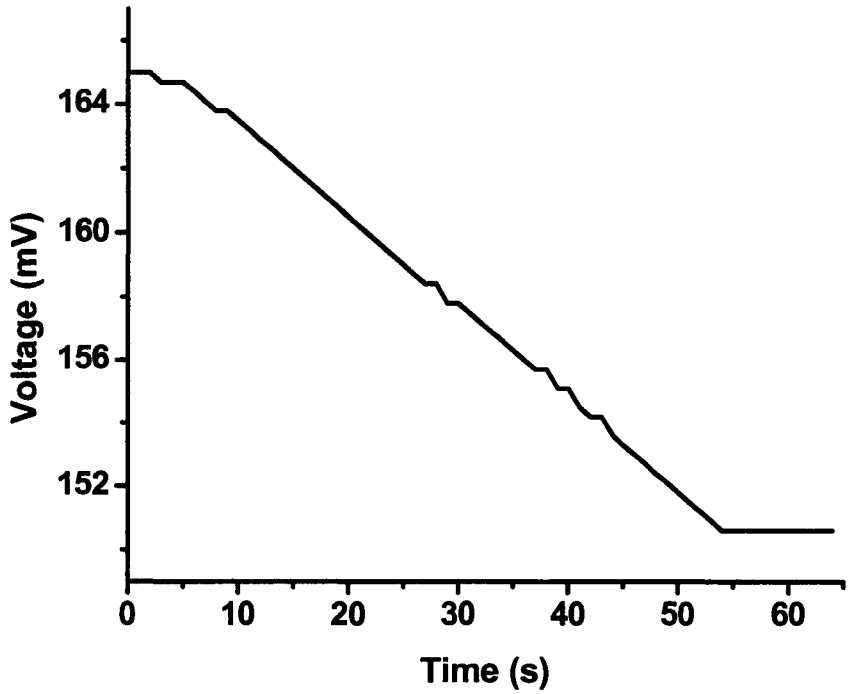

Figure 2.5 Typical voltage profile of EOF measurement.

microchannels to meet analytical requirements. Second, reversible sealing can effectively reuse the substrate pieces while irreversible sealing by air plasma oxidation can produce leak-free assembly. This prototyping method is applied throughout the whole dissertation.

2.6 Acknowledgments

Microfabrications were carried out at Mississippi State University and Colorado State University, respectively. The author thanks Mr. Jeffery Carter at MSU and Dr. Kevin Lear at CSU for the access to clean room facilities.

2.7 References

(1) Horng, R.-H.; Han, P.; Chen, H.-Y.; Lin, K.-W.; Tsai, T.-M.; Zen, J.-M. *Journal of Micromechanics and Microengineering* **2005**, *15*, 6-10.
(2) Fogarty, B. A.; Heppert, K. E.; Cory, T. J.; Hulbutta, K. R.; Martin, R. S.; Lunte, S. M. *Analyst (Cambridge, United Kingdom)* **2005**, *130*, 924-930.
(3) Muck, A., Jr.; Wang, J.; Jacobs, M.; Chen, G.; Chatrathi Madhu, P.; Jurka, V.; Vyborny, Z.; Spillman Scott, D.; Sridharan, G.; Schoning Michael, J. *Analytical chemistry* **2004**, *76*, 2290-2297.
(4) Fujii, S.; Tokuyama, T.; Abo, M.; Okubo, A. *Analyst* **2004**, *129*, 305-308.
(5) Rossier, J. S.; Vollet, C.; Carnal, A.; Lagger, G.; Gobry, V.; Girault, H. H.; Michel, P.; Reymond, F. *Lab on a Chip* **2002**, *2*, 145-150.
(6) Kricka, L. J.; Fortina, P.; Panaro, N. J.; Wilding, P.; Alonso-Amigo, G.; Becker, H. *Lab on a Chip* **2002**, *2*, 1-4.
(7) Kikutani, Y.; Horiuchi, T.; Uchiyama, K.; Hisamoto, H.; Tokeshi, M.; Kitamori, T. *Lab on a Chip* **2002**, *2*, 188-192.
(8) Jacobson, S. C.; Moore, A. W.; Ramsey, J. M. *Analytical Chemistry* **1995**, *67*, 2059-2063.
(9) Nakanishi, H.; Nishimoto, T.; Arai, A.; Abe, H.; Kanai, M.; Fujiyama, Y.; Yoshida, T. *Electrophoresis* **2001**, *22*, 230-234.
(10) Madou, M. J. *Fundamentals of Microfabricaion*, 2nd ed ed.; CRC Press: Boca Raton, 2002.
(11) Kim, M.-S.; Cho, S. I.; Lee, K.-N.; Kim, Y. K. *Sensors and Actuators, B:*

Chemical **2005**, *107*, 818-824.
(12) Rossier, J.; Reymond, F.; Michel, P. E. *Electrophoresis* **2002**, *23*, 858-867.
(13) McDonald, J. C.; Chabinyc, M. L.; Metallo, S. J.; Anderson, J. R.; Stroock, A. D.; Whitesides, G. M. *Anal Chem* **2002**, *74*, 1537-1545.
(14) Muck, A.; Svatos, A. *Rapid Commun Mass Spectrom* **2004**, *18*, 1459-1464.
(15) Llopis, S. D.; Stryjewski, W.; Soper, S. A. *Electrophoresis* **2004**, *25*, 3810-3819.
(16) Kelly, R. T.; Woolley, A. T. *Analytical Chemistry* **2003**, *75*, 1941-1945.
(17) Bao, N.; Xu, J.-J.; Dou, Y.-H.; Cai, Y.; Chen, H.-Y.; Xia, X.-H. *Journal of Chromatography, A* **2004**, *1041*, 245-248.
(18) Dahlin, A. P.; Wetterhall, M.; Liljegren, G.; Bergstrom, S. K.; Andren, P.; Nyholm, L.; Markides, K. E.; Bergquist, J. *Analyst* **2005**, *130*, 193-199.
(19) Li, H. F.; Lin, J. M.; Su, R. G.; Cai, Z. W.; Uchiyama, K. *Electrophoresis* **2005**, *26*, 1825-1833.
(20) McDonald, J. C.; Duffy, D. C.; Anderson, J. R.; Chiu, D. T.; Wu, H.; Schueller, O. J.; Whitesides, G. M. *Electrophoresis* **2000**, *21*, 27-40.
(21) Huang, X.; Gordon, M. J.; Zare, R. N. *Anal Chem* **1988**, *60*, 1837-1838.

CHAPTER III

ELECTROCHEMICAL DETERMINATION OF URINARY 4-AMINOPHENOL

During the year of 2001 when this dissertation work started, microchip CE-EC was seeing a tremendous growth in analyte category, electrode material, and instrumentation.[1-10] In addition to catechols, nitroaromatic explosives, glucose and phenolic pollutants were determined via microchip CE-EC.[1, 2, 9, 11] A wide variety of the substrate materials from glass and quartz to ceramics and polymers have been used because optical clarity of the substrate was not required for EC detection.[6, 9, 11, 12] Meanwhile, two different alignments of the working electrode had been employed for microchip CE-EC. The most common method was to place the detection cell just outside of the separation channel. This is called end-column or end-channel detection.[9] A second method is grounding the separation channel prior to the detection cell, which is commonly referred as decoupling. This is also known as off-column or off-chip detection.[9] Most publications involving microchip CE-EC used end-channel detection.

Two different ways were reported to place the working electrode outside of the separation channel. The first method mounted working electrode (wire or tube) at the end of the channel in a wall-jet arrangement.[6] Consequently, the CE effluent flowed off the channel and hit directly onto the surface of the working electrode. In a slightly different approach, the EC working electrode

was prepared by depositing a thin-film metal layer onto the outside of the chip where the CE channel exited.[13, 14] In this manner, the sensing electrode was incorporated directly onto the chip. Although reference and counter electrodes were still located separately in the reservoir, this approach had the potential to integrate all electrodes onto the microfluidic device. The integration of the working electrode with the microchip also leads to an inherent high mechanical stability of the detector assembly which may also improve baseline noise. It was my initial goal to use a microfabricated electrode system to develop portable clinical analyzers.

Phenols are one of the frequently employed model analytes in EC detection since they are electroactive at moderate redox potential.[9] Phenols are of considerable toxicological and environmental significance, therefore, they have been popular analyte for microchip CE-EC.[9] In occupational toxicology, 4-aminophenol (PAP) is used as a biological marker to screen for human aniline exposure.[15] Most of absorbed aniline is oxidized to PAP, which is excreted in urine.[16] The tentative maximum permissible concentration for PAP in urine is 30 mg PAP / 1 g creatinine.[17] High concentration PAP in vivo is thought to cause liver and kidney damage and may result in nephrotoxic effects.[18] In this chapter, electrochemical determination of PAP was employed to investigate the performance of the microfabricated Au thin-film microelectrode in a CE microchip. The detection of spiked PAP in human urine samples is also presented here.

3.1 Experimental

3.1.1 Sample and solution preparation

The pH values of Tris buffers were established by titrating the Tris solution with 0.1 M sodium hydroxide. Buffers were prepared weekly in deionized water and passed through a 0.20-μm sized syringe filter (Whatman, Florham Park, NJ). PAP stocks were prepared by dissolving PAP into 10 mM acetate buffer (pH 5.0) and stored at -20 °C until use. New PAP stocks were prepared every three days.The PAP sample solutions were prepared by diluting the stocks into 10 mM Tris buffer (pH 9.0).

Urine samples were obtained from healthy adult volunteers. The samples were refrigerated in sterile containers until use. All sample solutions and buffers were degassed in a sonicator (Fisher Scientific, FS 20) for 5 minutes and filtered before use.

3.1.2 Electrode fabrication

A 2.5-inch square glass plate was sequentially cleaned with piranha solution, deionized water, isopropanol, and deionized water. The plate was then dried with N_2 gas, and baked at 105°C for 5 minutes to remove any residual moisture. A thermal evaporator (Denton Vacuum, Cherry Hill, NJ) was used to sequentially deposit 50 Å of Ti and 1000 Å of Au onto the glass plate. After piranha cleaning, the metallized plate was coated with positive photoresist using a spin coater at 4000 rpm for 30 seconds. The desired

positive pattern mask was then placed on the coated plate and exposed to UV light source for 45 seconds. The plate was then developed and the photoresist patterns were left on top of the Au layer. The Au and Ti layers were etched using aqua regia (3:1 $HCl:HNO_3$) and Ti etch (2% HF/ 0.5% HNO_3) respectively. Finally, acetone was used to strip the remain photoresist from the electrode. The whole process of Au thin-film electrode fabrication is shown as Figure 3.1. Prior to use, the electrode plates were cleaned with piranha solution for 10 minutes. The width of the working electrode in the detection zone was 120 μm, as measured with an optical microscope. Reversible sealing was used to assemble the electrode plate with the PDMS replica. The layout of the chip is shown in Figure 3.2.

3.1.3 Microchip CE-EC

Gated injection[19] was used for injection in initial microchip CE-EC experiments. Electrochemical detection was performed in the amperometric mode using an electrochemical detector (CHI 812, Austin, TX) operating in a three-electrode configuration. A Ag/AgCl reference electrode and a platinum counter electrode were placed in the buffer waste reservoir, and a microfabricated Au thin-film electrode was placed at the exit of the separation channel. Alignment of the working electrode was accomplished during the sealing process. The distance between the exit of separation channel and the gold working electrode was 89 ± 10 μm (n = 5). In situ cleaning of the working

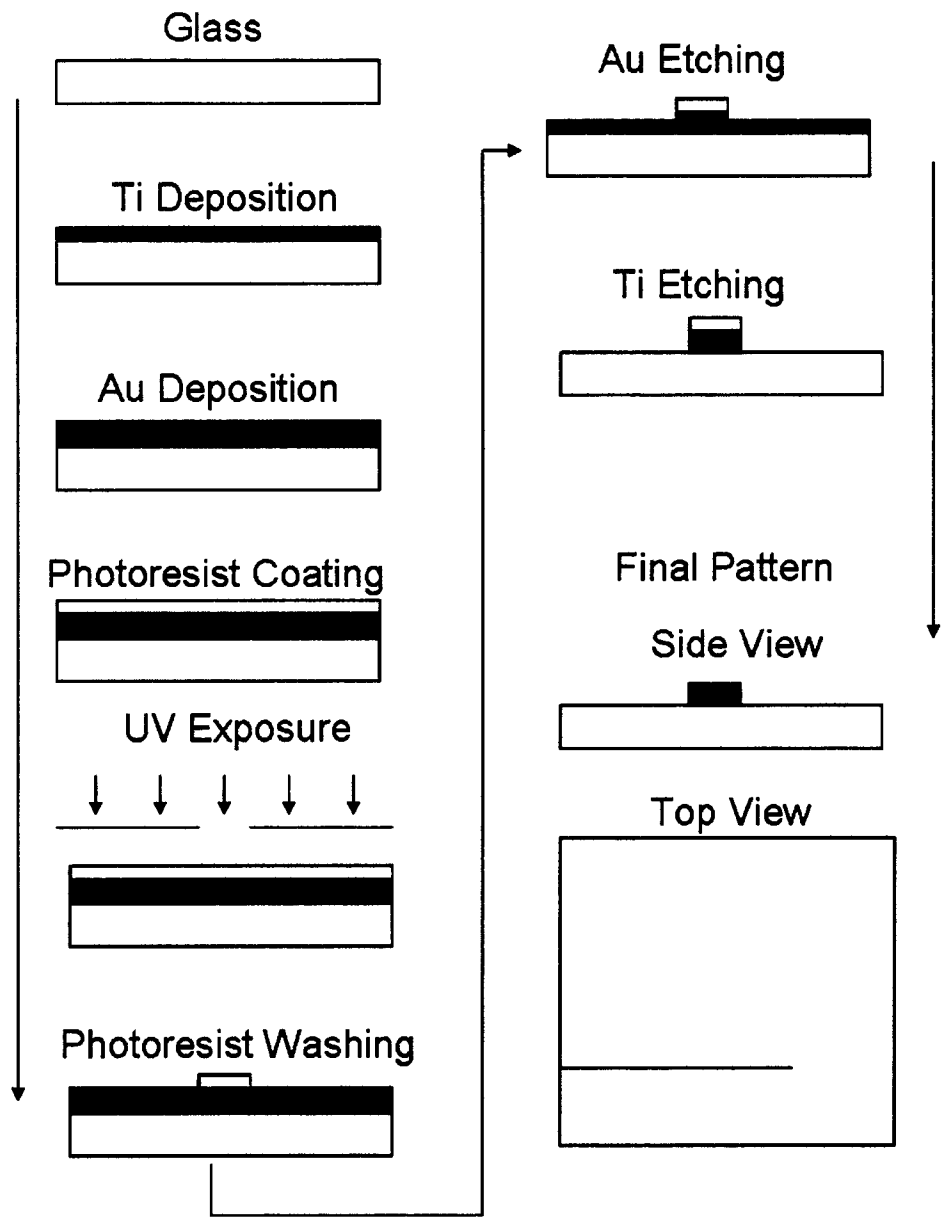

Figure 3.1 Fabrication of Au thin-film electrode (drawn not to scale)

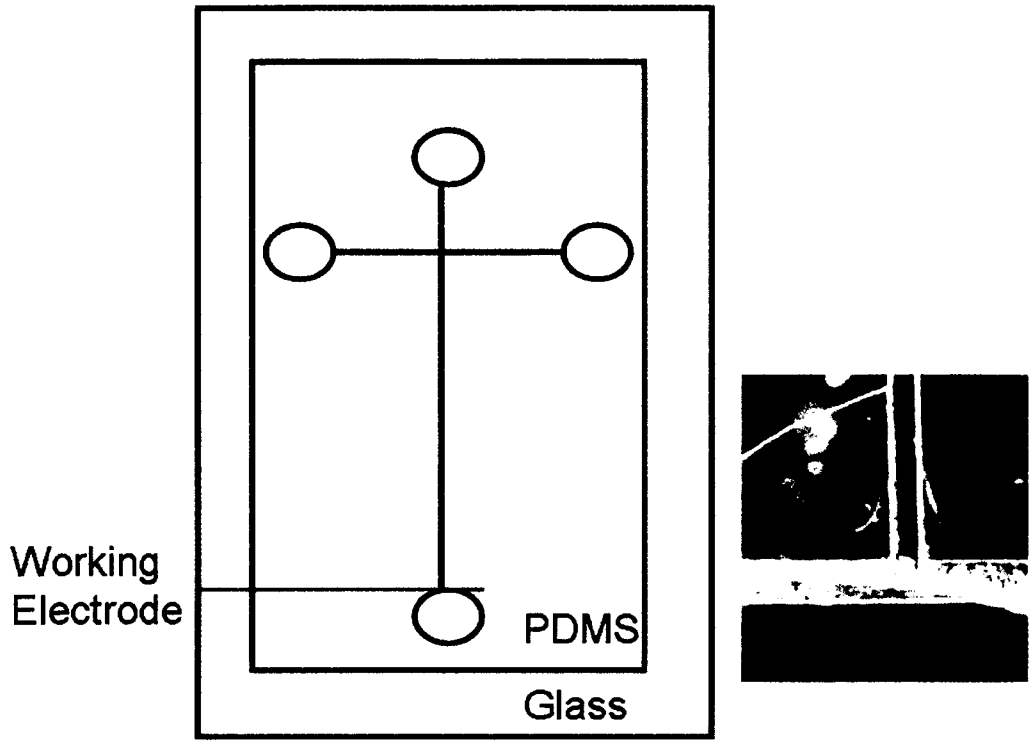

Figure 3.2 Schematic of microchip with on-chip working electrode. Reservior assignment: top, sample; left, sample waste; right, buffer; bottom, buffer waste (drawn not to scale); Right: picture of the alignment of working electrode

electrode was accomplished via cyclic voltammetry with twenty consecutive sweep segments from -0.8 to 1.2 V while buffer was electrokinetically pumped over the working electrode. Hydrodynamic voltammograms were from the chromatographic peak currents of PAP at different working electrode potentials.

3.2 Results and Discussion

3.2.1 Characterization of the system

Catechols are common analytes for EC detection and are frequently employed as model analytes because of their well-known mechanism of redox reaction.[9] Separations of dopamine and hydroquinone were performed to characterize the integrated glass/PDMS microchip with Au thin-film electrode. 3s-injection of 20 μM dopamine and 40 μM hydroquinone mixtures were achieved by gated injection. The running buffer was 10 mM pH 7 phosphate solution. Both analytes were oxidized at the working electrode and, therefore, represented by positive peaks for dopamine and hydroquinone, respectively (Figure 3.3). At this pH, dopamine is positively charged and hydroquinone is neutral. As a result, the first peak was dopamine and the second was hydroquinone. The separations were finished in 80s, however, the peak broadening was observed. There are two reasons: one is the adsorption of analytes onto PDMS; the other is the non-uniform flow in the channel. Since this is a glass/PDMS hybrid chip, three sides of the wall were PDMS,

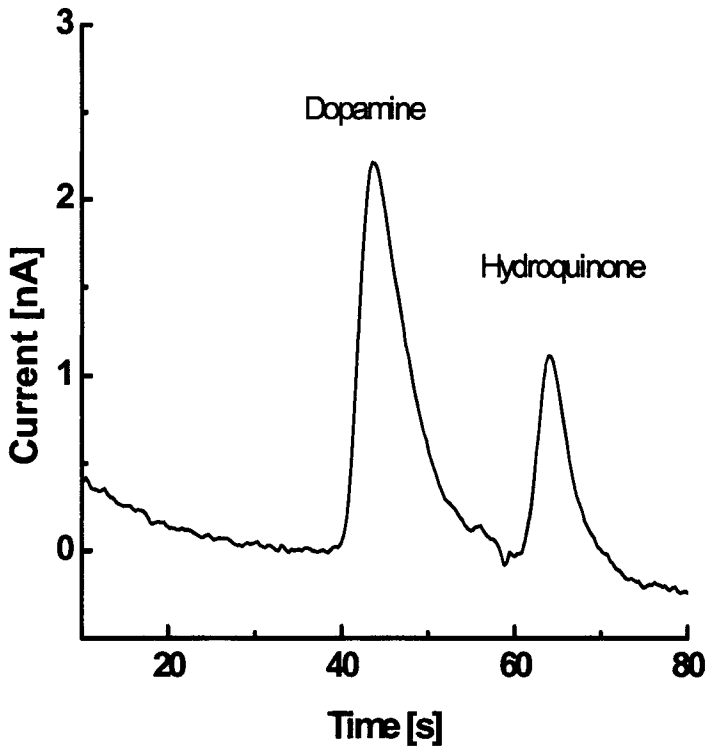

Figure 3.3 Electropherogram showing the separation of 20 μM dopamine and 40 μM hydroquinone. Separation conditions: separation voltage, 600 V; buffer, 10 mM pH 7.0 phosphate; injection, 3 s.

while the fourth wall is glass. The charge density of PDMS is different from glass. As a result, the electroosmotic flow on PDMS surface is different from that on glass resulting in non-uniform flow in the channel and peak broadening. These problems can be minimized by non-covalent coating to the separation channel.

3.2.2 Electrochemical reaction of PAP

Amperometric detection is based on electron transfer to or from the analyte of interest at an electrode surface. With an applied DC voltage, a redox reaction occurs at the electrode resulting in a current that is directly related to the analyte concentration. PAP is an easily oxidized compound which undergoes the following oxidation reaction at an electrode:

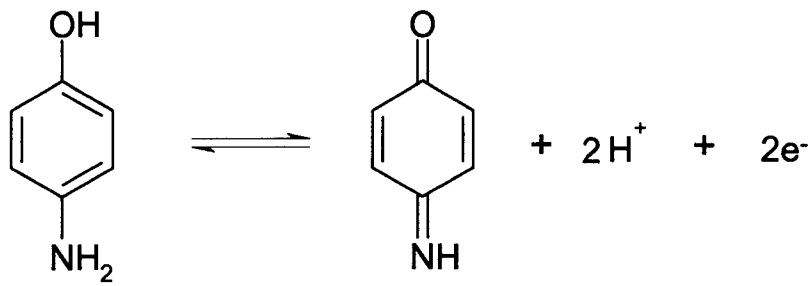

According to Heineman's reports, the oxidation potential of PAP was 250 mV vs. Ag/AgCl. However, since the separation voltage is grounded within the detection reservoir, the remaining separation field causes potential shifts at the working electrode. Therefore it is necessary to obtain a hydrodynamic

voltammogram (HDV) for a given analyte using the separation conditions that will be employed for the determination of PAP in urine. The HDV of PAP obtained from our experiments (Figure 3.4) verified the possibility of electrochemical detection of PAP at 300 mV vs Ag/AgCl. Figure 3.5 shows a typical electropherogram for PAP. The major advantage of this system is the reduced analysis time of PAP (35 s), compared to conventional CE or LC (minutes).

3.2.3 Optimization of injection time

The influence of injection time from 1 to 5 seconds on the PAP separation was investigated. The results were presented in Table 3.1. The peak height increased from 1 - 3 s where it reached a maximum. The peak areas, however, were linear with injection time 1 s - 5 s. The linear increase in peak area with injection time was expected as more PAP was injected into the separation channel. For the peak height, the larger volume of PAP solution leads to band broadening and column overloading, explaining why the peak height of signal reached a maximum. The relatively low theoretical plate numbers obtained with the present device are the result of the adsorption of the phenolic compound onto the surface of PDMS microchannel coupled with the materials mismatch of the microchip. But they are comparable to other reports of microchip CE-EC. When the influence of injection on separation efficiency was investigated, the number of theoretical plates per meter decreased with

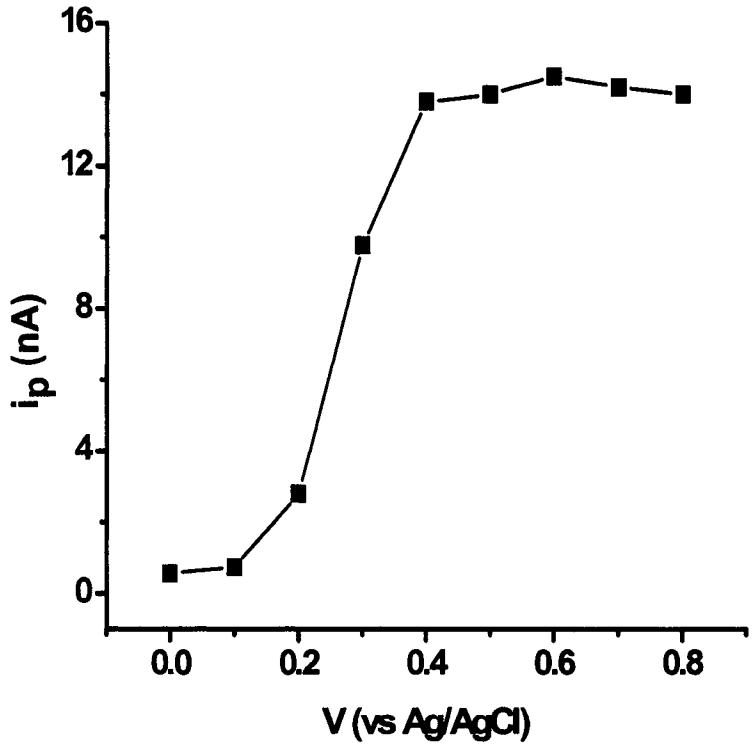

Figure 3.4: Hydrodynamic voltammogram of PAP. CE conditions: applied voltage, 180 V/cm; run buffer, 10 mM Tris (pH 9.0); injection time, 2 s.

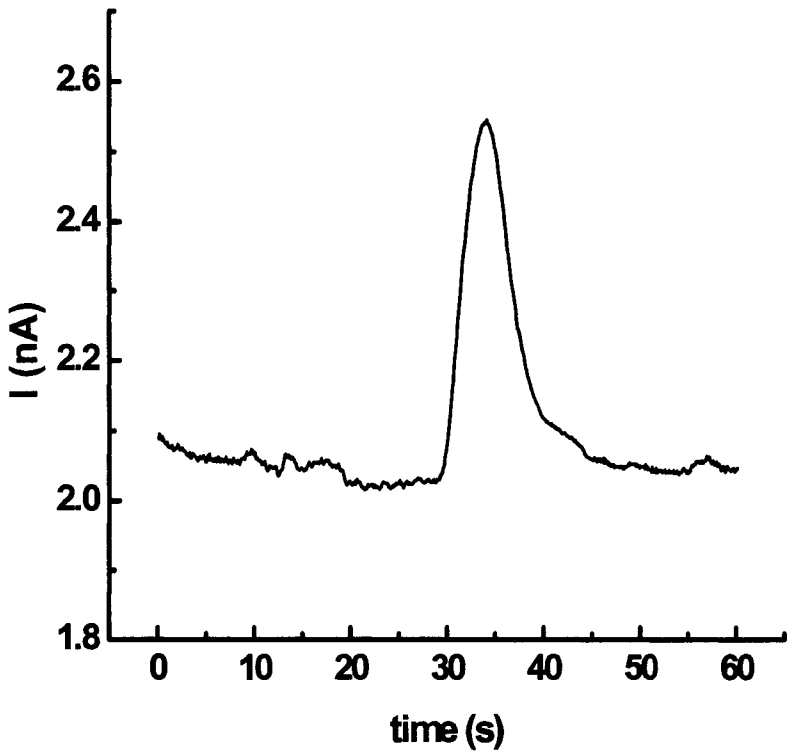

Figure 3.5: A typical electropherogram of PAP. CE conditions: applied voltage, 180 V/cm; run buffer, 10 mM Tris (pH 9.0); injection time, 2 s; working electrode potential: 300 mV vs. Ag/AgCl

Table 3.1 The Influence of Injection Time on PAP Detection

Injection Time (s)	Peak Height (nA)	Peak Area (10^{-8} C)	N (plates/m)
1	3.961	9.95	37372
2	5.295	19.41	18845
3	6.176	29.62	9487
4	6.306	34.72	6663
5	6.252	40.87	5227

increasing injection time. As a result, two seconds was used for injection time. This represented the best compromise between detection sensitivity and separation efficiency.

3.2.4 Linear calibration and limit of detection

The relationship between concentration and peak current was investigated. Six standard PAP solutions of differing concentration were tested. A good linear relationship was observed from 1 μM to 70 μM for peak current, with a correlation coefficient of 0.9991, shown in figure 3.6. The standard deviations (n = 6) for all five points were less than 2.0%. At 90 μM, the signal was no longer linear. In order to determine the absolute threshold for detection of PAP, we diluted the PAP standard solution to 1 μM which had a signal-to-noise ratio (S/N) of 4.3. According to the standard for LOD (S/N = 3), an estimated LOD of PAP would be 0.76 μM. Both the linear range and LOD obtained with the present device are comparable to the reported values using microchip CE which gave a linear range from 1 to 120 μM and a LOD of 5 μM.[20] The LOD and the linear range are appropriate for the reported maximum toxicological limit (423 μM) after dilution with buffer.[16]

3.2.5 Sample Analysis

Figure 3.7 shows a representative electropherogram of a urine sample diluted 20-fold. When the dilution of urine sample was decreased from 20 to

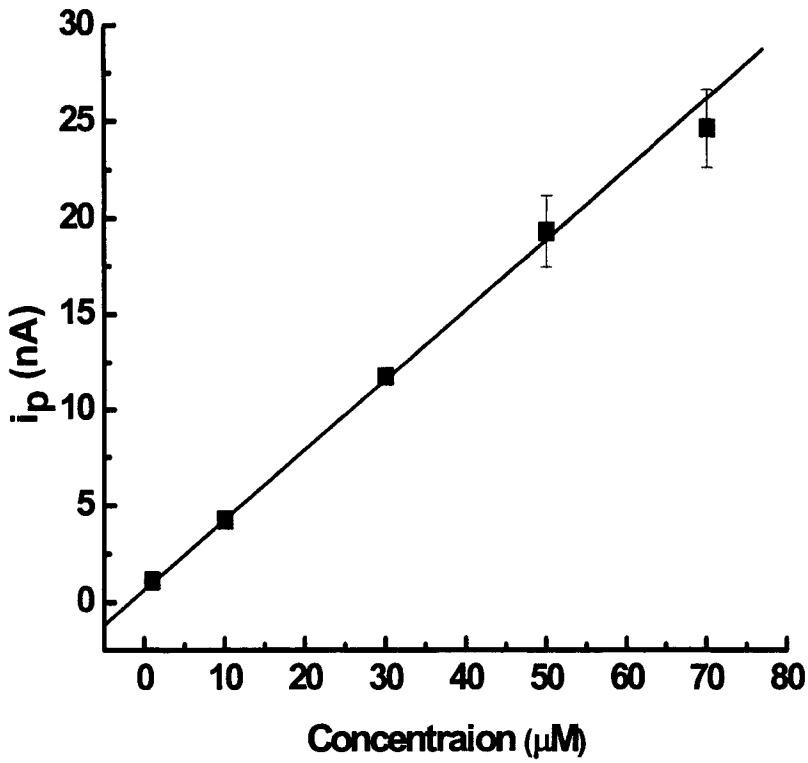

Figure 3.6: Linear relationship between the chromatographic peak current and PAP concentration. CE conditions were same as Figure 3.5.

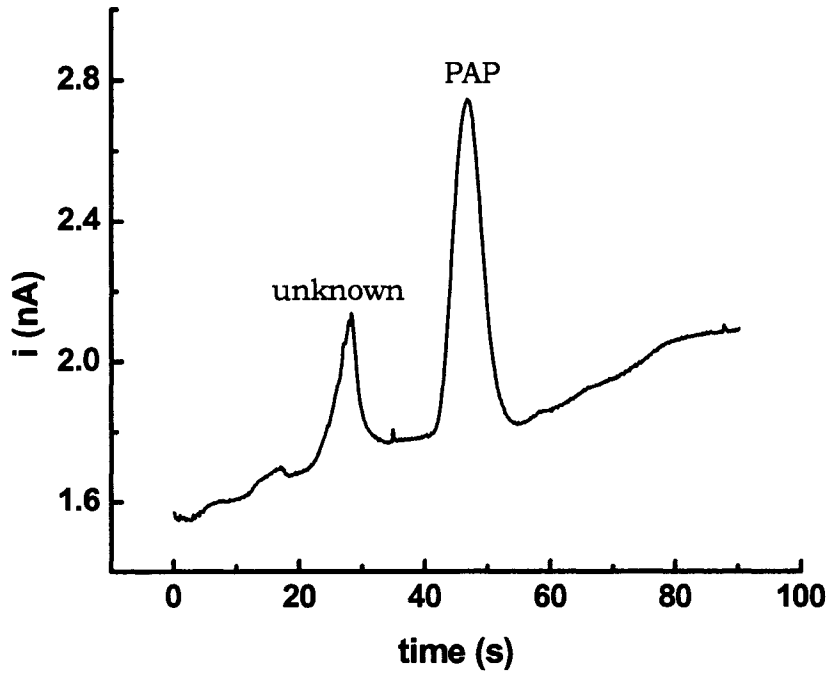

Figure 3.7: Electropherogram of PAP spiked urine sample. CE conditions were same as Figure 3.5. Urine sample was 5-fold diluted in 10 mM Tris buffer (pH 9.0) with 30 μM PAP.

5-fold, the PAP migration was increased from 35 s to 47 s. Urine is a complex matrix with high ionic strength. The velocity of an analyte in the capillary is the combination of electroosmostic flow (EOF) and electrophoretic mobility.[21] When the ionic strength of the sample increases, the EOF will decrease as the square root of the ionic strength.[21] Due to the decreased EOF, the migration rate of PAP was reduced. As a result, the migration time of PAP increased. No significant difference was observed for the migration time of standard PAP solution and 20-fold diluted urine sample. The observation further suggested that the high ionic strength of urine sample affected the migration of PAP. The migration time of standard PAP solutions prepared by different concentration buffers showed a 8.7% difference between the high concentration buffer and the low concentration buffer. These results further verified the explanation. A second concern is adsorption of urinary proteins and PAP to the capillary wall and working electrode after a few runs. Due to the low amount of proteins in urine, the insignificant effect is expected, which is demonstrated as the constant migration time of PAP with a relative standard deviation of 2.9% (n=15). However, to avoid the possible adsorption of samples, flushing the channel with methanol and replacing buffer and sample solutions after every eight runs was done, which proved useful to obtain the relatively small standard deviations.

As a major component of urine sample, uric acid may have severe interference to PAP determination. The peak of uric acid would appear after

PAP's appearance due to its electrophoretic mobility. According to hydrodynamic voltammograms, a potential of 0.3 V vs Ag/AgCl reference electrode, which was below the oxidation potential of uric acid (0.7 V), was chosen to detect PAP. This effectively shielded the uric acid. The peak before the PAP is still unknown. Further work is needed to identify this compound.

3.3 Conclusions

The aim of the present study was to develop a rapid, simple, and practical electrochemical approach for analysis of biological and environmental samples. Here, PAP was used a marker to investigate the performance of the microchip CE-EC device with Au thin-film electrode. Although the PAP in artificially spiked urine sample was quantified successfully, there were some issues that needed to be addressed. The size and weight of power supply for microchip CE system was the first concern. Second, the migration time of PAP shifted from time to time which was due to the non-uniform flow in channel. Third problem was the separation efficiency of PAP. The fourth consideration was the costly and tedious fabrication of Au thin-film electrode. Methods to overcome these drawbacks are presented in details in the following chapters of the dissertation.

3.4 Acknowledgments

The funding of this project was provided by Mississippi State University.

The fabrication of Au thin-film electrode was carried out in the clean room at Mississippi State University with the permission of Mr. Geoffrey Carter.

3.5 References:

(1) Wang, J.; Chatrathi, M. P.; Tian, B. *Anal Chem* **2001**, *73*, 1296-1300.

(2) Wang, J.; Ibanez, A.; Chatrathi, M. P.; Escarpa, A. *Anal Chem* **2001**, *73*, 5323-5327.

(3) Liu, Z.; Niwa, O.; Kurita, R.; Horiuchi, T. *J Chromatogr A* **2000**, *891*, 149-156.

(4) Martin, R. S.; Gawron, A. J.; Lunte, S. M. *Anal Chem* **2000**, *72*, 3196-3202.

(5) Radtkey, R.; Feng, L.; Muralhidar, M.; Duhon, M.; Canter, D.; DiPierro, D.; Fallon, S.; Tu, E.; McElfresh, K.; Nerenberg, M.; Sosnowski, R. *Nucleic Acids Res* **2000**, *28*, E17.

(6) Wang, J.; Chatrathi, M. P.; Tian, B. *Anal Chem* **2000**, *72*, 5774-5778.

(7) Gawron, A. J.; Martin, R. S.; Lunte, S. M. *Electrophoresis* **2001**, *22*, 242-248.

(8) Kamidate, T.; Kaide, T.; Tani, H.; Makino, E.; Shibata, T. *Anal Sci* **2001**, *17*, 951-955.

(9) Lacher, N. A.; Garrison, K. E.; Martin, R. S.; Lunte, S. M. *Electrophoresis* **2001**, *22*, 2526-2536.

(10) Martin, R. S.; Gawron, A. J.; Fogarty, B. A.; Regan, F. B.; Dempsey, E.; Lunte, S. M. *Analyst* **2001**, *126*, 277-280.

(11) Patzer, J. F., 2nd; Yao, S. J.; Xu, W.; Day, T. L.; Wolfson, S. K., Jr.; Liu, C. C. *Asaio J* **1995**, *41*, M409-413.

(12) Henry, C. S.; Zhong, M.; Lunte, S. M.; Kim, M.; Bau, H.; Santiago, J. J. *Analytical Communications* **1999**, *36*, 305-307.

(13) Liu, Y.; Wipf, D. O.; Henry, C. S. *Analyst* **2001**, *126*, 1248-1251.

(14) Liu, Y.; Fanguy, J. C.; Bledsoe, J. M.; Henry, C. S. *Anal Chem* **2000**, *72*, 5939-5944.

(15) Van Bocxlaer, J. F.; Clauwaert, K. M.; Lambert, W. E.; De Leenheer, A. P. *Clin Chem* **1997**, *43*, 627-634.

(16) *Casarett and Doull's Toxicology: The Basic Science of Poisons*, Fifth edition ed.; McGraw-Hill: New York, 1995.

(17) Liu, Z.; Li, J.; Dong, S.; Wang, E. *Analytical Chemistry* **1996**, *68*, 2432-2436.

(18) Pariente, F.; Hernandez, L.; Lorenzo, E. *Analytica Chimica Acta* **1993**, *273*, 399-407.

(19) Jacobson, S. C.; Ermakov, S. V.; Ramsey, J. M. *Analytical Chemistry* **1999**, *71*, 3273-3276.

(20) Rossier, J. S.; Ferrigno, R.; Girault, H. H. *Journal of Electroanalytical Chemistry* **2000**, *492*, 15-22.
(21) Weston, A.; Brown, P. R. *HPLC and CE Principles and Practices*; Academic Press: San Diego, 1997.

CHAPTER IV

BUILDING A PORTABLE HIGH-VOLTAGE POWER SUPPLY FOR MICROCHIP CE

The development of miniaturized or portable CE instrumentation must focus on the miniaturization of the detection system and/or the integration of the power supply and the detection system.[1-4] Currently, most of microchip CE experiments have been performed using conventional scale power supplies. If the final goal of the microanalytical devices is to allow point-of-care testing, the whole instrument needs to be made portable, including the power supply. So far, most notably, Hauser's group has described the construction of a battery-powered, field-portable CE instrument of carrying out amperometric, potentiometric, and conductivity detection.[1] However, this approach which employed a conventional fused-silica capillary for separation was not intended for microchip level application.

In the present chapter, the fabrication and performance of a portable high voltage power supply (HVPS) for microchip CE is described. First, a battery-powered HVPS was designed to provide 2-channel output using one positive DC-DC converter. Following that, a 3-channel HVPS was developed which consisted of two positive and one negative DC–DC converters, a microprocessor controlled timer, a battery and a transformer to recharge the battery. This arrangement allows the control of the potentials applied in the 0 to ± 4000 V range for a variety of microchip designs and can be easily adapted to

perform any type of injection. A microprocessor controlled timer was included in order to increase the reproducibility of injection. A rechargeable battery was used to feed the DC–DC converters to reduce noise levels (compared to standard 110 V transformers). Finally, because all the controls are built in, simple push button operation can be achieved with no computer programming.

4.1 Construction of 2-Channel HVPS

The first generation of HVPS consisted of one DC-DC converter (6A12P6C). The complete circuit diagram is shown in Figure 4.1. The converter had the possibility of drawing an output voltage between 0 and 6000 V and a maximum power of 30 W. These specifications were able to meet the power requirements for operation of any microchips. In addition, the converter was small (70.2 cm^3), light (142 g) and inexpensive (< US $200). The HVPS consisted of following parts: battery, voltage divider, DC-DC converter, voltammeter, and switches. The DC-DC converter was battery powered. There were two output terminals, as seen in Figure 4.1. Output 1 was controlled by a voltage divider underneath the DC-DC converter (Figure 4.1). A second voltage divider on the left side of DC-DC converter was employed to adjust the output 2 in Figure 4.1 of DC-DC converter The outputs were monitored by two voltammeters. This was the first draft of power supply construction. One advantage of this HVPS was that it could provide 2-channel output which could meet the requirement of gated injection. Drawbacks, however, existed. The first drawback lay in the power source of the DC-DC converter. The lifetime of battery was not monitored and the voltage input

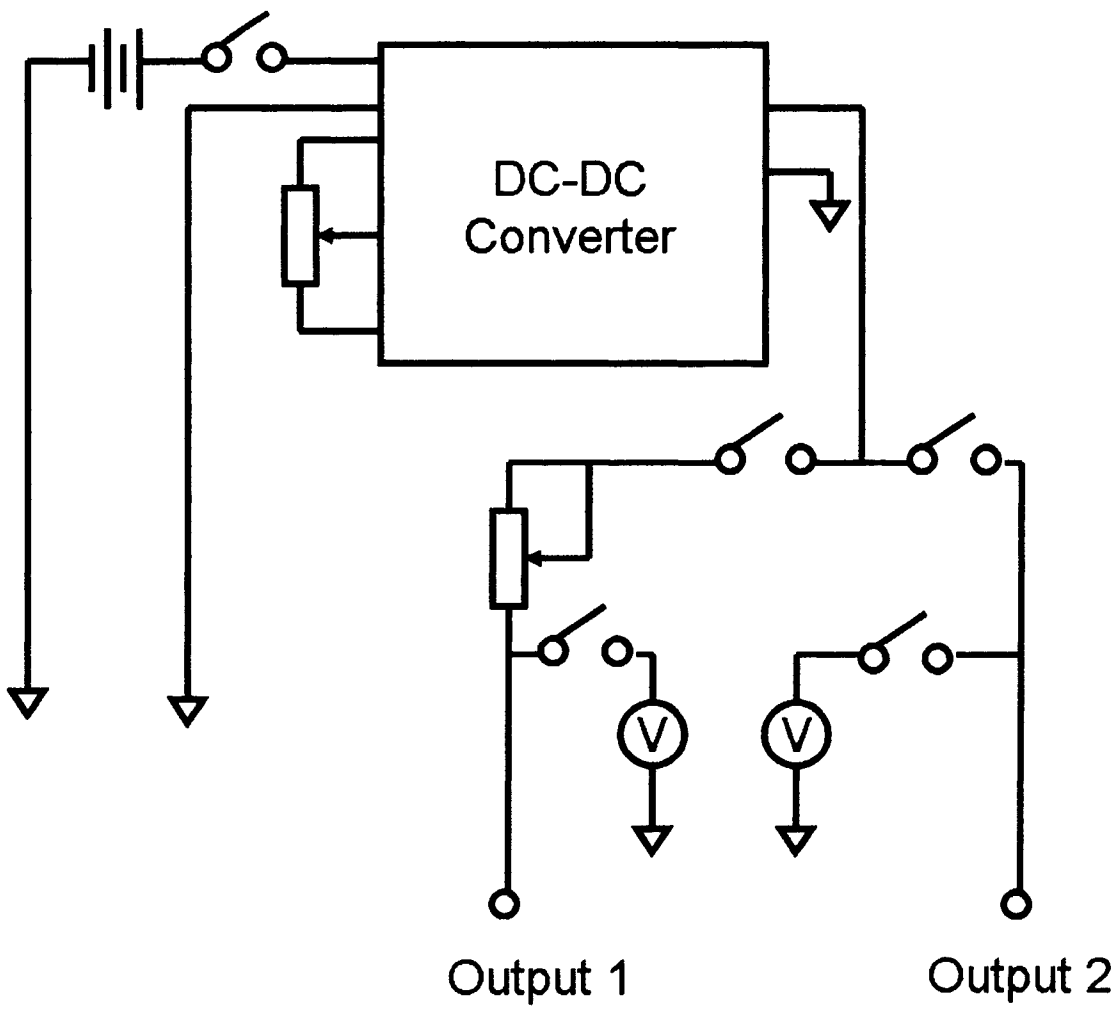

Figure 4.1 Circuitry of 2-channel output HVPS

to DC-DC converter needed to be regulated. A good way to solve it was to connect one voltage regulator to the battery which could protect the DC-DC converter when subjected to an excessive power overload condition. The second drawback was the reproducibility of operations. All operations were made manually by turning on or off the switches. The output of the HVPS should be controlled electronically. More improvements to the HVPS were made.

4.2 Construction of 3-Channel HVPS

With the help of Paul Anderson and Carlos Garcia, a 3-channel HVPS was built using 2 positive (6A12P4C) and 1 negative (6A12P4N) DC–DC converters. The regulation of the output voltage was performed by the use of a potentiometer and monitored with a digital display placed in the top panel (Fig. 4.2A). A switch was connected before each DC–DC converter to control the individual channels. The outputs of each DC–DC converter were connected to a two-pole banana connector in the rear panel of the HVPS (Fig. 4.2B). The size of the plastic box used to contain all the parts, including the battery and the transformer, was 9.5 3 × 18.43 × 26.4 cm. The total weight of the system (including the transformer and the battery) was 3.5 kg.

Two different designs were used as the power source of the DC-DC converter. The first design used a 110 V transformer and a current rectification circuit. The second scheme used a 110–16 V transformer to charge a 12 V battery, which was used to feed the DC–DC converters (Fig. 4.3A).

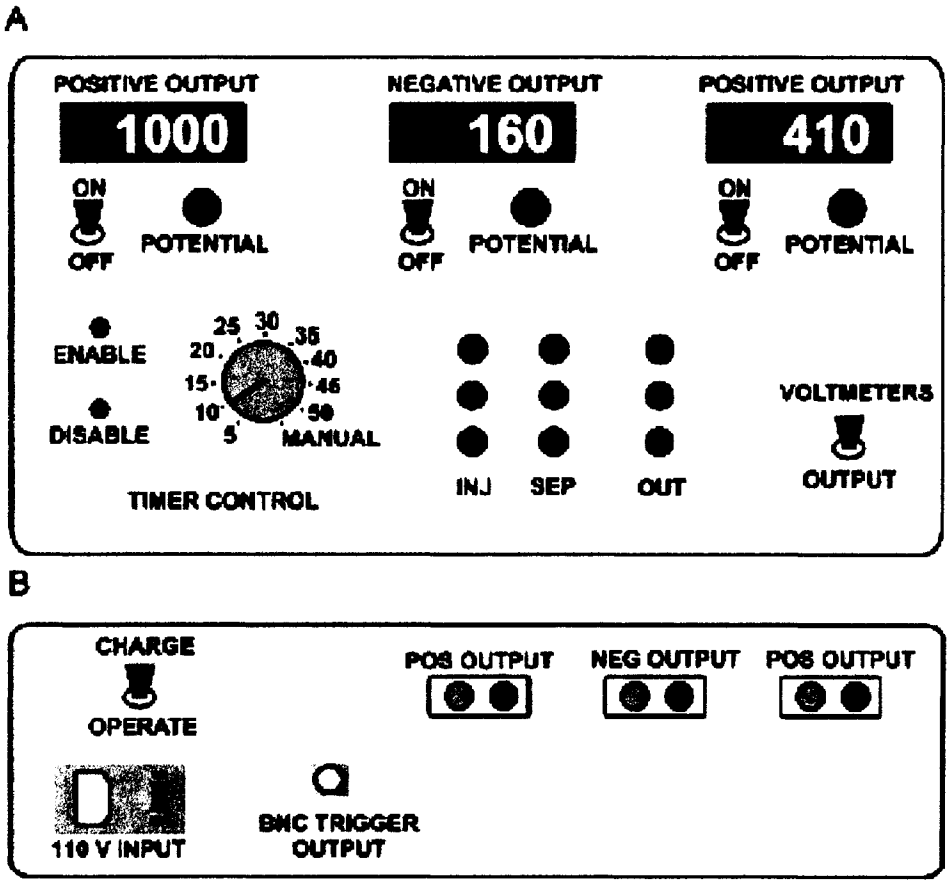

Figure 4.2 Front panel (A) and rear panel (B) of the 3-channel HVPS

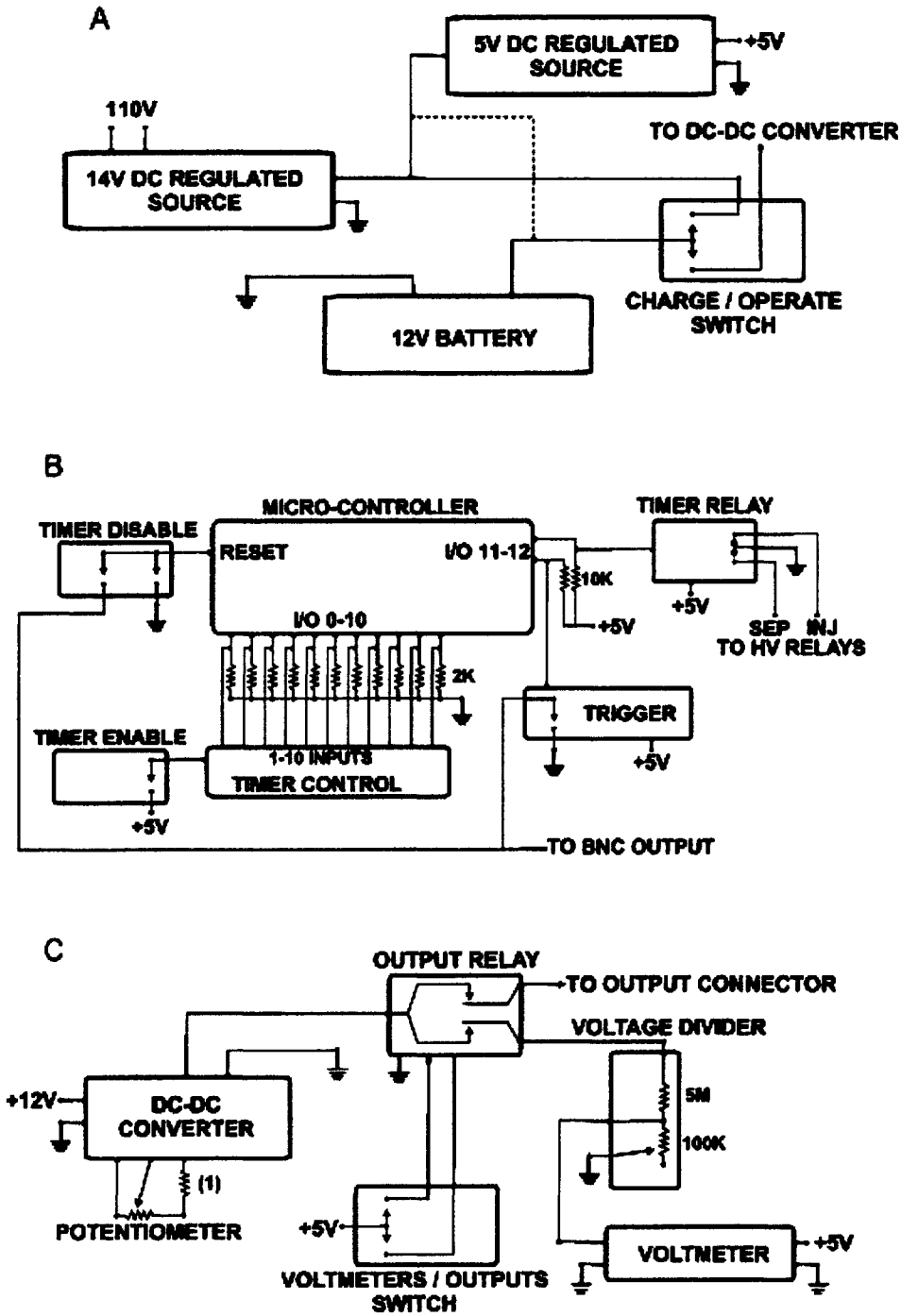

Figure 4.3 Circuit diagram to connect the battery to the DC–DC converters (A), microprocessor controlled timer circuitry (B) and circuit corresponding to connect either the voltmeters or the outputs (C).

Under both setups a +5 V line was connected to the transformer and used to feed the high-voltage relays. However, if no 110 V is available (e.g. field operation), the +5 V input can be taken from the battery (dotted connection in Fig. 4.3A). A three-position switch was connected to the battery to allow either recharge or use. The charge lifetime of the battery, measured under typical operation conditions was 8 hours. If a fully portable HVPS was needed and only the battery was used, the charge lasted 2 h due to the power consumption of the relays (0.5 mA).

To perform injections, different sets of voltages were applied during the injection and separation modes. In order to automate the process, a microprocessor controlled timer circuit was designed according to Fig. 4.3B and burned on a printed circuit board. It can be observed that the 11 I/O of the microprocessor can be activated by the timer controller knob. This allows the selection between 10 pre-selected injection times and one open position to manually control the injection time. Two pushbuttons were employed to enable or disable the timer. As mentioned before, the different injection times were written in the microprocessor code in the 5–50 s range using 5 s intervals. For specific applications these times can be easily reprogrammed. According to the manufacturers, the reset time for the relays is 5 ms while the microprocessor can perform 10000 operations/s. Assuming 2 relay operations (open and close) and 4 microprocessor operations (push button, open relays, close relays and activation of the trigger), the total operation time takes about 20 ms. This enables the control of injection times even below the second range with a high accuracy (> 99% for a 0.1 s injection). The connections between the timer connectors (in the front panel, Figure 4.2 A) and

the DC–DC outputs (in the back panel, Figure 4.2 B) were performed by the use of external wires. These external connections facilitate simple and rapid changes in the configuration. High voltage relays were used in order to allow the operation of the HVPS at higher potentials (up to ±4000 V). If standard relays are used, only lower potentials (up to ±1000 V) can be applied. In order to avoid feedback between the power supplies through the voltmeters circuitry, a switch was included to connect the DC–DC converters to either the voltmeters or the corresponding outputs (Fig. 4.3C).

4.3 Operation of the HVPS

For most microchip applications, two operation modes are needed: injection and separation. Normally, the analysis begins with the HVPS in the separation mode, where buffer is flowing through the separation channel. When the timer starts, the microprocessor opens 3 high-voltage relays corresponding to the 3 separation inputs and closes 3 high-voltage relays corresponding to the 3 injection inputs for the specified injection time. At the end of the injection, the HVPS outputs are switched back to the separation mode. One output of the microprocessor timer was connected to an external trigger in order to start the detector simultaneously with the beginning of the separation. The typical potentials used during injection and separation are summarized in Table 4.1.

4.4 Injection demonstration

Three different injection methods (pinched, gated, and diffusion) were used to

Table 4.1 Parameters used to perform pinched, gated and diffusion injection

(a) Parameters used to perform pinched injection

Reservoir	Containing	Injection	Separation
A	Buffer	+410	+1500
B	Buffer	-160	+410
C	Sample	+410	+410
D	Waste	Ground	Ground

(b) Parameters used to performed gated injection

Reservoir	Containing	Injection	Separation
A	Sample	+500	+500
B	Buffer	Ground	Ground
C	Buffer	Floating	+750
D	Waste	Ground	Ground

(c) Parameters used to perform diffusion injection

Reservoir	Containing	Injection	Separation
A	Buffer	Floating	+500
B	Buffer	Floating	Ground
C	Sample	Floating	+750
D	Waste	Ground	Ground

test the capabilities of the HVPS. A solution of 1 mM fluorescein, prepared in the running electrolyte, was used to follow injection at a double-T injector.

To perform pinched injection, the outputs of the DC–DC converters were connected according to Table 4.1. Due to the lower resistance value of the A–B channel (with respect to B–C), a 1 MΩ resistor was included to avoid Joule heating during the injection procedure. The timer circuit switches the potentials applied to reservoirs A and C while the potential applied to the reservoir B is constant and the reservoir D is always grounded. A sequence of photomicrographs showing the injection (before, during and after) is shown in Fig. 4.4A. A well defined sample plug (1.3 nL) is injected. A small amount of diffusive leaking towards the detection reservoir is noted. This leaking is the result of the required ground in the detection reservoir due to the presence of the detection electrodes.

To perform gated injection, only the positive DC–DC converters were used. It can be observed that in this case, only the potential applied to the reservoir B is changed (on/off). During the injection, reservoir B is floating, while during the separation, +750 V was applied between reservoirs B and D. Again, a sequence of photomicrographs (before, during and after the injection) is shown in Fig. 4.4B where a well defined sample plug is injected.

Diffusion or hydrodynamic injection was another injection method that was investigated. In separation mode, the settings for diffusion injection were same as those of gated injection. In injection mode, all potentials applied to the reservoirs were turned off instead of floating potential from reservoir B. The sample diffuses

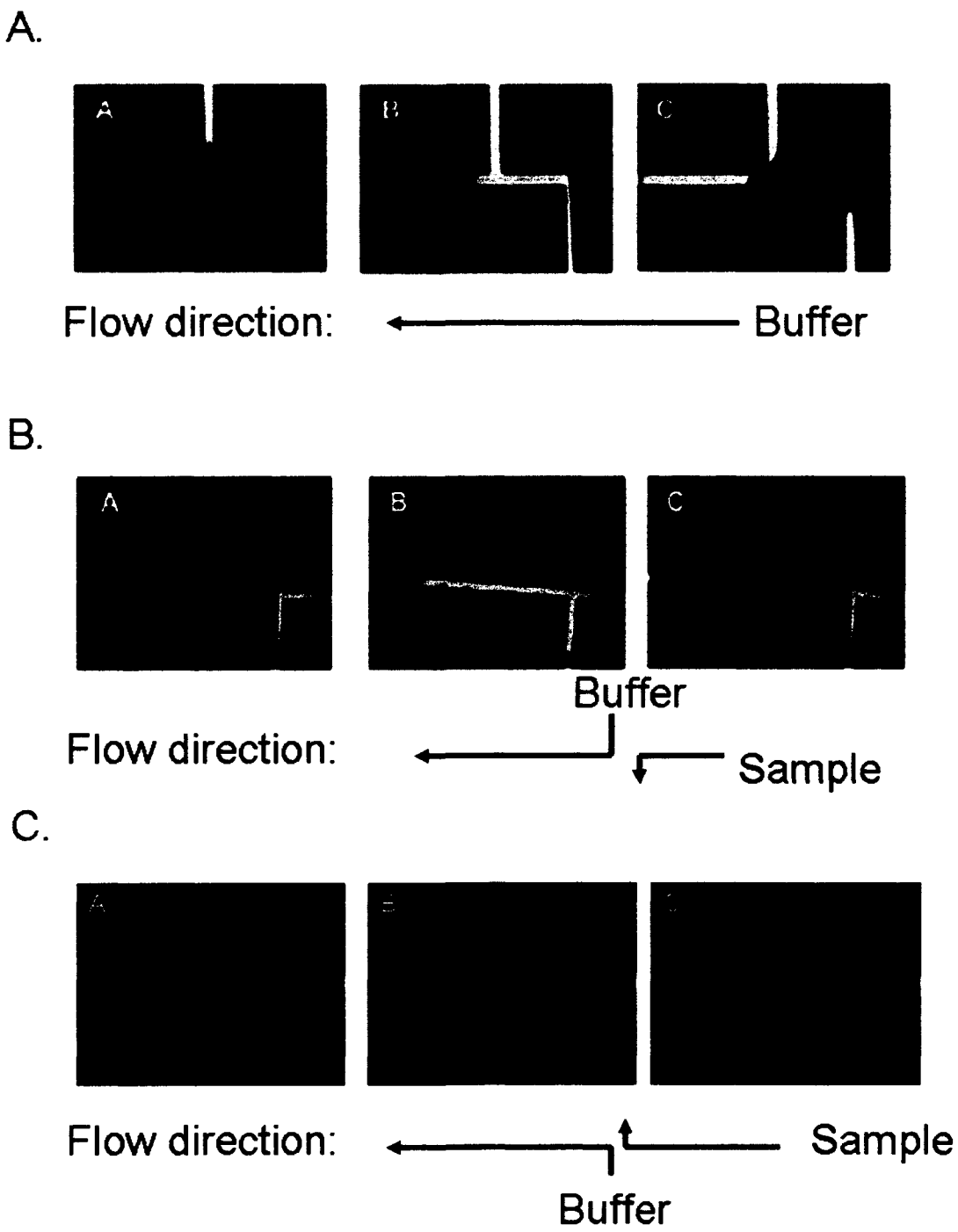

Figure 4.4 (A) Pinched injection. (B) Gated injection. (C) Diffusion injection

into the separation channel due to the concentration gradient. The image of diffusion injection is shown in Fig. 4.4C while the parameters for voltages are listed in Table 4.1.

4.5 HVPS Noise

Although most of the separation current is driven through the ground electrode, a small portion is always introduced through the detection electrodes. This input is the main source for noise when electrochemical detection is used, limiting the lower detectable concentration of the analyte. In order to evaluate the contribution of the two different inputs (battery and transformer) used to feed the HVPS, the background noise level was measured. The experiments were performed applying 300–1800 V in 300 V steps, using 5 mM borate (pH = 9.5), 2.4 mM SDS as the electrolyte. In Fig. 4.5A the average peak-to-peak noise values are shown for both configurations. As expected, higher noise values were obtained when the transformer was used to feed the HVPS as compared to the battery powered HVPS. In Fig. 4.5B, a comparison baseline obtained at 900 V between the battery and the transformer powered HVPS, is shown. Under these conditions, the average peak-to-peak noise level was 490 ± 60 pA (n = 25) for the transformer and 8 ± 7 pA (n = 25) for the battery.

4.6 Conclusions

The construction of a simple three-channel HVPS that meets the requirements to perform CE separations at the microchip scale under a wide

A

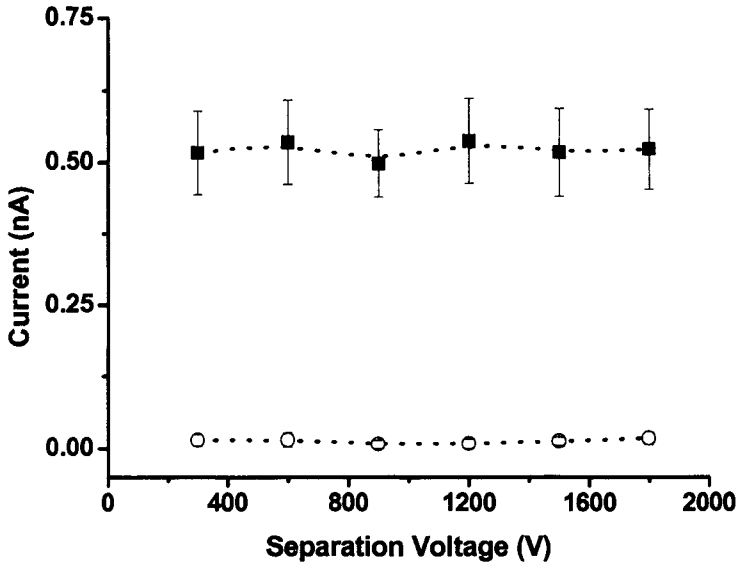

B

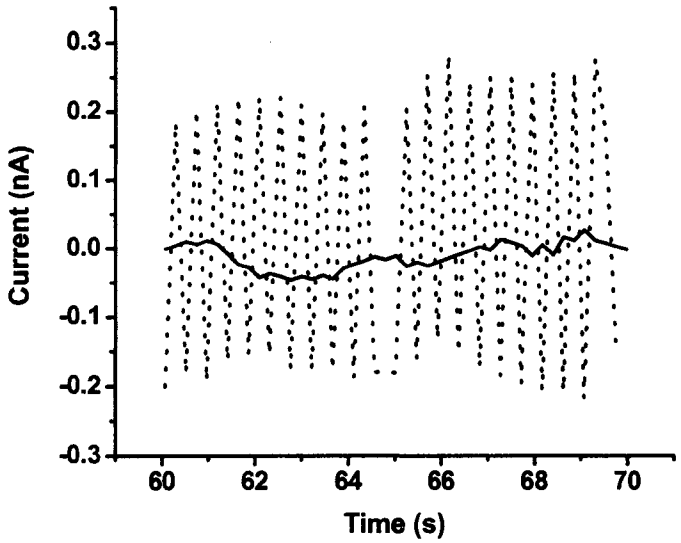

Figure 4.5 (A) Comparison of peak–peak noise baseline noise level values for the 110 V transformer (■) and 12 V battery (O) powered HVPS. (B) Comparison of baseline obtained for the transformer (---) and battery (—) powered HVPS. *E* = 900 V.

variety of conditions was described. The possibility of performing pinched, gated, and diffusion injection by changing the external connections between the DC–DC converters outputs and the timer inputs was also demonstrated. The inclusion of a microprocessor controlled timer simplifies the analysis and allows triggering of the detector simultaneously with the separation process. Once the HVPS is wired the operation is very simple. One of the advantages of the presented design is the use of a rechargeable internal battery to feed the HVPS, decreasing the noise with respect to the 110 V transformer. The present design does not need a PC to control the injection and allows on-site analysis without loss of performance.

4.7 Acknowledgments

The author appreciates Mr. Paul Anderson's dedicated work toward building the 3-channel HVPS. Without his help, the 3-channel HVPS can not become a reality. The author also thanks Dr. Carlos Garcia for his help in imaging sample injections and noise level investigation.

4.8 References

(1) Kappes, T.; Galliker, B.; Schwarz, M. A.; Hauser, P. C. *TrAC, Trends in Analytical Chemistry* **2001**, *20*, 133-139.
(2) Kappes, T.; Hauser, P. C. *Analytical Communications* **1998**, *35*, 325-329.
(3) Schwarz, M. A.; Galliker, B.; Fluri, K.; Kappes, T.; Hauser, P. C. *Analyst* **2001**, *126*, 147-151.
(4) Li, J.; Tremblay, T.-L.; Thibault, P.; Wang, C.; Attiya, S.; Harrison, D. J. *European Journal of Mass Spectrometry* **2001**, *7*, 143-155.

CHAPTER V

SIMPLE AND SENSITIVE ELECTRODE DESIGN FOR MICROCHIP CE-EC

At the time of carrying out urinary PAP determination, on-chip thin-film electrodes were widely used because they were able to be incorporated on the microchip substrate using microfabrication techniques.[1-3] As mentioned in the summary of PAP project, there are several disadvantages of thin-film electrodes. First, the microfabrication process requires a clean-room facility, which increases the microchip cost. Second, the lifetime of a microfabricated electrode can be affected by the running buffer and other experimental conditions.[4] Once the electrode fouls, a new chip must be made, which further increases the cost and time of the analysis. Microfabricated electrodes can also delaminate as a result of their use and/or cleaning. Moreover, the alignment of the electrode is a significant concern when irreversible sealing is used for the assembly of the microchip. Finally, the Au thin-film electrode can not be permanently deposited on PDMS surface due to the weak interaction between PDMS and Au.[5]

A new method to integrate working electrodes with PDMS microchips was highly desired. End-channel off-chip working electrodes have been used to overcome some of above drawbacks by several groups.[6-11] The end-channel off-chip electrode design refers to the system where the detection electrode is placed just outside of the separation channel and is separate from the microchip.[12, 13] This mode was predominantly used in the early stage of

microchip CE-EC because the distance between the channel exit and the working electrode allows sufficient decoupling of the separation voltage from the working electrode and detector without an additional decoupler.[7, 14-16] Moreover, the systems are generally easier to construct than microfabricated systems and provide an ultra-stable electrode. The coupling of off-chip electrodes with a microchip CE device, however, creates complications in obtaining precise spacing between the separation channel exit and the working electrode.[17] The distance between the channel outlet and working electrode affects the post-capillary band broadening. If the gap between the separation channel exit and the working electrode is too large, the sample plug diffuses into the detection reservoir before the analyte can be detected resulting in a loss in peak efficiency and intensity. If the gap is too small, it may be subject to lower isolation from the separation voltage and the noise increases. In addition, if the detection surface of the working electrode and the side of the microchip are not exactly parallel to one another, the working electrode collides with the edge of the microchip as it is moved toward the channel exit, preventing optimal alignment. To reach an optimal alignment of the working electrode, a 3-D position controller must be used, which reduces to portability and increases the cost and complexity.[17] To overcome some of these disadvantages, Ertl et al. developed a new end-channel detection scheme.[18] The approach utilized a sheath-flow-supported CE-EC system that allows efficient detection of analytes at a distance of up to 250 μm from the separation channel exit. In general, however, end-channel detection

produces higher background currents and is less sensitive than the other detection modes.

In-channel detection, a new approach to the integration of electrodes in microchip CE-EC devices, was presented by Martin et al.[19] Martin's team created a flow-onto CE-EC microchip band electrode detector by placing carbon paste within a channel of the PDMS layer outside the exit of the separation channel. The analytes migrated over the electrode while still confined to the channel, thus eliminating band-broadening. A vast improvement (4.6-fold) in the performance of EC detection for microchip CE was achieved, compared to the commonly used end-channel alignment even without use of decoupler.[19] However, the system required an electrically isolated potentiostat making the instrumentation complex.

The goal of this part of my thesis work was to develop a simple and sensitive electrode system for microchip CE-EC devices while minimizing the fabrication complexity. A novel design using a metallic microwire as the in-channel working electrode for microchip CE-EC is presented here. The microwire is aligned across the separation capillary using a premolded channel perpendicular to the separation channel in the PDMS. The method provides excellent chip-to-chip reproducibility of the working electrode location. Furthermore, because more surface area of the wire is exposed to the flow than either microfabricated or off-chip electrodes, higher collection efficiency is expected. Characterization of such a working electrode design is described in this chapter. Chapters VI and VII discuss some of the applications of the new system.

5.1 Experimental

5.1.1 Wire materials

Metallic microwires made of 99.9 % platinum (diameter 0.025 and 0.050 mm), 99.99 % gold wire (diameter 0.025 mm) and 99.99 % copper wire (diameter 0.025mm) were obtained from Goodfellow (Huntingdon, England).

5.1.2 Integration of microwire with microchip

The pattern of microchannel network was designed using FreeHand software and printed on a transparency mask. The pattern was then transferred to the master mold using the method described in Chapter II. After the PDMS with the channel network were fabricated, the detection wire was placed in the electrode channel. A PDMS replica with the working electrode and a blank piece of PDMS were placed simultaneously in an air plasma cleaner and oxidized for 45 s. The two pieces were then brought into conformal contact directly after removal from the plasma cleaner to form an irreversible seal. The final layout of microchip with working electrode is shown in Figure 5.1. The exclusive use of PDMS removes some of the band broadening mentioned in Chapter III in the determination of PAP.

5.1.3 Microchip CE-EC

Pinched injection through a double-T injector was employed for these experiments using the HVPS described in Chapter IV. The voltage setting for pinched injection is listed in Table 5.1.

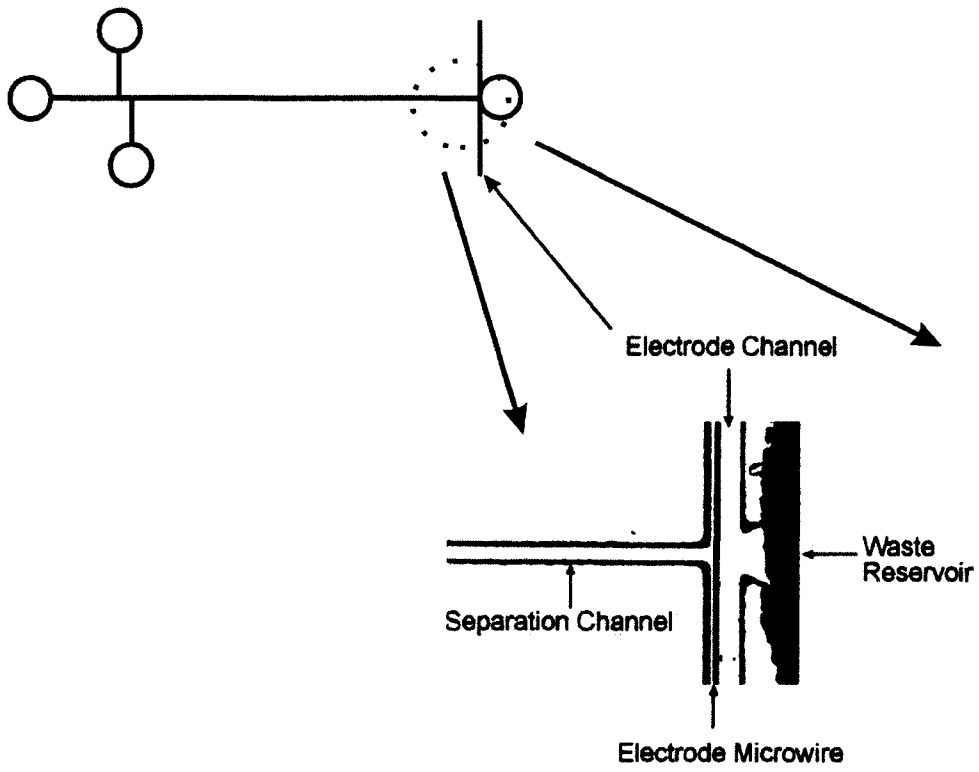

Figure 5.1: Top) Schematic of the microchip showing placement of the electrode alignment channel. Bottom) Photograph showing electrode alignment in a completed microchip

Table 5.1 Potential settings for separation and injection

Reservoir	Separation (V)	Injection (V)
Sample	+410	+410
Buffer	+1500	+410
Sample waste	+410	-160
Buffer waste	Ground	Ground

Amperometric electrochemical detection was employed (CHI812, CH Instruments) in a two-electrode configuration. Platinum wire (1 mm diameter) was used as the counter electrode. The working electrode materials and sizes varied between experiments. The electrode materials studied were platinum, gold, and copper, with diameters of 25 and 50 μm. After the electrode was aligned and sealed in place, a 0.80 mm copper wire was attached to the exposed wire end with conductive silver paint and held in place with glue to facilitate electrical contact. In situ cleaning of the working electrode was done every 20 runs via cyclic voltammetry with 20 sweeps segments from 0 V to 1.2V at the rate of 0.1 V/s while the buffer was electrokinetically pumped over the electrode.

5.2 Results and discussion

5.2.1 Electrode materials

The detector performance is strongly influenced by the material of working electrode. The selection of the working electrode depends primarily on the redox behavior of the target molecules and background current over the applied potential region. Selectivity in microchip CE-EC can therefore be obtained through judicious choice of the working electrode material and the applied potential. There are a wide variety of the electrode materials that can be incorporated, including carbon ink, carbon fiber, gold, platinum, palladium, and copper.[12] The influence of different electrode materials on the performance of two-electrode electrochemical detector in our simplified CE-EC was investigated.

Copper, gold, and platinum microwires were used as the working electrode, respectively. Electropherograms for catechol at each electrode material are shown in Figure 5.2. For the copper electrode, the separation current decreased with time. This is probably caused by the oxidation of copper electrode since our detection potential (0.8 V) is higher than copper oxidation potential (0.35 V). While Cu electrodes are not normally used for direct amperometric detection, it was used in this case as a simple demonstration of the concept and for comparison to other electrode materials. The migration time for catechol is different for each electropherogram but this is the result of inconsistent EOF which is common with irreversibly sealed PDMS.[20] This problem can be minimized by the non-covalent coating to the channel surface.[21, 22] The response for the Au and Pt electrodes is consistent with other reports for similar systems using the same electrode materials.[3] These results demonstrate our ability to easily incorporate electrodes of different sizes and materials in the microchip.

5.2.2 Limit of dection

The limit of detection (LOD) was determined as a function of electrode size. Electropherograms for 100 nM dopamine detected at a 50 μm electrode and 250-nM dopamine measured at a 25 μm electrode are shown in Figure 5.3. The experimental LOD of dopamine associated with 25 μm Au electrode is 250 nM and the LOD for the 50-μm Pt electrode is 100 nM with a 3:1 signal to noise ratio. The improvement in detection limit for the 50-μm electrode over the 25 μm electrode is in part because the 50 μm electrode has a larger surface area than

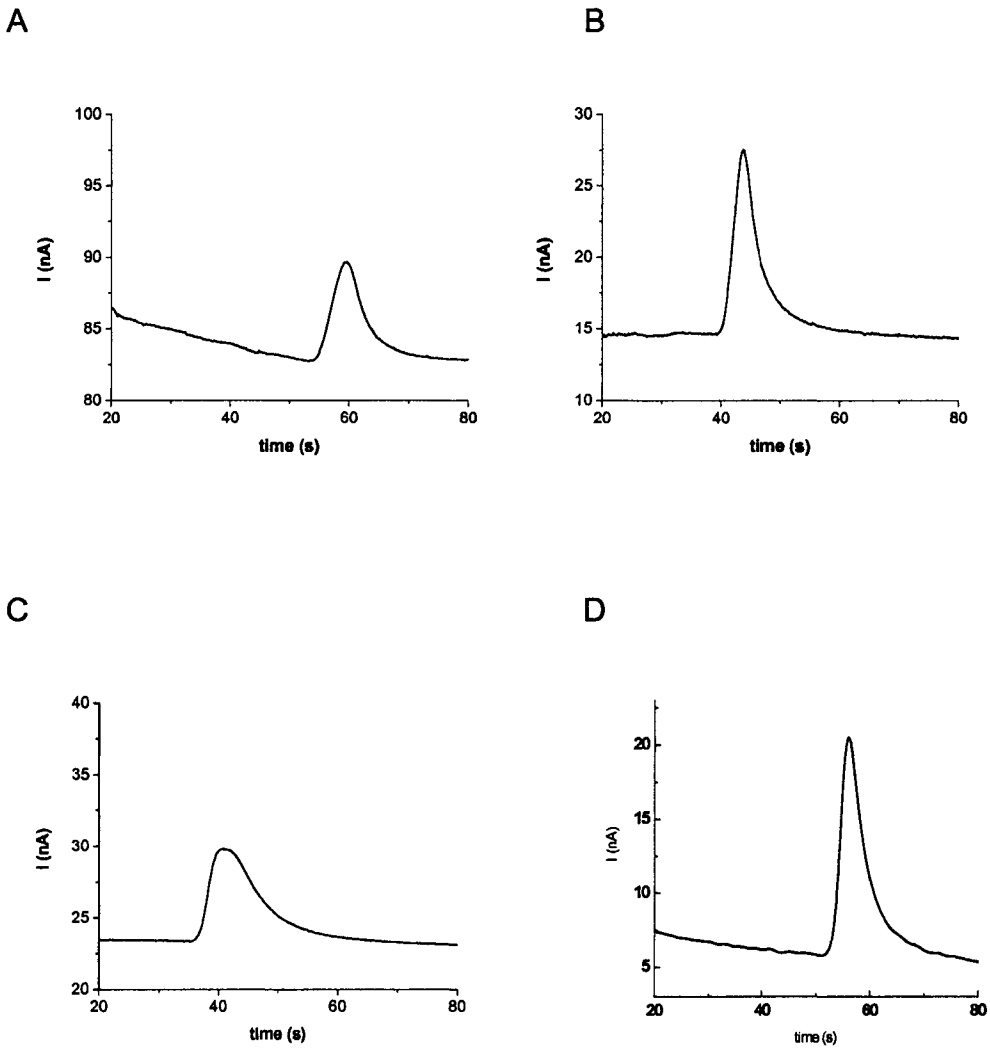

Figure 5.2: Electropherograms of 100 μM catechol: A) 25 μm Cu electrode B) 25 μm Au electrode C) 25 μm Pt electrode D) 50 μm Pt electrode. Experimental conditions: Separation voltage: 1500 V; Pinched injection time: 45 s; Running buffer: 20 mM TES (pH 7)

A

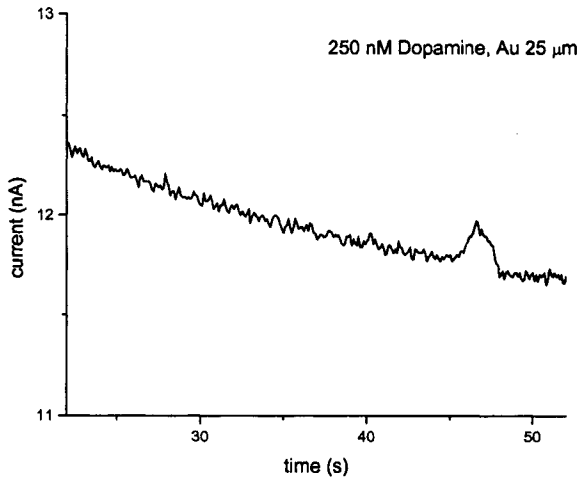

B

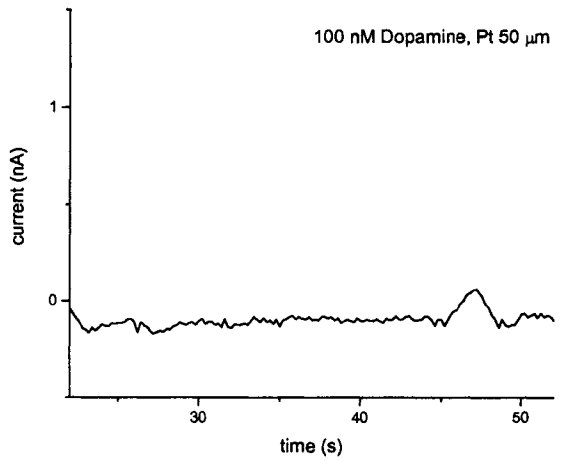

Figure 5.3 A) LOD of dopamine for 25 μm Au electrode (250 nM). B) LOD of dopamine for 50 μm Pt electrode (100 nM). Experimental conditions were the same as Figure 5.2.

25 μm electrode. The detection limit is the lowest reported to date without use of a decoupler.[23] The dynamic range of dopamine for 25 μm Pt electrode microchip was also investigated. The linear range for dopamine was found to be from 0.1 to 100 μM with an R^2 value of 0.993 and a sensitivity of 12.445 nC/μM.

5.2.3 Flow Profile

The low detection limit achieved with the 50 μm wire can not be the result of only the difference in the size of the electrode. Another consideration is the flow around the electrode. Figure 5.4 shows a schematic of the flow around the electrode in the separation channel. For the 25 μm electrode, there is more distance between the electrode and the channel wall compared to the 50 μm electrode. This should result in a higher collection efficiency at the larger electrode. The collection efficiency was calculated for both electrode sizes using Faraday's equation (Q = nFC). Theoretically, 1.2 nL of dopamine (100 μM) injected into the separation channel should have a peak area of 11.58 nC. The total charge passed as measured by the peak area was 4.21 nC and 10.49 nC for 25 μm and 50 μm electrodes, respectively. The collection efficiency given by the ratio of measured value to theoretical value for 25μm and 50 μm electrode is 36% and 90%, respectively, which is higher than microfabricated electrode (15-20%). The results demonstrate that the 50μm electrode dramatically improves the collection efficiency as a result of electrode alignment in the channel. This improvement in the collection efficiency results from the shorter diffusional pathlength for the analytes to the electrode surface.

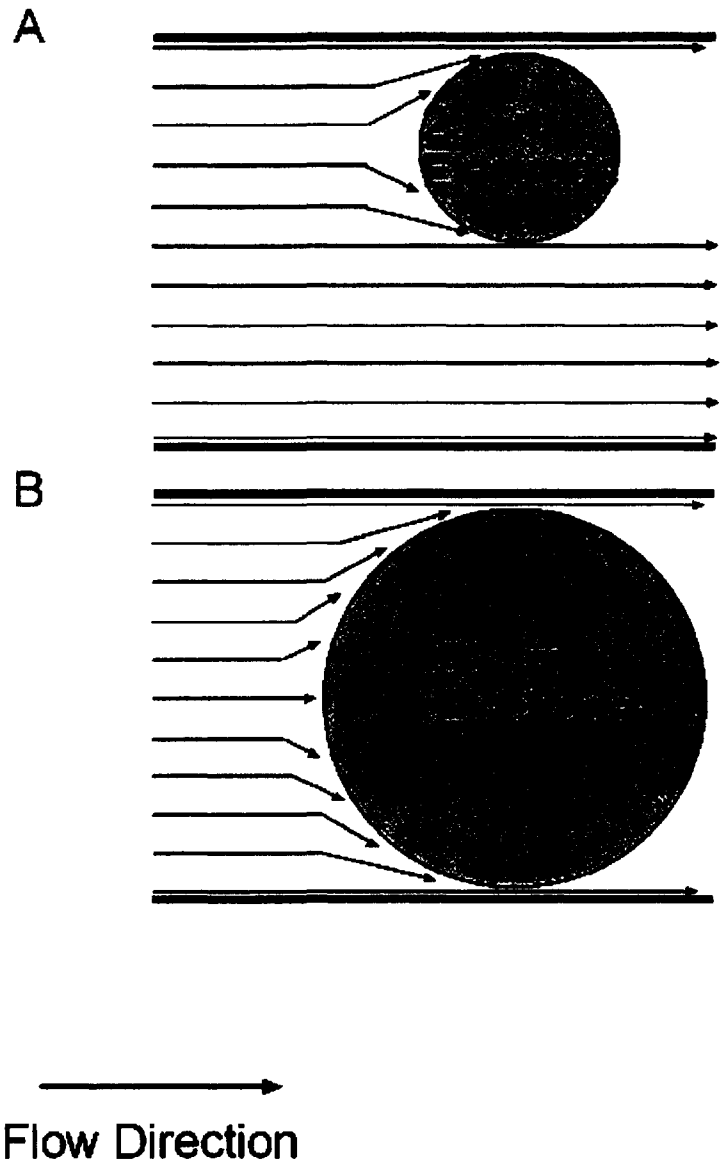

Figure 5.4 Schematic of flow around the microwire electrode in microchannel, drawn to scale. Location of the 25 μm electrode can vary vertically in the channel.

5.2.4 Electrode size

The electrode size plays an important role in the separation efficiency and resolution as well. The separation efficiency of dopamine and catechol was investigated for two different electrode sizes, 25 μm and 50 μm (Figure 5.5). For the 25 μm electrode, the two peaks from the oxidation of dopamine and catechol were well resolved (R = 1.54), while for 50 μm electrode, the resolution was 0.85. The separation efficiencies for the dopamine peak were 1923 plates/m for the 25 μm electrode and 1338 plates/m for the 50 μm electrode, respectively. The difference in separation efficiency is expected as the width of the electrode increases. The corresponding plate heights (H) are 0.52 mm and 0.75 mm for the 25 μm and 50 μm electrodes respectively, mirroring the increase in electrode width. Although the separation efficiencies are low, they can be improved for both electrodes by reducing the injection volume and modifying the surface of the PDMS. The trends in the separation efficiency and resolution are still valid irrespective of the large injection volume.

5.3 Conclusions

A simple, flexible and sensitive microwire working electrode design was presented in this chapter. The alignment of the working electrode was easy to complete by simply putting the microwire into the prepatterned electrode channel before sealing the chip. The microwire design exposes more surface area to the flow thus high collection efficiency is achieved. A 100 nM LOD of dopamine was reached, making the lowest level reported without using a decoupler. To

A

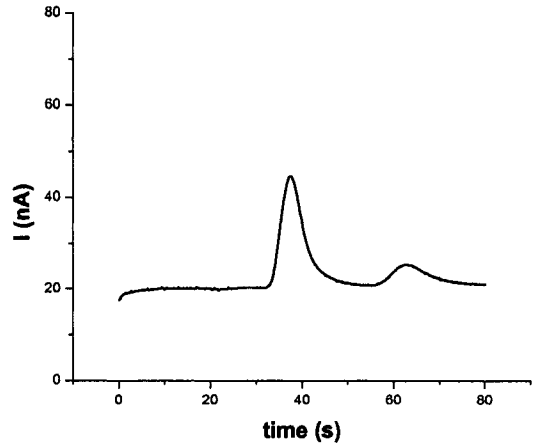

B

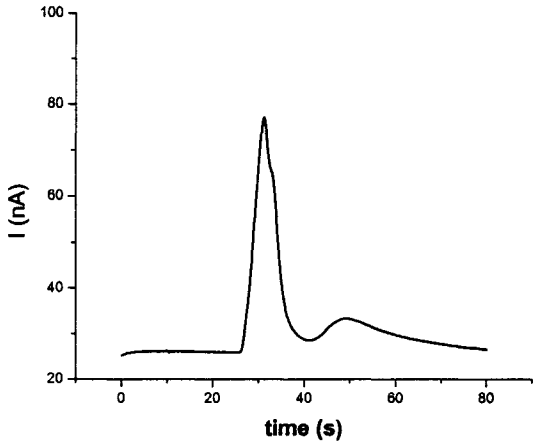

Figure 5.5 Separations of 100 μM dopamine and catechol. A) 25 μm Au electrode; B) 50 μm Pt electrode. Experimental conditions were the same as Figure 5.2

increase the system sensitivity, more work such as employing a decoupler can be completed. The only change that should be made is to add a second electrode channel prior to the working electrode channel and align the decoupler wire into the second channel. The presented working electrode design should have a wide variety of applications.

5.4 Acknowledgments

The project was supported by Colorado State University. The author also thanks Jonathan Vickers for his help in this project.

5.5 References

(1) Wang, J.; Pumera, M.; Chatrathi, M. P.; Rodriguez, A.; Spillman, S.; Martin, R. S.; Lunte, S. M. *Electroanalysis* **2002**, *14*, 1251-1255.
(2) Woolley, A. T.; Lao, K.; Glazer, A. N.; Mathies, R. A. *Anal Chem* **1998**, *70*, 684-688.
(3) Martin, R. S.; Gawron, A. J.; Lunte, S. M. *Anal Chem* **2000**, *72*, 3196-3202.
(4) Lunte, S. M.; Martin, R. S.; Lunte, C. E. *Electroanalytical Methods for Biological Materials* **2002**, 461-490.
(5) Lee, K. J.; Fosser, K. a.; Nuzzo, R. G. *Adv. Funct. Mater.* **2005**, *15*, 557-566.
(6) Gawron, A. J.; Martin, R. S.; Lunte, S. M. *Electrophoresis* **2001**, *22*, 242-248.
(7) Martin, R. S.; Gawron, A. J.; Fogarty, B. A.; Regan, F. B.; Dempsey, E.; Lunte, S. M. *Analyst* **2001**, *126*, 277-280.
(8) Wang, J.; Chen, G.; Muck, A., Jr.; Shin, D.; Fujishima, A. *J Chromatogr A* **2004**, *1022*, 207-212.
(9) Coltro, W. K.; da Silva, J. A.; da Silva, H. D.; Richter, E. M.; Furlan, R.; Angnes, L.; do Lago, C. L.; Mazo, L. H.; Carrilho, E. *Electrophoresis* **2004**, *25*, 3832-3839.
(10) Lee, H.-L.; Chen, S.-C. *Talanta* **2004**, *64*, 750-757.
(11) Castano-Alvarez, M.; Fernandez-Abedul, M. T.; Costa-Garcia, A. *Analytical and Bioanalytical Chemistry* **2005**, *382*, 303-310.
(12) Lacher, N. A.; Garrison, K. E.; Martin, R. S.; Lunte, S. M. *Electrophoresis* **2001**, *22*, 2526-2536.

(13) Vandaveer, W. R. I. V.; Pasas-Farmer, S. A.; Fischer, D. J.; Frankenfeld, C. N.; Lunte, S. M. *Electrophoresis* **2004**, *25*, 3528-3549.
(14) Garcia, C. D.; Henry, C. S. *Electroanalysis* **2005**, *17*, 223-230.
(15) Wang, J.; Zima, J.; Lawrence Nathan, S.; Chatrathi Madhu, P.; Mulchandani, A.; Collins Greg, E. *Analytical chemistry* **2004**, *76*, 4721-4726.
(16) Zhong, M.; Zhou, J.; Lunte, S. M.; Zhao, G.; Giolando, D. M.; Kirchhoff, J. R. *Analytical Chemistry* **1996**, *68*, 203-207.
(17) Fanguy, J. C.; Henry, C. S. *Electrophoresis* **2002**, *23*, 767-773.
(18) Ertl, P.; Emrich, C. A.; Singhal, P.; Mathies, R. A. *Anal Chem* **2004**, *76*, 3749-3755.
(19) Martin, R. S.; Ratzlaff, K. L.; Huynh, B. H.; Lunte, S. M. *Anal Chem* **2002**, *74*, 1136-1143.
(20) Ocvirk, G.; Munroe, M.; Tang, T.; Oleschuk, R.; Westra, K.; Harrison, D. J. *Electrophoresis* **2000**, *21*, 107-115.
(21) Liu, Y.; Fanguy, J. C.; Bledsoe, J. M.; Henry, C. S. *Anal Chem* **2000**, *72*, 5939-5944.
(22) Liu, Y.; Wipf, D. O.; Henry, C. S. *Analyst* **2001**, *126*, 1248-1251.
(23) Osbourn, D. M.; Lunte, C. E. *Anal Chem* **2003**, *75*, 2710-2714.

CHAPTER VI

ANALYSIS OF ANIONS IN AEROSOL PARTICLES

One advantage of microwire electrode design is the flexibility of coupling more than one microwire with the microfluidic device when multiple electrodes are needed. This can be accomplished by adding more electrode alignment channels in PDMS. In this chapter, a microchip CE-EC system with multiple (up to three) microwires is presented. This system was employed in the analysis of anions in airborne particles.

An aerosol is a suspension of fine solid or liquid particles in gas.[1, 2] Identification and quantification of chemical components in aerosols provide important information to investigate air pollution sources, sinks, transports and their effects on human health and the environment.[3-8] Inorganic anions, especially sulfate and nitrate, contribute significantly to particulate matter mass.[2, 9-11] Both sulfate and nitrate are frequently major components of regional haze.[12] Currently, analysis of aerosol inorganic ions relies heavily on ion chromatography (IC) techniques.[2, 9, 13, 14] In the past several years, researchers have successfully coupled IC with novel aerosol collectors for near real-time aerosol ionic quantification.[2] Although these instruments represent the state-of-the-art in aerosol analysis, large consumption of sample and reagents, and size and cost of the instrumentation prevent them from massive deployment by large monitoring networks such as those operated by

The Environmental Protection Agency (EPA) and the Interagency Monitoring of Protected Visual Environments (IMPROVE, National Park Service) network.[9, 13] Development of novel aerosol instrumentation with portability and simple and sensitive analysis is of utmost importance in the study of aerosol chemistry.

Microchip CE-EC is a perfect system for the analysis of airborne particles. Although most analyte species in the atmosphere are not electrochemically active, conductivity detection can still be coupled with microchip CE.[15-19] Conductivity detection is based on the change in bulk solution conductivity or resistance between two electrodes when an analyte band passes through the electrode gap. Conductivity detection is ideal for inorganic ion detection since the ions cause a change in the conductivity between electrodes. Most microchip CE devices using conductivity detection employ contactless conductivity detection where the working electrodes are electrically isolated from the separation potential by an insulating layer.[20-22] Although this mode is effective in isolating working current from the separation current leading to a high sensitivity, it requires more complex high frequency waveforms and does not lend itself to development of a simple inexpensive detector which is needed for atmospheric research. In a contact conductivity detection mode, the working electrodes are placed in direct contact with the solution and thus a lower excitation frequency is required. This detection mode has already proven sensitive when used at the microchip scale.[15]

The goal of this chapter is to develop small, sensitive, affordable aerosol analysis systems that are complimentary to the existing techniques for long term in field monitoring of aerosols. A simple and effective microchip CE system with contact conductivity detection to analyze sulfate and nitrate in airborne particles is described here. The experimental conditions, including electrode materials, ionic strength of running buffer, and electrode configuration, were optimized. The quantification of sulfate and nitrate in aerosol samples was carried out and compared with IC. To the best of our knowledge, this represents the first extension of microchip CE to the analysis of aerosol samples.

6.1 Experimental

6.1.1 Preconditioning the microchannel

The microchip channels were first treated with 0.1 M NaOH for 30 mins, followed by H_2O rinsing for 15 mins. The channel was coated with 3% (w/v) polybrene aqueous solution for at least 30 minutes. The positively charged polybrene covered the microchannel wall due to the electrostatic interaction between the polymer and the silanol group on the channel surface. (Coating the channel with polyelectrolytes was the focus of my M.S. degree at Mississippi State University) As a result, a positively charged surface was generated which reversed the direction of electroosmotic flow in the microchannel. 75 μL of sample was placed in the sample reservoir, while 70

μL of buffer solution was placed in all other reservoirs to effect hydrodynamic injection. Prior to running, high voltage was applied for 30 min to stabilize the system. Injections were performed hydrodynamically for 15 s according to Chapter IV. The potential settings for injection and separation mode are listed in Table 6.1.

6.1.2 Microchip CE with conductivity detection

Conductivity detection was carried out using Crystal 1000 detector (ATI Unicam, Madison, WI) in contact mode. Three different electrode configurations with varying numbers of on-column microwires were employed in these experiments.

For the one-electrode on-column system, the first working electrode, either Au or Pd microwire, was placed inside an electrode alignment channel located at the end of the separation channel, directly in front of the detection reservoir in a configuration very similar to that used for amperometric detection described in the previous chapter (Figure 6.1). The second working electrode (Pt) and the ground electrode to complete the separation circuit were placed in the buffer waste reservoir. The solution resistance outside of the channel is negligible compared to the solution resistance inside the channel and therefore, the active portion is the channel region between the wire and the reservoir.

Table 6.1 Voltage configurations for hydrodynamic injection

Reservoir	Separation Mode	Injection mode	Volume (μL)
Sample	-400 V	No voltage	75
Sample waste	Ground	No voltage	70
Buffer	-400 V	No voltage	70
Buffer waste	Ground	No voltage	70

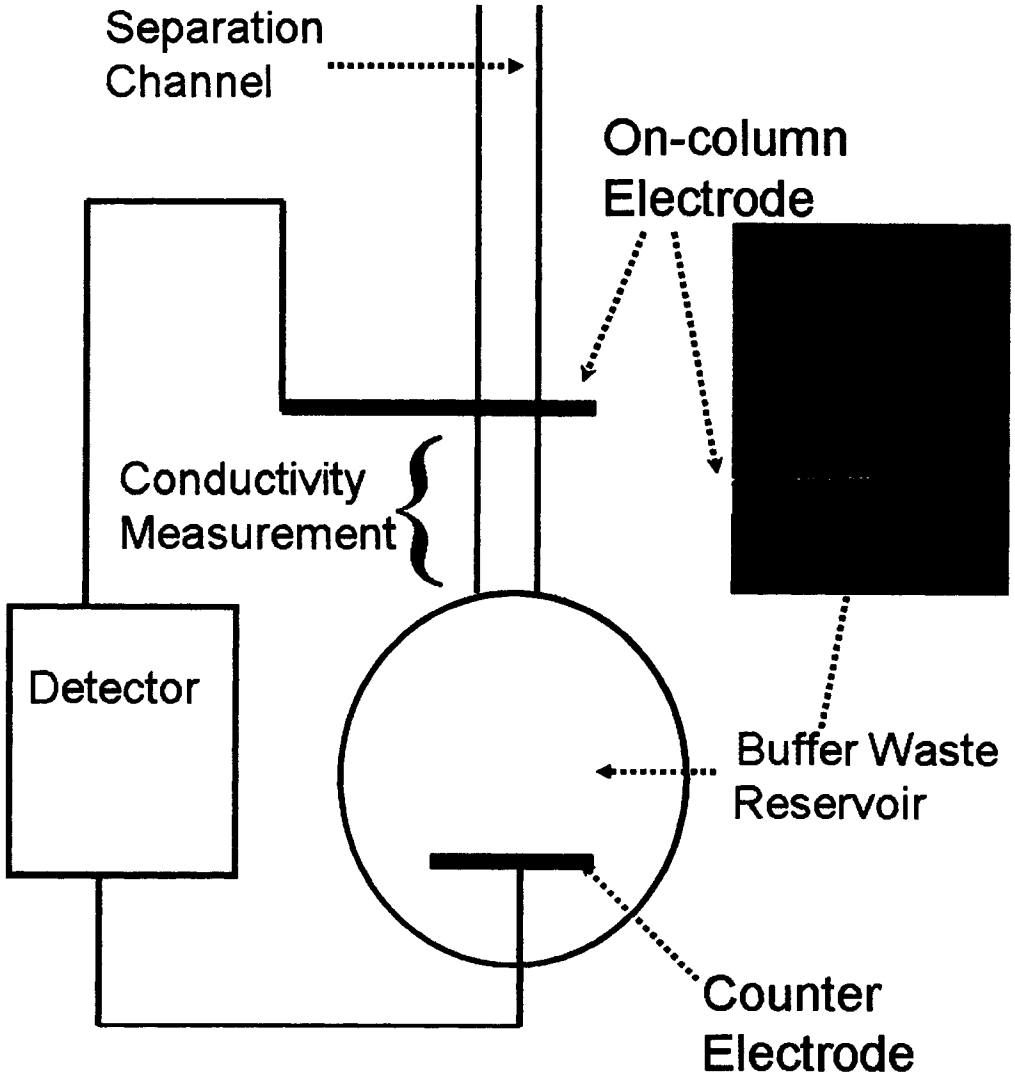

Figure 6.1 One-electrode on-column configuration for microchip CE-EC.

For the two-electrode on-column system, both working electrodes (Au microwires) were placed in the electrode channels at the end of the separation channel (Figure 6.2). The ground electrode to complete the separation circuit was placed in the buffer waste reservoir. The conductivity detector measures the solution resistance between the two working electrodes.

The third configuration places three electrodes, one ground and two working electrodes in the electrode channels, respectively. As shown in Figure 6.3, Pd wire is employed as the decoupler to isolate the electrophoretic current from the detector. Again, the solution resistance between two working electrodes (Au microwires) was monitored.

6.2 Results and Discussion

6.2.1 Electrode materials

One advantage of the microwire electrode design used in these studies is the wide variety of the electrode materials that can be incorporated, as was demonstrated previously.[23] The influence of electrode material on the performance of conductivity detector was investigated in a one-electrode on column mode. Au and Pd microwires (25 μm in diameter) were used as the working electrode, respectively. Pd wire was investigated because of its H_2 absorbing ability and the potential to incorporate it anywhere in the channel. Electropherograms for sulfate (first peak) and nitrate (second peak) at each

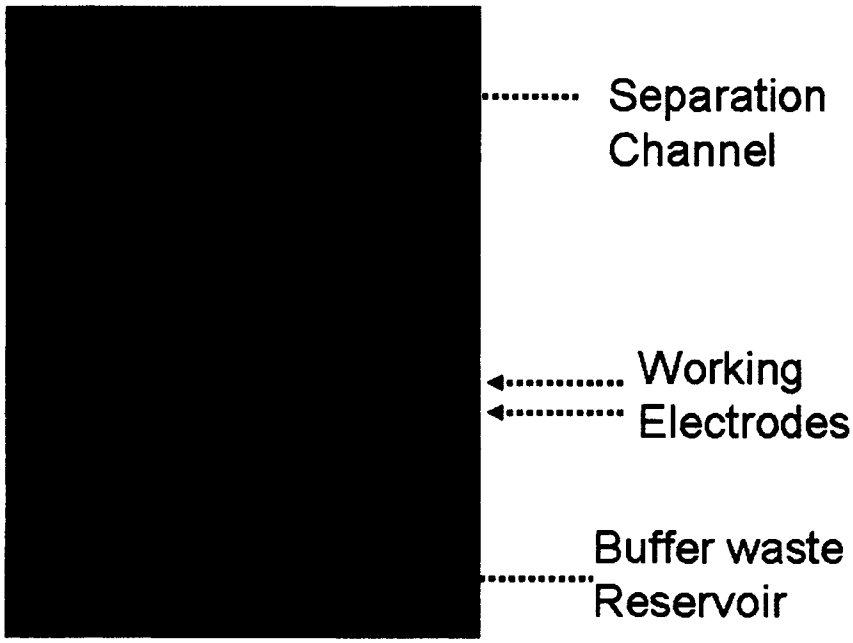

Figure 6.2 Two-electrode on-column system.

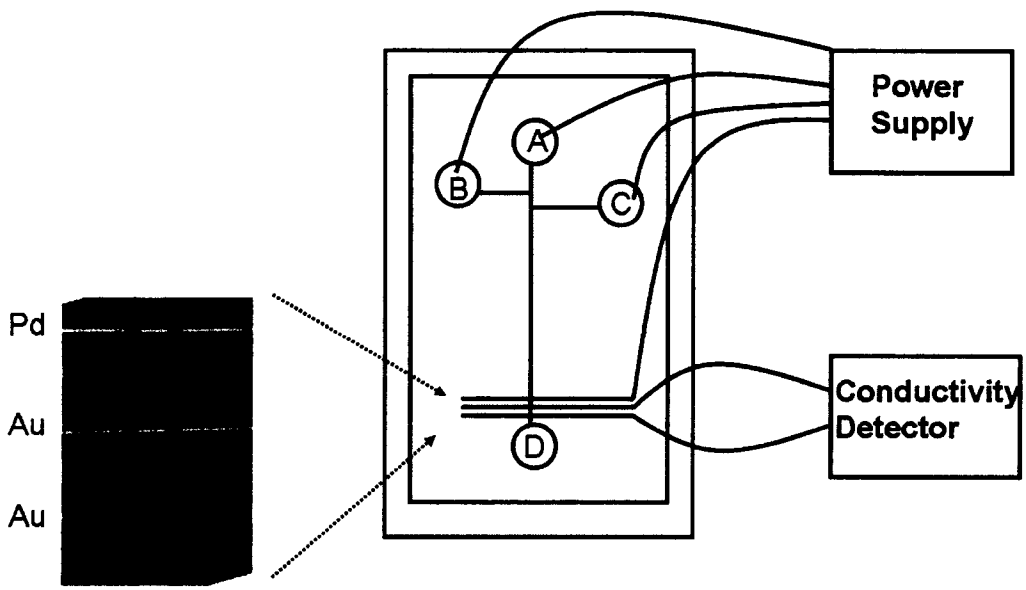

Figure 6.3 Three-electrode system; Left: photograph of working electrode and decoupler alignment. A. sample reservoir, B. sample waste reservoir, C. buffer reservoir, D. buffer waste reservoir

electrode material are shown in Figure 6.4. Both microwire electrodes showed similar conductivity response to sulfate and nitrate.

The limit of detection (LOD) and the dynamic range of sulfate and nitrate were obtained for both Au and Pd electrode. The experimental results are shown as Table 6.2. The experimental LOD of sulfate and nitrate associated with Au electrode is 1 μM with a 3:1 signal to noise ratio and the LOD for Pd electrode is 10 μM. The linear range for sulfate (Au chip) was found to be from 1 to 250 μM with an R^2 value of 0.998 and a sensitivity of 823 μV/μM. The linear range for nitrate (Au wire) was found to be from 5 to 500 μM with an R^2 value of 0.989 and a sensitivity of 498 μV /μM. The linear range for sulfate (Pd wire) was found to be from 10 to 100 μM with an R^2 value of 0.994 and a sensitivity of 809 μV /μM. The linear range for nitrate (Pd wire) was found to be from 60 to 500 μM with an R^2 value of 0.998 and a sensitivity of 288 μV /μM. The improvement in detection limit for the Au electrode over the Pd electrode is in part because Au is more conductive than Pd. Au electrodes were used for the remaining of the experiments.

6.2.2 Ionic Strength

The ionic strength of mobile phase can affect the sensitivity and resolution of CE separations when conductivity is used. The effects of running buffer concentration were therefore investigated to optimize sensitivity and resolution. The migration time of NO_3^- increased from 84s to 168s when the

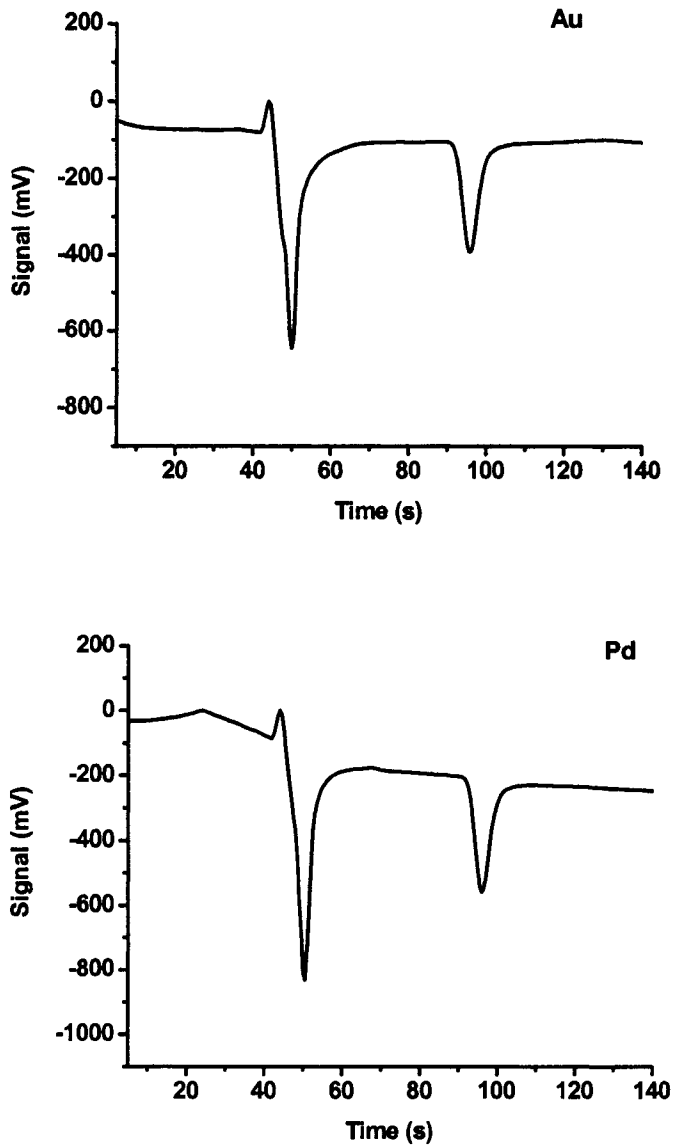

Figure 6.4: Separation of sulfate and nitrate. A. Au working electrode; B. Pd working electrode. Experimental conditions: separation voltage, -400V; hydrodynamic injection, 10 s; sample concentration, 1 mM.

Table 6.2: result comparison between Au and Pd working electrode microchip

		Au	Pd
Sulfate	LOD(μM)	1	10
	Linear range(μM)	1-250	10-100
	R^2	0.998	0.994
	Sensitivity(mV/μM)	0.823	0.809
Nitrate	LOD(μM)	1	10
	Linear range(μM)	5-500	60-500
	R^2	0.989	0.998
	Sensitivity(mV/μM)	0.498	0.288

buffer concentration increased from 5 mM to 20 mM, while the migration time of SO_4^{2-} changed from 57 s to 68 s. This is consistent with the effect of ionic strength on EOF. The dependence of bulk solution mobility on ionic strength is given by $\mu_{eof} \propto c^{-1/2}$.[24] When buffer concentration increases, the EOF will decrease as the square root of the buffer concentration.

The effects of ionic strength on the detection sensitivity were also investigated using a 1 mM SO_4^{2-} and NO_3^- solution as the standard. The peak height of sulfate and nitrate reached a maximum, 845 and 397 mV, respectively, when the concentration of running buffer was 10 mM. When the buffer was at 5 mM, the peak height of SO_4^{2-} and NO_3^- was 583 and 370 mV. When 20 mM buffer was used, the peak heights for SO_4^{2-} and NO_3^- were 509 and 165 mV, respectively. At higher concentration, the working electrode was overloaded with charged species in the solution. 10 mM buffer provided the best signal response and was employed as the running electrolyte solution.

6.2.3 Reproducibility

One concern with long-term aerosol sample analysis is reproducibility. The analyte migration time was considered as an indicative factor of day-to-day, run-to-run, and chip-to-chip reproducibility. For single day use, the average value of sulfate and nitrate migration time was 53.1±4.7 s and 93.0±3.5 s (n=14), respectively. The seven day average for sulfate and nitrate migration time was 50.9±3.6 s and 97.7±7.7 s, respectively. The consistent

migration time is due to the consistency of EOF in polybrene coated channels.[25] The good reproducibility of the coatings suggests validity as a long-term monitoring system.

6.2.4 Multiple-electrode system

Above experimental results were obtained using one-electrode on-column system. The drawback of the one-electrode mode was the inconsistency of the distance between the first working electrode and the exit of the separation channel. To fix the problem, two-electrode mode was employed. Although the gap distance between two working electrodes are constant, new problems appeared. For example, bubbles were formed on the working electrode surface due to the high electric field in channel. A third generation three-electrode chip was investigated. Meanwhile, to generate more uniform microchannel surface, a second layer of PB was deposited. Prior to the second PB layer coating, dextran sulfate was pumped through the channel to generate a negatively charged surface to bind to the PB. The coating procedures are shown as Figure 6.5.

Interferences from high electric field and electrophoretic current are observed as an increase in background noise. The degree of interference is associated with the concentration and conductivity of the electrolyte within the separation channel.[26] Under the high electric field of electrophoresis, electrolysis of water can also result in production of hydrogen. The generated

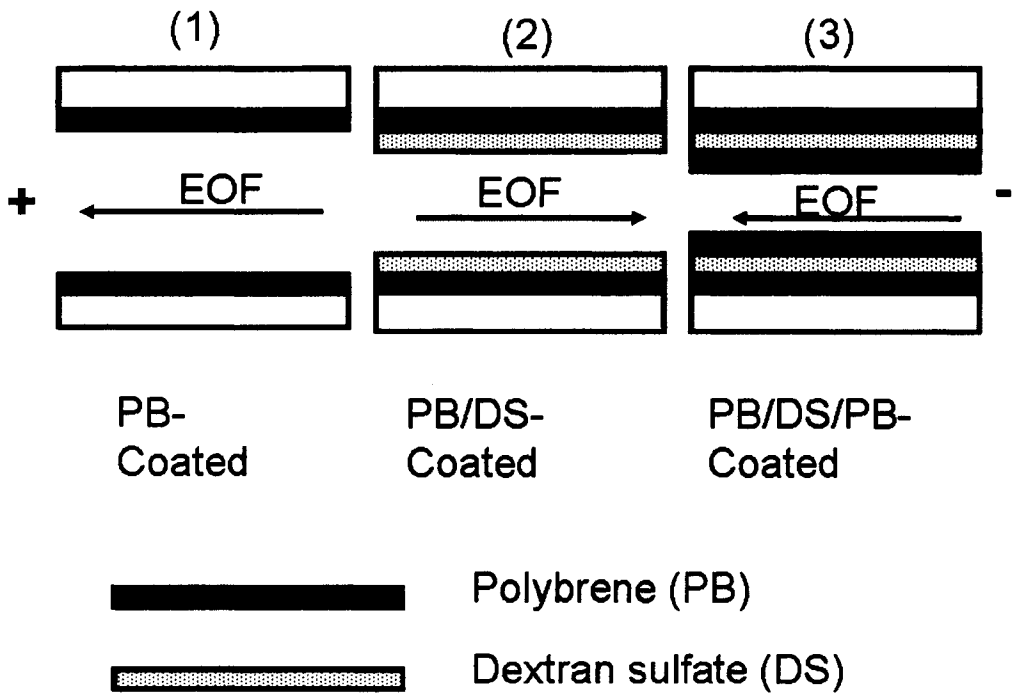

Figure 6.5 Multiple layer coating for microchannel.

hydrogen is accumulated on the electrode surface and forms gas bubbles that block the channel. If a Pd electrode is used, the hydrogen adsorbs onto the Pd surface then diffuses into bulk phase. As a result, hydrogen is removed from the Pd surface before the gas bubbles are formed.[27]

6.2.5 Sample Analysis

Three different previously prepared liquid aerosol samples were analyzed using microchip CE-conductivity detection. The samples were collected on a filter and extracted in DI water. Electropherograms are shown in Figure 6.6. The two negative peaks correspond to SO_4^{2-} and NO_3^-, respectively, while the positive peak is due to water. The water peak appears in the real samples that were extracted with water. Laboratory standards were prepared in buffer and therefore did not contain this negative peak. The concentrations for three different samples were compared to the results obtained by ion chromatography (Table 6.3). The results for SO_4^{2-} and NO_3^- are consistent with IC results

6.3 Conclusions

Analyses of sulfate and nitrate in aerosol particles were demonstrated in a microfluidic device with conductivity detection. This work represents the first application of microchip CE with conductivity detection to the determination of the chemical composition of aerosol samples. Three different electrode

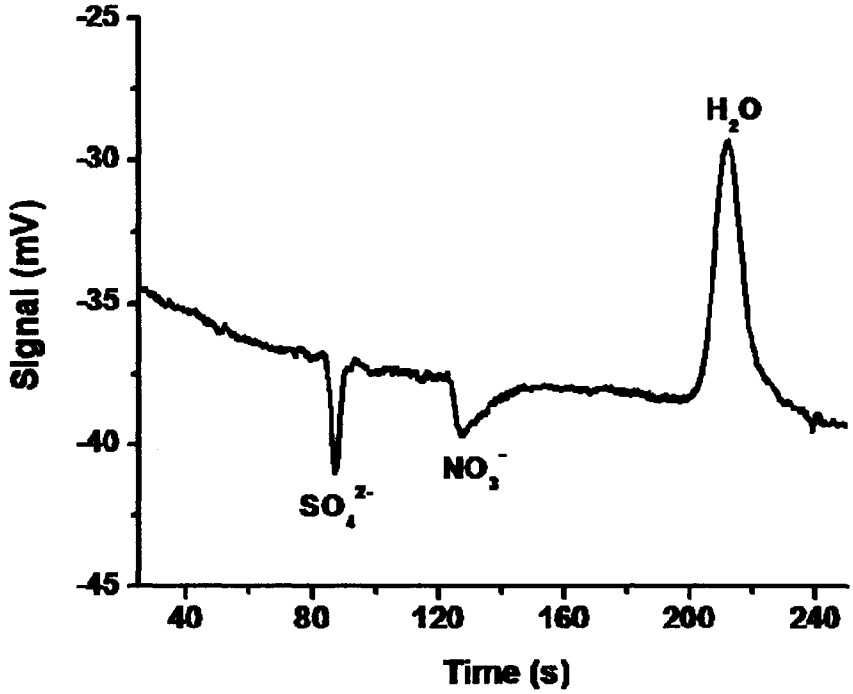

Figure 6.4. A representative electropherogram for a real aerosol sample.

Table 6.3: Comparison of sample analysis between microchip and IC.

Sample	SO_4^{2-}		NO_3^-	
Number	Microchip	IC	Microchip	IC
021503	41	44	62	53
021403	55	61	123	114
020103	101	90	108	115

* unit: μM

configurations further demonstrate the flexibility of microwire working electrode design for microchip CE-EC.

6.4 Acknowledgments

Financial support of this project was from EPA and DOE. The author thanks Dave MacDonald, Dr. Xiao-Ying Yu, and Dr. Jeffery Collett for their collaborative work.

6.5 References

(1) Baek, B. H.; Aneja, V. P. *J Air Waste Manag Assoc* **2004**, *54*, 623-633.
(2) Al-Horr, R.; Samanta, G.; Dasgupta, P. K. *Environ Sci Technol* **2003**, *37*, 5711-5720.
(3) Hollander, W.; Stober, W. *Arch Toxicol Suppl* **1986**, *9*, 74-87.
(4) Winchester, J. W. *Biol Trace Elem Res* **1990**, *26-27*, 195-212.
(5) Ziemann, P. J.; McMurry, P. H. *J Colloid Interface Sci* **1997**, *193*, 250-258.
(6) Deboudt, K.; Flament, P.; Weis, D.; Mennessier, J. P.; Maquinghen, P. *Sci Total Environ* **1999**, *236*, 57-74.
(7) Ames, R. B.; Hand, J. L.; Kreidenweis, S. M.; Day, D. E.; Malm, W. C. *J Air Waste Manag Assoc* **2000**, *50*, 665-676.
(8) Polissar, A. V.; Hopke, P. K.; Poirot, R. L. *Environ Sci Technol* **2001**, *35*, 4604-4621.
(9) Yan, Z.; Yanyan, L.; Fritz, J. S.; Haddad, P. R. *J Chromatogr A* **2003**, *1020*, 259-264.
(10) Blanchard, C. L.; Hidy, G. M. *J Air Waste Manag Assoc* **2003**, *53*, 283-290.
(11) Sukhapan, J.; Brimblecombe, P. *ScientificWorldJournal* **2002**, *2*, 1138-1146.
(12) Hogrefe, O.; Schwab, J. J.; Drewnick, F.; Lala, G. G.; Peters, S.; Demerjian, K. L.; Rhoads, K.; Felton, H. D.; Rattigan, O. V.; Husain, L.; Dutkiewicz, V. A. *J Air Waste Manag Assoc* **2004**, *54*, 1040-1060.
(13) Nanni, E. J.; Lovette, M. E.; Hicks, R. D.; Fowler, K. W.; Borgerding, M. F. *J Chromatogr Sci* **1990**, *28*, 432-436.
(14) Lin, J. J. *Environ Int* **2002**, *28*, 55-61.

(15) Galloway, M.; Stryjewski, W.; Henry, A.; Ford, S. M.; Llopis, S.; McCarley, R. L.; Soper, S. A. *Anal Chem* **2002**, *74*, 2407-2415.
(16) Dolnik, V.; Liu, S.; Jovanovich, S. *Electrophoresis* **2000**, *21*, 41-54.
(17) Zemann, A. *G.I.T. Laboratory Journal, Europe* **2003**, *7*, 60-62.
(18) Ling, B. L.; Baeyens, W. R. G.; Dewaele, C. *Analytica Chimica Acta* **1991**, *255*, 283-288.
(19) Liu, Y.; Wipf, D. O.; Henry, C. S. *Analyst* **2001**, *126*, 1248-1251.
(20) Wang, J.; Pumera, M.; Collins, G.; Opekar, F.; Jelinek, I. *Analyst* **2002**, *127*, 719-723.
(21) Guijt, R. M.; Baltussen, E.; van der Steen, G.; Frank, H.; Billiet, H.; Schalkhammer, T.; Laugere, F.; Vellekoop, M.; Berthold, A.; Sarro, L.; van Dedem, G. W. *Electrophoresis* **2001**, *22*, 2537-2541.
(22) Pumera, M.; Wang, J.; Opekar, F.; Jelinek, I.; Feldman, J.; Lowe, H.; Hardt, S. *Anal Chem* **2002**, *74*, 1968-1971.
(23) Liu, Y.; Vickers Jonathan, A.; Henry Charles, S. *Analytical chemistry* **2004**, *76*, 1513-1517.
(24) Weston, A.; Brown, P. R. *HPLC and CE Principles and Practices*; Academic Press: San Diego, 1997.
(25) Liu, Y.; Fanguy, J. C.; Bledsoe, J. M.; Henry, C. S. *Anal Chem* **2000**, *72*, 5939-5944.
(26) Wu, C. C.; Wu, R. G.; Huang, J. G.; Lin, Y. C.; Hsien-Chang, C. *Anal Chem* **2003**, *75*, 947-952.
(27) Wang, J. *Electroanalysis* **2005**, *17*, 1133-1140.

CHAPTER VII

USING CAPILLARY ELECTROPHORESIS TO STUDY BIOLOGICAL OXIDATION REACTIONS

The second application of developed system was to study biological oxidation reactions, mainly the behavior of reactive oxygen species (ROS). The cell damaging effects of ROS such as hydrogen peroxide (H_2O_2), superoxide ion (O_2^-) and hydroxyl radical ($OH^\bullet$) have been implicated in many diseases (cancer, Alzeimer's and Parkinson's) and in aging.[1] The presence of antioxidants, both natural and dietary, effectively balances the formation and removal of ROS in biological systems.[2] Glutathione (GSH, L-γ-glutamyl-L-cysteinylglycine) is the most abundant naturally occurring low-molecular mass water-soluble antioxidant, as well as an essential cofactor for antioxidant enzymes, in mammals.[3] GSH is present in many physiological fluids and animal and microbial cells.[4] GSH provides protection for biological organisms against oxidative injury through its chemical and/or enzymatic conversion to glutathione disulfide (GSSG).[5] There is also increasing evidence for the involvement of GSH in metabolic regulation, signal transduction and regulation of gene expression.[6-8] The high electron-donating capacity of GSH combined with its high intracellular concentration (mM) endows GSH with reducing power, which is used to regulate a complex thiol-exchange system.[9] Moreover, GSH is important for protein preservation

in most living cells and participates in diverse biological processes.[10] The change of GSH concentration in biological fluids or tissues may be a useful biomarker in certain disorders such as leukemia, diabetes, and DNA base damage.[2] From a medical perspective, the GSH/GSSG ratio serves as a sensitive indicator of oxidative stress and a key marker for the redox status of cells.[11] A thorough understanding of the oxidative reactions involving GSH in aqueous solution should be useful for obtaining a better understanding of cellular oxidative damage as well as evaluating the ability of antioxidants to protect biological systems.

There have been several methods reported for GSH analysis.[11-16] In biological samples, the most commonly used technique is Ellman's method which involves in a reaction between 5,5'-dithiobis(2-nitrobenzoic acid) and GSH.[16, 17] Indirect measurement of GSH is made by spectrophotometrically monitoring the absorbance change of the reaction product, 2-nitro-5-mercapto-benzoic acid, at 410 nm. Another approach is the use of enzymatic methods which immobilize glutathione peroxidase on an electrode surface.[2] This enzyme catalyzes the oxidation of GSH to GSSG in the presence of hydrogen peroxide. GSSG is subsequently monitored by direct spectroscopic measurement at 305 nm. Although spectroscopic techniques offer simplicity, they can only follow one reagent and can therefore miss important information. Other methods that have been used in the analysis of GSH include gas chromatography-mass spectrometry, liquid

chromatography-mass spectrometry, electron paramagnetic resonance spectroscopy and nuclear magnetic resonance spectroscopy.[14, 18, 19] High-performance liquid chromatography (HPLC) has recently become the method of choice for measuring GSH and related thiols in biological samples.[14] HPLC techniques are highly specific, sensitive and reproducible. The simultaneous determination of GSH and other thiols in a single assay may be achieved by the appropriated choice of column, derivatization and elution protocols and detection system. The methods are less susceptible to the interference problems than direct spectroscopic methods and provide the separation between the reactants and products. Electrochemical, fluorometric and ultraviolet detections have all been coupled with HPLC to analyze GSH.[18] Kachur et al proposed a HPLC method to simultaneously monitor the concentration change of GSH, H_2O_2, and GSSG for copper-catalyzed oxidation of GSH.[20]

Capillary electrophoresis (CE) is a well-known ultrasmall-volume analytical separation technique for the analysis of charged species in biological samples.[21] Compared to HPLC, CE provides higher separation efficiency while consuming less reagent and sample. CE has been used primarily for the determination of GSH and GSSG in red blood cells.[22-27] To date no reports have dealt with the use of CE to study the oxidation reactions of GSH, especially microchip CE. However, there is a fundamental gap between understanding GSH behavior and microchip CE application. In this

chapter, conventional CE is used to investigate the oxidation of GSH by H_2O_2 in the presence of known accelerants and antioxidants. Preliminary data on simultaneous analysis of GSH and GSSG by microchip CE-EC is also presented.

7.1 Experimental Methods

7.1.1 CE-UV

CE analyses were carried out using a Beckman MDQ Capillary Electrophoresis system (Beckman Coulter, Fullerton, CA) with a photodiode array detector operating at 214 nm. Before each run, the capillary was rinsed with 1.0 M NaOH for 3 min, deionized H_2O for 2 min, and running buffer for 3 min, respectively. Sample solution was injected for 5 s at 0.5 psi. The separation was carried out by applying 20 kV voltage across the capillary. The capillary was 360 μm outer diameter and 75 μm inner diameter with a total length of 57 cm and an effective length of 47 cm.

7.1.2 Kinetic Experiments

Sample was made by first adding a certain amount of GSH stock solution (GSH stock solution was prepared in 0.01 M HCl) to sample vial following by dilution with running buffer to the desired concentration (1 mM). The reaction was initiated by adding an amount of H_2O_2 to the sample vial. The reaction products were immediately analyzed by CE. All reactions and sample

preparations were performed at room temperature (22°C). A similar procedure was used to assess the effect of other compounds on GSH oxidation. Solutions containing 1 mM GSH and Fe^{2+}, Cu^{2+}, ascorbic acid or catechin were prepared by combining the stock solutions with the running buffer. Once the H_2O_2 stock solution was added to the sample vial, the CE separation program was started.

7.2 Results/Discussion

7.2.1 Simultaneous Analysis of GSH, H_2O_2, and GSSG by CE-UV

The oxidation of GSH by H_2O_2, with or without catalysts, has been previously studied by several other groups.[20, 27] Normally in these studies, the simultaneous determination of GSH, GSSG and H_2O_2 was made by colorimetric methods after chromatographic separations.[20, 27] The analysis of GSH oxidation by a separation method has the advantage of being able to follow all solution species and not just the concentration of a single component. Our goal here is to demonstrate a CE method that can be used to measure the conversion of GSH to GSSG in the presence of oxidants and antioxidants, as part of a long term effort to characterize the role of antioxidants in disease. Figure 7.1 displays a typical electropherogram for the oxidation of GSH by H_2O_2 generating GSSG. We are unsure of the molecular structure of the last peak, however, it is clearly more negative than GSSG. With increasing time, GSH and H_2O_2 were consumed to produce GSSG. The peak areas of GSH,

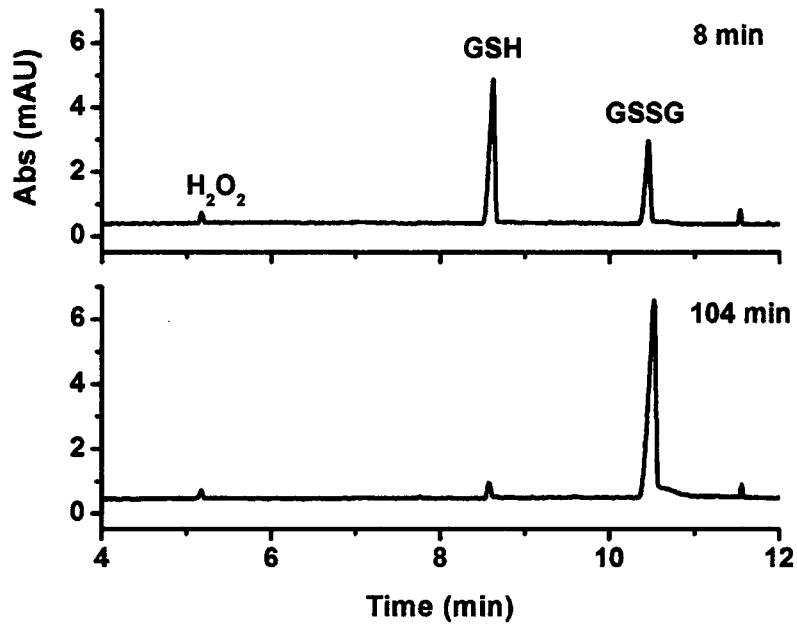

Figure 7.1. Representative eletropherogram for GSH oxidation. Experimental condition: starting concentration: GSH, 1 mM; H_2O_2, 1 mM; Separation voltage: 20 kV; Running buffer: 30 mM pH 7.0 phosphate; Capillary length: 57 cm.

GSSG and H_2O_2 were found to be linear over concentration ranges of 0.1 – 2.0 mM for all three compounds by measuring the peak area of serial standard dilutions for each species. The estimated detection limit at 214 nm is 30.0 μM (S/N = 3). These detection limits are not as sensitive as electrochemical methods, which normally reach sub-micromolar detection limits.[28] However, the goal of this project is to follow kinetics of conversion and therefore detection limit is not an issue.

7.2.2 Separation Optimization

To simultaneously monitor the concentration of GSH, GSSG and H_2O_2 during reaction process, the separation efficiency and resolution of all three compounds must be optimized. Run buffer concentration and pH conditions were therefore investigated to optimize the separation. Migration times and peak magnitudes of GSH and GSSG were recorded to analyze the separation efficiency and resolution.

Run Buffer Concentration. Variation of ionic strength changes the electroosmotic flow (EOF). As a result, the migration velocity of analyte molecules in the capillary changes, which further affects the separation efficiency and resolution.[29] Separations of GSH and GSSG were performed using different buffer concentrations (Figure 7.2A). The migration time of GSH increases from 7.6 min to 13.3 min and the migration time of GSSG increases from 9.3 min to 17.2 min when the running buffer concentration increases from

A.

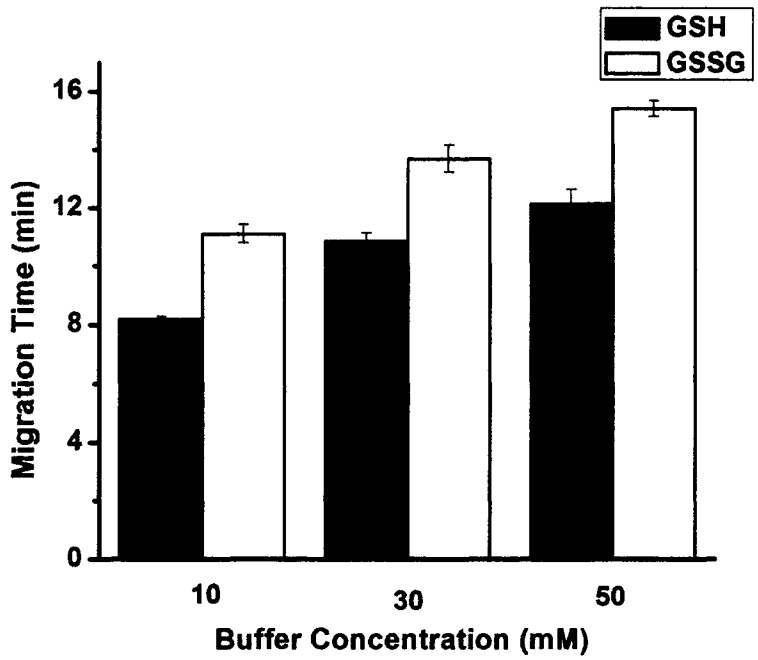

B.

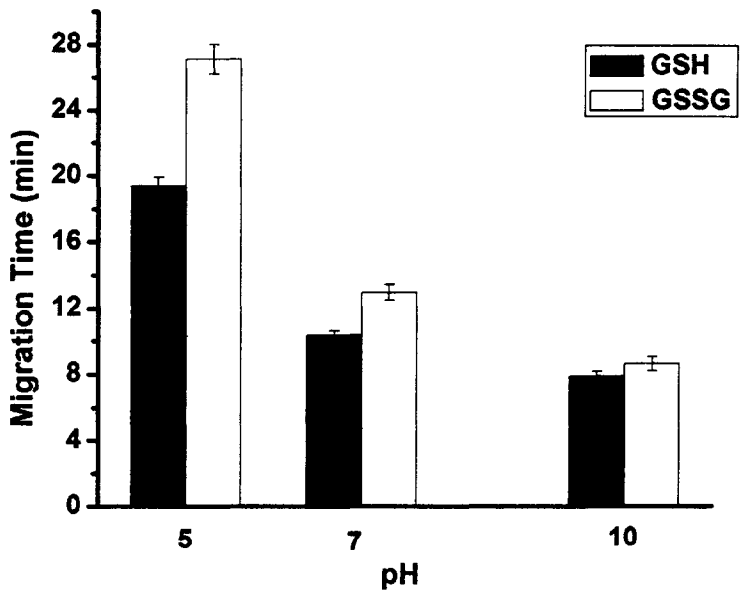

Figure 7.2. Optimization of separation conditions. A). Running buffer concentration, B). Running buffer pH value. Concentration: GSH, 1 mM; GSSG, 1 mM.

10 mM to 50 mM. The separation efficiency varied from 1.08×10^4 to 2.64×10^4 plates/m for GSH and 6.08×10^4 to 2.13×10^4 plates/m for GSSG. The resolution increased from 3.70 to 7.50 as the ionic strength increased. Based on these results, the buffer strength was set at 30 mM as the best compromise of time, resolution, and separation efficiency.

pH. The pH of the run buffer is another important factor that affects EOF and separations.[29] Three different pH values, 5.0, 7.0, and 10.0, were investigated. The migration times decreased from 19.0 min to 7.9 min, and from 27.1 min to 8.6 min for GSH and GSSG respectively when pH was increased from 5.0 to 10.0. Neutral pH (7.0) was chosen because it gave relatively short analysis time and is close to physiological pH.

7.2.3 Kinetics and Reaction Rate

Initial rates of GSSG formation were monitored to obtain reaction order for two reactants, GSH and H_2O_2. The value of the initial rate is given by

$$Rate = \frac{d[GSSG]}{dt} = k[GSH]^a[H_2O_2]^b$$

where k is reaction constant, a is the reaction order for GSH, and b is the reaction order for H_2O_2. Figure 7.3 shows the formation of GSSG versus time using different starting molar ratios of GSH to H_2O_2. When the starting concentration of GSH was varied from 1 mM to 2 mM while keeping H_2O_2 concentration constant (1 mM), two initial rates were calculated. The initial rate for 1 mM GSH oxidation was 298/min, and the initial rate for 2 mM GSH

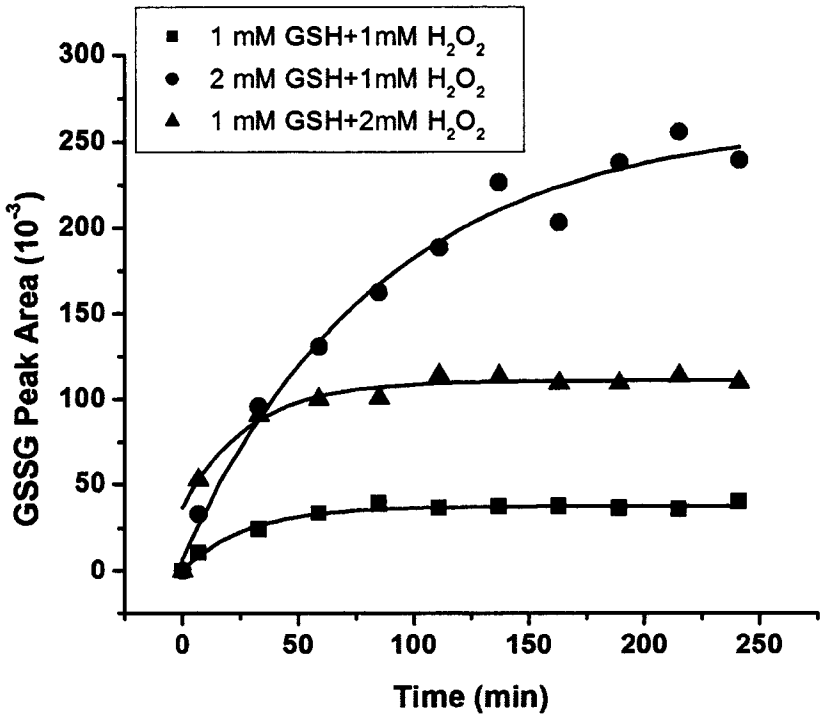

Figure 7.3. Formation of GSSG at different molar ratio of GSH and H_2O_2. The starting concentrations of GSH and H_2O_2 were shown in figure. Experimental conditions were same as Figure 7.1.

oxidation was 1567/min. The reaction order for GSH was thus determined as 2. When starting concentration of GSH was maintained at 1 mM and the concentration of H_2O_2 was varied from 1 mM to 2 mM, similar procedures can be taken. The initial rate for 1 mM H_2O_2 starting concentration was 298/min, and the initial rate for 2 mM H_2O_2 starting concentration was 791/min. The reaction order for H_2O_2 was calculated as 1. Therefore the overall oxidation should be 2 mol GSH with 1 mol of H_2O_2 generating 1 mol GSSG. The data matches well accepted stoichiometric reaction:[27]

$$H_2O_2 + 2GSH \longrightarrow GSSG + H_2O.$$

This step shows our ability to accurately profile chemical kinetics using CE. A secondary byproduct of the oxidation is seen as a small peak after GSSG in Figure 7.1. Numerous byproducts can be formed during the formation of GSSG in the presence of H_2O_2 [27].

7.2.4 Fenton Chemistry

As reported, the auto-oxidation of GSH (i.e., the direct reaction between GSH and molecular oxygen in air) is a spin-forbidden process.[30] Therefore, the auto-oxidation reaction was not expected to contribute significantly to the formation of GSSG. To verify this, the amount of air auto-oxidation was measured. Consecutive injections of GSH were made over 200 min, and the peak area of GSH decreased from 1.55×10^5 to 1.47×10^5. The 5% decrease of GSH peak area indicated that only a very small amount of GSH was oxidized

by dissolved oxygen in the solution. As reported, Fenton chemistry is responsible for most biological oxidative damage.[31] Trace transition metal ions, Cu^{2+} and Fe^{2+}, were therefore introduced into GSH solution to investigate the effect (Figure 7.4). Both Cu^{2+} and Fe^{2+} accelerated thiol auto-oxidation through the formation of reactive superoxide ions. The presence of 0.05 mM Cu^{2+} changed the initial rate from 44.1 to 111.6/min while 0.05 mM Fe^{2+} accelerates the oxidation from 44.1 to 242.9 (Figure 7.4). As a comparison, 0.05 mM Fe^{3+} was also introduced into GSH solution. No acceleration of the reaction was observed as shown in Figure 6.4, because Fe^{3+} does not participate in the reaction. When Cu^{2+} was added into the mixture of GSH and H_2O_2, the initial rate of oxidation was tremendously increased from 298/min to 1341/min. Formation of highly reactive hydroxyl radical due to Fenton chemistry is the cause of the further oxidation acceleration.

7.2.5 Antioxidants

The presence of antioxidants was investigated to further demonstrate the ability of CE to profile the oxidation process of GSH. Figure 7.5A is a representative electropherogram of GSH oxidation in the presence of catechin. The shoulder on the catechin peak is unidentified but may be the oxidation product of catechin. Catechin is a naturally occurring flavonoid compound and known for its antioxidant properties.[32, 33] Ascorbic acid is another naturally occurring antioxidant in biological systems.[34, 35] GSH was premixed with

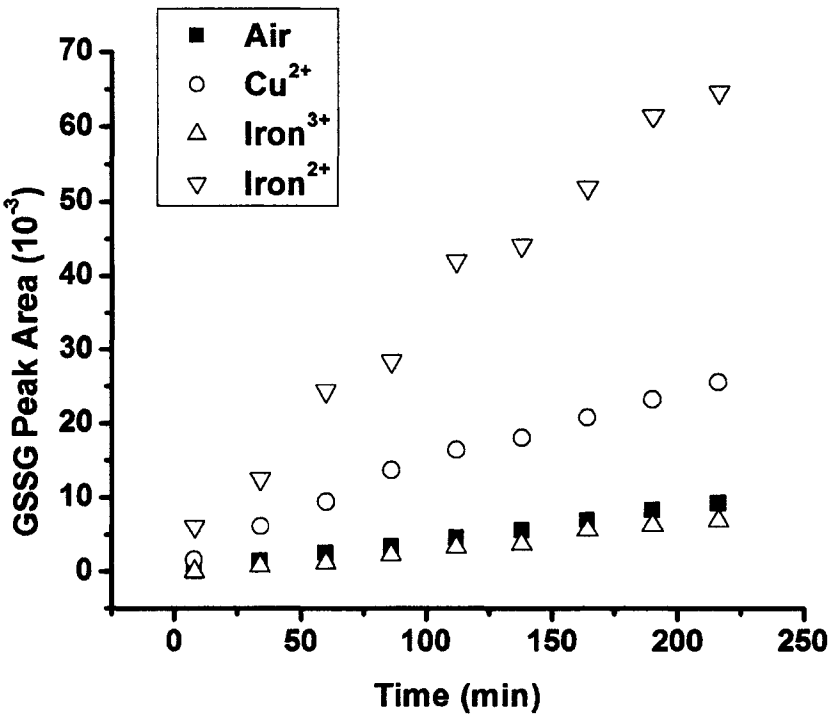

Figure 7.4. Formation of GSSG in the presence of Cu^{2+}, Fe^{2+} and Fe^{3+}. Concentrations: metal ions, 50 μM; GSH, 1 mM. Experimental conditions were same as Figure 7.1.

A

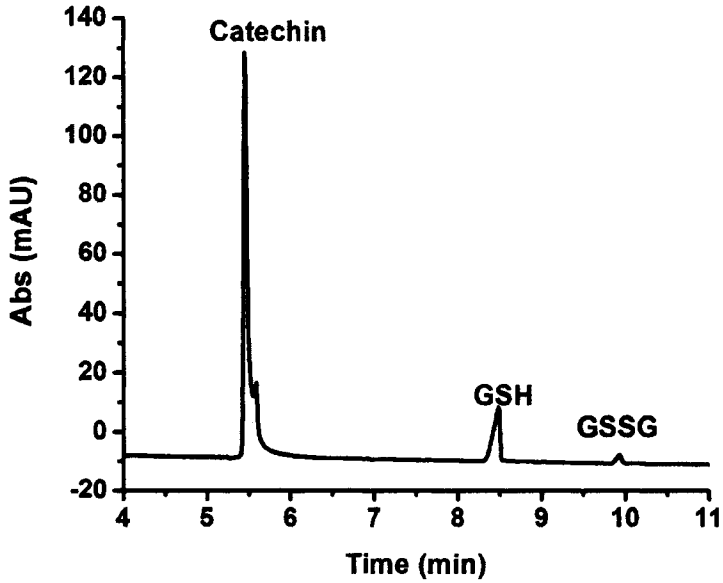

B.

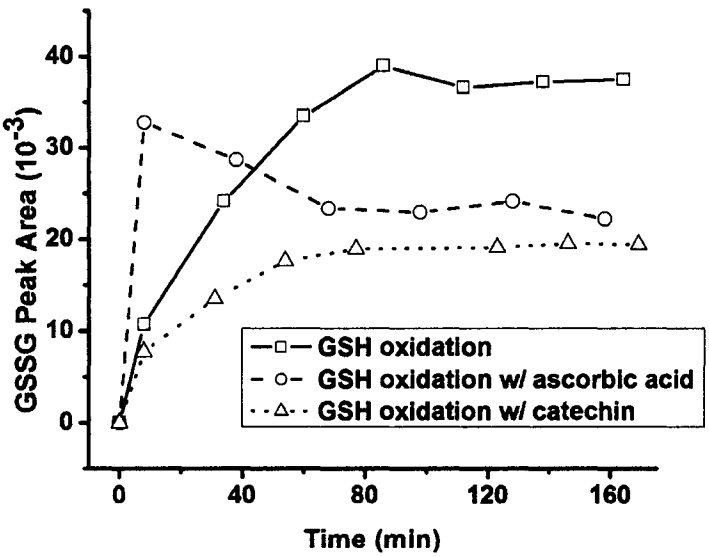

Figure 7.5. Oxidation of GSH at the presence of other antioxidants. A). Representative electrophegram of GSH oxidation with other compounds, GSH 1mM; catechin 1mM; Cu^{2+} 50 μM. B). Formation of GSSG at the presence of 1 mM catechin or 1 mM ascorbic acid in GSH oxidation by H_2O_2

catechin or ascorbic acid, followed by introduction of H_2O_2. Figure 7.5B shows that both catechin and ascorbic acid reduce GSH oxidation although oxidation processes are slightly different. The final concentration of GSSG was decreased more than 40% in the presence of antioxidants. To demonstrate the prevention properties by antioxidants, two more experiments were carried out. The auto-oxidation of GSH is a very slow process as shown in Figure 7.6A. When catechin was introduced into the GSH solution, the initial rate of GSSG formation decreased from 21.7/min to 4.0/min. Even for the case of GSH auto-oxidation accelerated by Cu^{2+}, the oxidation process was still decreased as the initial rate went from 111.6/min to 66.5/min (Figure 7.6B). This decrease is significant, showing the potential of catechin to protect GSH in a biological system. The standard reduction potential of catechin is lower than that of GSH,[36] which results in catechin reacting with ROS in the solution first. Less ROS will be able to oxidize GSH, resulting in less GSH oxidation.

7.2.6 Microchip CE

The desired goal of this project is to develop a miniaturized device that is desired for simultaneous detection of GSH and GSSG from cells experiencing different levels of oxidative stress. Although a lot of small molecules have been detected by microchip CE-EC, and although the EC method is simple, rapid, sensitive and versatile, the direct electrochemical determination of GSH and GSSG is very difficult. Electrode fouling is a major problem for direct

A

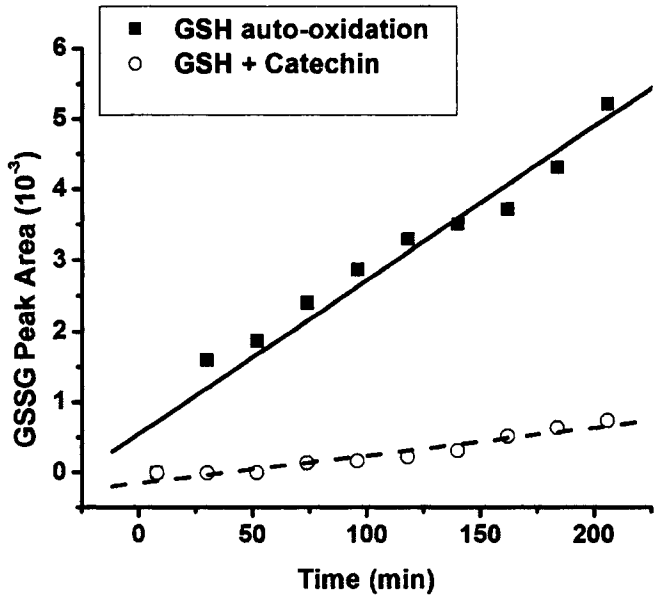

B

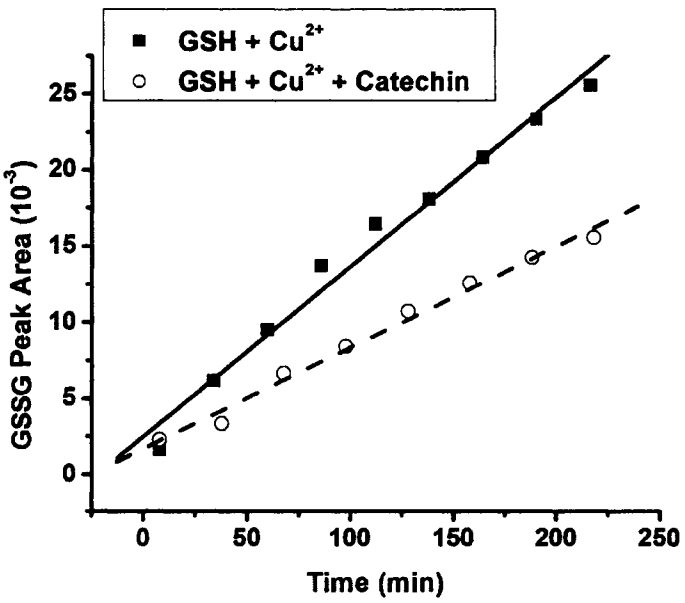

Figure 7.6. A). Auto-oxidation of GSH at the presence of catechin, GSH 1mM and catechin 1mM. B). Comparison of GSSG formation with and without catechin when Cu^{2+} is present.

amperometric detection when using noble metal electrodes. Chemically modified electrodes have been used to oxidize thiols but do not respond to disulfides. Anodically pretreated diamond electrodes have been employed to detect GSH and GSSG, however, the cost of the electrode prevents its extensive use. Pulsed amperometric detection (PAD) involves the application of a triple-step potential waveform, consisting of a detection potential (E1), where oxidation of adsorped analyte occurs, followed by a large positive potential (E2) for oxidative cleaning of the electrode surface, and finally, a large negative potential (E3) for reductive cleaning and adsorption of the analytes. The electrode fouling due to the adsorped analytes is decreased allowing direct detection of both thiols and disulfides.

Figure 7.7 shows preliminary data for the simultaneous detection of GSH and GSSG using a design discussed in Chapter V in PAD mode. The separation was accomplished in 150 s. The running buffer was 20 mM pH 7.0 TES, and the pinched injection time was 25 s. The chemistry involved in the electrochemical redox reaction of GSH and GSSG was not well understood. It was reported that different electrode materials have different redox mechanisms. On boron-doped diamond electrodes oxygen transfer reactions occur mainly by mediation of electrogenerated •OH radicals from H_2O discharge on the electrode surface. Under acidic conditions, the oxidized product at that type of electode is GSO_3H for GSH, while GSSG has 3 products, GSOSG, GSOOSG, and GSO_3H. Again, this is just the first

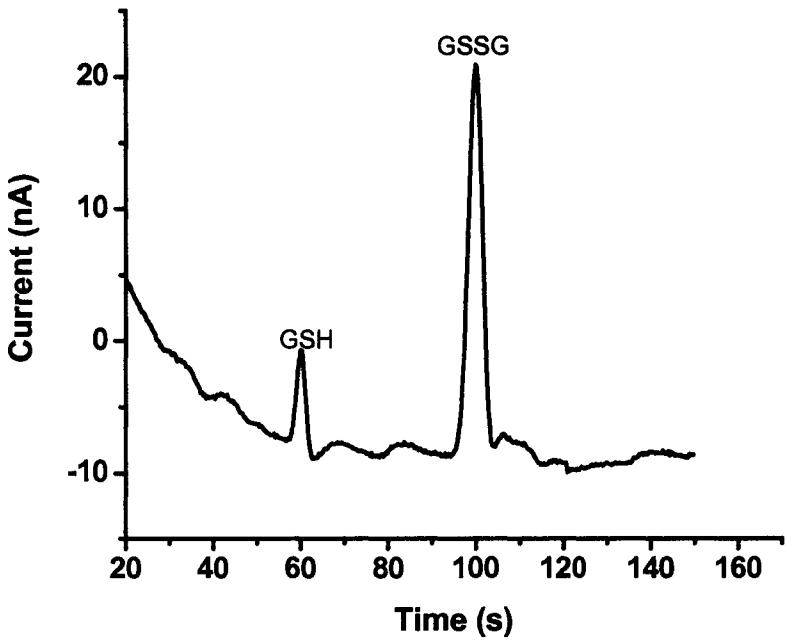

Figure 7.7. Separation of 100 μM reduced (GSH) and oxidized (GSSG) glutathione. Experimental conditions: PAD waveform, E1, 0.8 V; t1 0.20 s; E2, 1.4 V; t2, 0.05 s; E3, -0.5 V; t3, 0.05 s; separation voltage, 1000 V; injection, 25 s; running buffer, 30 mM pH 7.2 TES

preliminary experiment showing simultaneous detection of GSH and GSSG. Experimental conditions require further optimization for cell-based studies.

7.3 Conclusions

This is the first report that studies the oxidation of GSH by H_2O_2 using CE to monitor product formation. The environmental effects (presence of transitional metal ions and antioxidants) on the oxidation of GSH were investigated. The antioxidants reduce the oxidation of GSH, while transition metal ions catalyze GSH oxidation. Thorough understanding of these effects will be useful in understanding GSH oxidation in biological systems and as a result of dietary antioxidant therapy.

7.4 References

(1) Stamler, J. S.; Hausladen, A. *Nat Struct Biol* **1998**, *5*, 247-249.
(2) Rover, L., Jr.; Kubota, L. T.; Hoehr, N. F. *Clinica chimica acta; international journal of clinical chemistry* **2001**, *308*, 55-67.
(3) Meister, A. *Hepatology* **1984**, *4*, 739-742.
(4) Meister, A.; Anderson, M. E. *Annu Rev Biochem* **1983**, *52*, 711-760.
(5) De Vega, L.; Perez Fernandez, R.; Martin Mateo, M. C.; Bustamante Bustamante, J.; Mendiluce Herrero, A.; Bustamante Munguira, E. *Renal Failure* **2002**, *24*, 421-432.
(6) Anderson, J. V.; Davis, D. G. *Physiol Plant* **2004**, *120*, 421-433.
(7) Anderson, E. I.; Wright, D. D. *Exp Eye Res* **1982**, *35*, 11-19.
(8) Anderson, C. P.; Tsai, J. M.; Meek, W. E.; Liu, R. M.; Tang, Y.; Forman, H. J.; Reynolds, C. P. *Exp Cell Res* **1999**, *246*, 183-192.
(9) Wilson, W. R.; Anderson, R. F. *Int J Radiat Oncol Biol Phys* **1989**, *16*, 1001-1005.
(10) Muscari, C.; Pappagallo, M.; Ferrari, D.; Giordano, E.; Capanni, C.; Caldarera, C. M.; Guarnieri, C. *Journal of Chromatography, B: Biomedical Sciences and Applications* **1998**, *707*, 301-307.
(11) Pastore, A.; Federici, G.; Bertini, E.; Piemonte, F. *Clinica chimica acta; international journal of clinical chemistry* **2003**, *333*, 19-39.

(12) Awasthi, S.; Ahmad, F.; Sharma, R.; Ahmad, H. *Journal of chromatography* **1992**, *584*, 167-173.
(13) Bozzi, A.; Parisi, M.; Strom, R. *Biochemistry and Molecular Biology International* **1996**, *40*, 561-569.
(14) Cereser, C.; Guichard, J.; Drai, J.; Bannier, E.; Garcia, I.; Boget, S.; Parvaz, P.; Revol, A. *Journal of chromatography. B, Biomedical sciences and applications* **2001**, *752*, 123-132.
(15) Eady, J. J.; Orta, T.; Dennis, M. F.; Stratford, M. R. L.; Peacock, J. H. *British Journal of Cancer* **1995**, *72*, 1089-1095.
(16) Mergel, D.; Andermann, G.; Andermann, C. *Methods and findings in experimental and clinical pharmacology* **1979**, *1*, 277-283.
(17) Raggi, M. A.; Mandrioli, R.; Sabbioni, C.; Mongiello, F.; Marini, M.; Fanali, S. *Journal of Microcolumn Separations* **1998**, *10*, 503-509.
(18) Reid, M.; Jahoor, F. *Curr Opin Clin Nutr Metab Care* **2000**, *3*, 385-390.
(19) Camera, E.; Picardo, M. *Journal of Chromatography, B: Analytical Technologies in the Biomedical and Life Sciences* **2002**, *781*, 181-206.
(20) Kachur, A. V.; Koch, C. J.; Biaglow, J. E. *Free Radic Res* **1998**, *28*, 259-269.
(21) Lunte, S. M.; Malone, M. A.; Zuo, H. *Current Separations* **1994**, *13*, 75-79.
(22) Piccoli, G.; Fiorani, M.; Biagiarelli, B.; Palma, F.; Potenza, L.; Amicucci, A.; Stocchi, V. *Journal of Chromatography, A* **1994**, *676*, 239-246.
(23) Jin, W.; Dong, Q.; Ye, X.; Yu, D. *Analytical Biochemistry* **2000**, *285*, 255-259.
(24) Jin, W.; Li, W.; Xu, Q. *Electrophoresis* **2000**, *21*, 774-779.
(25) Jin, W.; Li, X.; Gao, N. *Analytical Chemistry* **2003**, *75*, 3859-3864.
(26) Carru, C.; Zinellu, A.; Pes, G. M.; Marongiu, G.; Tadolini, B.; Deiana, L. *Electrophoresis* **2002**, *23*, 1716-1721.
(27) Abedinzadeh, Z.; Gardes-Albert, M.; Ferradini, C. *Can J Chem* **1989**, *67*, 1247-1255.
(28) Schwarz, M. A.; Hauser, P. C. *Lab on a Chip* **2001**, *1*, 1-6.
(29) Liu, Y.; Fanguy, J. C.; Bledsoe, J. M.; Henry, C. S. *Anal Chem* **2000**, *72*, 5939-5944.
(30) Luo, D.; Smith, S. W.; Anderson, B. D. *J Pharm Sci* **2005**, *94*, 304-316.
(31) Spear, N.; Aust, S. D. *Arch Biochem Biophys* **1995**, *324*, 111-116.
(32) Shui, G.; Wong, S. P.; Leong, L. P. *J Agric Food Chem* **2004**, *52*, 7834-7841.
(33) Apak, R.; Guclu, K.; Ozyurek, M.; Karademir, S. E. *J Agric Food Chem* **2004**, *52*, 7970-7981.
(34) Herrero-Martinez, J. M.; Simo-Alfonso, E. F.; Ramis-Ramos, G.; Deltoro, V. I.; Calatayud, A.; Barreno, E. *Environmental Science and Technology* **2000**, *34*, 1331-1336.
(35) Davey, M. W.; Bauw, G.; Van Montagu, M. *Journal of Chromatography, B: Biomedical Sciences and Applications* **1997**, *697*, 269-276.

(36) Yang, B.; Kotani, A.; Arai, K.; Kusu, F. *Chem Pharm Bull (Tokyo)* **2001**, *49*, 747-751.

CHAPTER VIII

CONCLUSIONS

When this dissertation work started, PDMS/glass hybrid microchip was the dominant format for microchip CE-EC. A very important factor for electrochemical detection is the working electrode. Both integrated thin-film and off-chip electrodes have been reported for microanalytical devices. Thin-film electrodes predominated at that time because of the compactness and suitability for batch fabrication from well developed photolithography techniques. The microfabrication of the thin-film electrode provided a high precision and good reproducibility on electrode sizes. The disadvantages of this electrode design, however, are obvious. First, the fabrication of thin-film electrodes requires a clean room facility, which increases the overall cost. Second, the lifetime of the electrode is limited by experimental conditions. Third, alignment of the thin-film electrode is difficult when irreversible sealing is used. Fourth, weak adhesion of Au to PDMS requires a different substrate material to incorporate Au electrode. Finally, separation efficiency is decreased by the use of different substrate materials. The goal of this dissertation work was to develop a miniaturized CE-EC system with enough sensitivity, flexibility, and portability to analyze biological and environmental samples.

The beginning of the dissertation project followed the trend in microchip CE-EC at that time and used a PDMS/glass hybrid chip with a Au thin-film

electrode on the glass substrate. Every problem mentioned above was encountered in the determination of 4-aminophenol. A new microchip CE-EC system was thus developed. The first change made was the employment of PDMS as the substrate for all microchannel walls. To incorporate the EC detection with PDMS chips, a new design of working electrode was developed. This design added one electrode alignment channel perpendicular to the separation channel in PDMS. A metallic microwire was placed in this electrode channel acting as the working electrode. The new working electrode proved to be simpler, more sensitive and have a higher collection efficiency than the microfabricated Au thin-film electrode. 100 nM LOD of dopamine was achieved for amperometric detection, which was the lowest report by microchip CE-EC without a decoupler. In addition, the alignment of the working electrode showed excellent reproducibility. Another advantage of microwire design is the flexibility of adding more microwires or electrodes to the chip. The developed microchip CE-EC (conductivity) system with multiple on-column electrodes was then applied to aerosol analyses and antioxidant profiling. The amount of sulfate and nitrate in aerosol samples were quantified. The results using our system matched other methodologies. This is the first presentation of using microchip CE-EC system to analyze inorganic anions in airborne particles. Besides aerosol sample analysis, oxidation reaction of GSH was studied using conventional CE-UV system. This was the first attempt in profiling antioxidant behaviors in the presence of known accelerants and antioxidants with CE

methodology. In addition, preliminary data showed simultaneous detection of GSH and GSSG could be made by the developed microchip CE-EC system. These developments in my research have been reported in several journals. Details of the publications are listed in Chapter IX.

CHAPTER IX

PUBLICATION LIST

1. Yan Liu, Charles S. Henry, Using Capillary Electrophoresis to Study Biological Behavior, J. Chromatography B, 2005, in preparation.

2. Yan Liu, Charles S. Henry, Polyelectrolyte Coating for Microchip Capillary Electrophoresis, Microchip Capillary Electrophoresis: Methods and Protocols, Humana Press, 2005, in press.

3. Yan Liu, David A MacDonald, Xiao-Ying Yu, Jeffrey L. Collett, Jr., Charles S. Henry, Analysis of Anions in Aerosol Particles by Microchip Capillary Electrophoresis, Analytical Chemistry, 2005, in preparation

4. Yan Liu, Jonathan A. Vickers, Charles S. Henry, Simple and Sensitive Electrode Design for Microchip Electrophoresis/Electrochemistry, Analytical Chemistry, 2004, 76, 1513-1517

5. Yan Liu, Carlos D. Garcia, Charles S. Henry, Recent Progress in the Development of μTAS for Clinical Analysis, Analyst, 2003, 128, 1002-1008

6. Carlos D. Garcia, Yan Liu, Paul Anderson, Charles S. Henry, Versatile 3-channel High-Voltage Power Supply for Microchip Capillary Electrophoresis, Lab-on-a-Chip, 2003, 3, 324-328

7. Yan Liu, David O. Wipf, Charles S. Henry, Conductivity Detection for Monitoring Mixing Reactions in Microfluidic Devices, Analyst, 2001, 126, 1248-1251

8. Yan Liu, Joseph C. Fanguy, Justin M. Bledsoe, Charles S. Henry, Dynamic Coating Using Polyelectrolyte Multilayers for Chemical Control of Electroosmotic Flow in Capillary Electrophoresis Microchips, Analytical Chemistry, 2000, 72, 5939-5944